No. 6, October 2002

# The Isaac Newton Group of Telescopes

NEWSLETTER

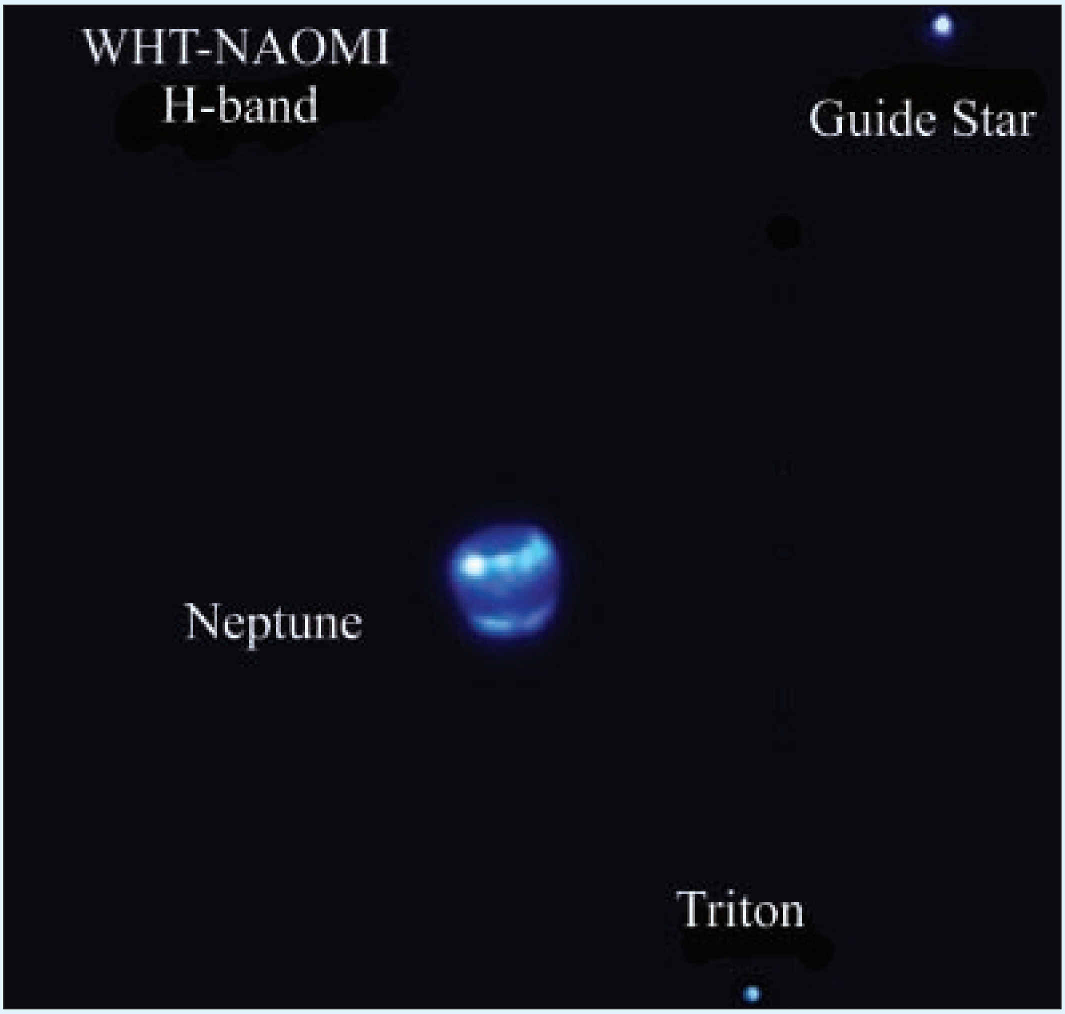


*NAOMI Neptune in H band (1.6 microns). 120-sec integration, using as wavefront reference a star (V ~10, top right) which happened to be nearby on the night. Neptune's diameter is 2.3 arcsec. The clouds are prominent in H band because of a strong methane line at a wavelength close to 1.6 micron. Triton is visible near the bottom of the image (see article by C. R. Benn et al. on page 21).*

## Message from the Director

*Dear Reader,*

Whilst the telescopes on La Palma keep going strong, a large number of changes are taking shape at the ING. Last winter important decisions were taken by PPARC Council that have a profound influence on the UK's ground-based astronomy programme. As a result, the UK is now a member of the European Southern Observatory, but these decisions also imply a siginificant shift in the balance of resources. One particular implication is a reduction of funds for the ING telescopes in the future.

In order to offset the reduction of funding from PPARC, a formal partnership with the Instituto de Astrofísica de Canarias has been agreed. This collaboration will further strengthen international collaboration between the European partners at the ORM, and at the same time reduce the impact of the reduced UK funding.

Nevertheless, the overall reduction in resources enforces a number of important changes at

# THE ISAAC NEWTON GROUP OF TELESCOPES

The Isaac Newton Group of Telescopes (ING) consists of the 4.2 m William Herschel Telescope (WHT), the 2.5 m Isaac Newton Telescope (INT) and the 1.0 m Jacobus Kapteyn Telescope (JKT), and is located 2,350 m above sea level at the Roque de Los Muchachos Observatory (ORM) on the island of La Palma, Canary Islands, Spain. The WHT is the largest telescope of its kind in Western Europe.

The construction, operation, and development of the ING Telescopes is the result of a collaboration between the United Kingdom and the Netherlands. The site is provided by Spain, and in return Spanish astronomers receive 20 per cent of the observing time on the telescopes. The operation of the site is overseen by an International Scientific Committee, or Comité Científico Internacional (CCI).

A further 75 per cent of the observing time is shared by the United Kingdom, the Netherlands and the Instituto de Astrofísica de Canarias (IAC). On the JKT the international collaboration embraces astronomers from Ireland. The remaining 5 per cent is reserved for large scientific projects to promote international collaboration between institutions of the CCI member countries.

The ING operates the telescopes on behalf of the Particle Physics and Astronomy Research Council (PPARC) of the United Kingdom, the Nederlandse Organisatie voor Wetenschappelijk Onderzoek (NWO) of the Netherlands and the IAC in Spain. The Roque de Los Muchachos Observatory, which is the principal European Northern hemisphere observatory, is operated by the IAC.

(Continued from front cover)

ING that will not go unnoticed by ING staff or the astronomical community that we serve. In this Newsletter you will read how the changes impact on the service delivered to our user community (see article on page 19).

Another significant development since the previous Newsletter is the creation of a new observatory advisory body. The creation of this advisory group with wide international participation and a wide brief, was proposed during the observatory review last year. I am particularly pleased with the strong membership of this group, and trust that their experience will help outline future directions of the observatory.

Apart from the unavoidable 'politics' that surrounds the observatory, we are not losing sight of the significant astronomical results that are being produced. The articles based on observations with INGRID, S-CAM, CIRSI, NAOMI and ULTRACAM provide for a number of excellent highlights.

I hope you enjoy reading this Newsletter !

René G. M. Rutten

## The ING Board

The ING Board oversees the operation, maintenance and development of the Isaac Newton Group of Telescopes, and fosters collaboration between the international partners. It approves annual budgets and determines the arrangements for the allocation of observing time on the telescopes. ING Board members are:

Prof. Janet Drew, *Chairperson* – London
Dr. Wilfried Boland – NWO, Leiden
Dr. Gavin Dalton – Oxford
Dr. Ramón García López – IAC, La Laguna
Dr. Tom Marsh – Southampton
Dr. Ronald Stark – NWO, The Hague
Prof. Thijs van der Hulst – Groningen
Dr. Colin Vincent – PPARC, Swindon
Dr. Simon Berry, *Secretary* – PPARC

## ING Director's Advisory Group

Last year the Isaac Newton Group of Telescopes had its second independent international review of the observatory, initiated by the ING Board. The conclusions from the review were very encouraging (for a summary, see the October 2001 issue of this Newsletter). One of the recommendations of the review was that ING should set up a Director's Advisory Group. Such a group would assist the observatory in defining the strategic direction for operation and development of the telescopes. It would also provide an international perspective and act as an independent contact point for the community to present its ideas. This new group replaces the instrumentation Working Group that fulfilled part of this function to date.

Dr Mark McCaughrean (Potsdam) has kindly agreed to chair this new advisory committee. Further members are: Thijs van der Hulst (Groningen), Ramón García López (IAC, La Laguna), Phil James (Liverpool) and Nial Tanvir (Hertfordshire).

## The ING Newsletter

ISSN 1575–8958 (printed version)
ISSN 1575–9849 (electronic version)
Legal License: TF–1959/99

Published in Spain by THE ISAAC NEWTON GROUP OF TELESCOPES (ING).

Apartado 321; 38700 Santa Cruz de La Palma; Canary Islands; Spain.
Telephone: +34 922 425400
Fax: +34 922 425401
URL: `http://www.ing.iac.es/`

**Editorial team:** J. Méndez, R. Rutten, D. Lennon and Johan Knapen.
**Designer:** J. Méndez.
**Preprinting:** Gráficas El Time. Tel.: +34 922 416651
**Printing:** Gráficas Sabater. Tel.: +34 922 623555

The ING Newsletter is primarily published on-line at `http://www.ing.iac.es/PR/newsletter/` in html and pdf format. Notification of every new issue is given by e-mail using the [INGNEWS] mailing list. More information on [INGNEWS] can be found on page 29. Requests for one-off printed copies can be emailed to Javier Méndez (*jma@ing.iac.es*).

The ING Newsletter is published twice a year in March and September. If you wish to submit a contribution, please contact Javier Méndez (*jma@ing.iac.es*). Submission deadlines are 15 July and 15 January.

# INGRID: Early Science Results

The ING's Red Imaging Device (INGRID) saw first light on the William Herschel Telescope in March 2000. In over 2 years of operation the instrument has proven to be a highly efficient infrared imager. Below we present four articles with science results from INGRID data.

## Bar Strengths in Galaxies as Measured from INGRID Images

J. H. Knapen[1], D. L. Block[2], R. Buta[3], I. Puerari[4], B. G. Elmegreen[5], S. Stedman[6], D. M. Elmegreen[7]

*1: ING and University of Hertfordshire; 2: University of the Witwatersrand; 3: University of Alabama; 4: INAOE; 5: IBM; 6: University of Hertfordshire; 7: Vassar College*

We describe results from our study of a sample of spiral galaxies of a wide range of Hubble types on the basis of near-IR imaging obtained with INGRID on the WHT. We focus on the determination of bar torques, or bar strengths, from our images, and show that this bar strength only very weakly correlates with de Vaucouleurs bar type, or with bar axis ratio.

### 1. INGRID on the WHT

INGRID, the near-IR (NIR) camera for the WHT, has been in routine operation at the Cassegrain focus for almost two years now. In the three semesters from August 2000 until January 2002, it has been in scheduled use for 37, 35, and 35 nights (including NAOMI science runs, excluding commissioning and service), or 20% of the time. This makes INGRID the second-most used instrument on the WHT, after ISIS. The scientific areas that have been attacked with INGRID span an enormous range, from observational cosmology to brown dwarfs and giant planets. INGRID's main attraction is the relatively large field-of-view, of just over 4 arcmin, coupled with a pixel size of 0.24 arcsec which samples all except the very best seeing conditions. Here, we present results obtained from a number of PATT-supported observing runs, aimed at imaging nearby and relatively face-on spiral galaxies.

### 2. Barred Galaxies

One of the main attractions of observing in the NIR is that one is much less susceptible to the attenuation of emission by dust. Compared to the visual ($V$-band), extinction by dust is a full order of magnitude less in the NIR $K$-band, at 2.2 microns. Since at rest wavelength (i.e., in nearby galaxies) the NIR light also traces a relatively old stellar population, NIR imaging is the technique of choice to observe the "stellar backbone" of galaxies: the old stellar population which, by assumption of a mass-to-light ($M/L$) ratio, will give an estimate of the mass. We imaged a complete sample of 57 galaxies with INGRID for this reason: to study the old stellar component, not affected by dust extinction. In one of the lines of our overall project, the INGRID $K_s$ imaging will be compared with $B$ and $R$ broad-band images, as well as with narrow-band H$\alpha$ images which trace young, massive stars and current star formation. This comparison can indicate how mass and star formation are concentrated in spiral arms, and why they are concentrated to a different degree.

In this short article, though, we will focus on bars in galaxies. About 75% of all disk galaxies have bars (Sellwood & Wilkinson, 1993; Knapen, 1999), where stars move on elongated periodic orbits and thus support a non-axisymmetric potential. Gas in bars shocks and loses angular momentum, which implies that bars form a mechanism to transport material inward in a rotationally supported galactic disk. This explains why bars are relevant for questions related to the origin, evolution, and maintenance of stellar and non-stellar activity in or around the nuclei of galaxies: massive black holes, AGN or (circum)nuclear starbursts all need fuel to maintain their activity and whereas enough gas is available in the disk at large, moving this gas inwards implies making it lose a considerable amount of angular momentum.

NIR imaging is the best way of finding and classifying bars. At optical wavelengths, the bar may be masked by the combined effects of emission from young stars, and extinction by dust. There are a number of well-known and spectacular examples of bars which are unrecognisable in the visible, but well-defined in the NIR (e.g., Block & Wainscoat, 1991; Block et al., 1994). However, statistical studies (e.g., Mulchaey & Regan, 1997; Knapen, Shlosman & Peletier, 2000; Eskridge et al., 2000) have shown that the overall bar fraction only goes up by 10–15% in the NIR as compared to classification from optical imaging. Still, the NIR is much preferred for any detailed and/or quantitative studies of bars, because the bar parameters can be measured much more cleanly there than in the optical.

## 3. Determining Bar Strength

Of the main structural parameters of bars: length, axis ratio, luminosity distribution, and strength, the latter has proved to be by far the most elusive observationally. Theoretically, bar strength can be defined rather easily as some measure of the ratio of non-axisymmetric, or tangential, over axisymmetric gravitational force. Observationally, bar "strength" has often been measured as bar ellipticity, or axis ratio, but this is strictly speaking incorrect. This is easy to illustrate by imaging a very elliptical bar in a galaxy which also has a massive bulge. In that case, the net gravitational pull felt by a particle (be it gaseous or stellar) in the bar will be that caused by the bar, but offset significantly by the axisymmetric gravitational pull of the bulge. Thus, the net bar strength in that case can be much less than in the case of a less elliptical bar in a bulge-less galaxy.

A quantitative observational measure of bar strength has recently been developed by Buta & Block (2001), based on an old of idea of Combes & Sanders (1981). Buta & Block calculate the maximum, $Q_b$, of the ratio of the tangential force to the mean axisymmetric radial force. Technically, this is done by a Fourier analysis of deprojected images, under the assumption of a constant mass-to-light ratio. This means that the observational input data must be NIR images with a high signal-to-noise ratio, which in turn implies a preference for bright, thus nearby, galaxies. This is where INGRID is ideal: the 4.2-m WHT mirror ensures a high S/N ratio, whereas the field of view of 4.2 arcmin facilitates the imaging of disks of nearby galaxies. We thus derived bar strengths, $Q_b$, for those galaxies in our sample of 57 galaxies where this could be determined (45 of them, the images of the others are not of high enough S/N ratio).

The galaxies in our sample were selected to have an angular diameter of more than 4.2 arcmin and an inclination of less than 50 degrees. Our sample covers the complete range in Hubble type for spiral galaxies, as well as in Elmegreen spiral arm class (Elmegreen & Elmegreen, 1987), from flocculent to grand-design. As an example, we show, in Figure 1, $V$ and $K_s$-band images of the SA(rs)b galaxy Messier 88 (NGC 4501), where the $V$-band image was obtained with ING's 1-m JKT. This $K_s$-band image is one of our deepest, with a total on-source integration time of over one hour. The $V\!-\!K_s$ colour index image clearly shows the location of the star-forming spiral arms (as lighter shades) and the dust lanes which accompany them (darker).

## 4. Results

In Figure 2 we show nine of our sample galaxies, ranked in terms of increasing bar strength or torque. The locations where the ratio of the tangential force to the mean axisymmetric radial force reaches a maximum are indicated in each galaxy image by four filled black or yellow dots. Figure 3 shows a montage of $K_s$ images of 9 two-armed spiral galaxies in our sample, ranked vertically in terms of bar torque, and horizontally in terms of pitch angle class, where class a contains the most tightly wound spirals.

Combining our results on the bar strength $Q_b$ with those obtained by Buta & Block (2001) for 30 galaxies, we now have a sample of 75 galaxies with bar strengths determined from NIR imaging. In Figure 4, we plot the bar strength $Q_b$ against the deprojected bar axis ratio, often used as a bar "strength" indicator, for those galaxies where the latter number has been published by Martin (1995). Whereas there is a general trend, as expected, where the most elongated bars (high

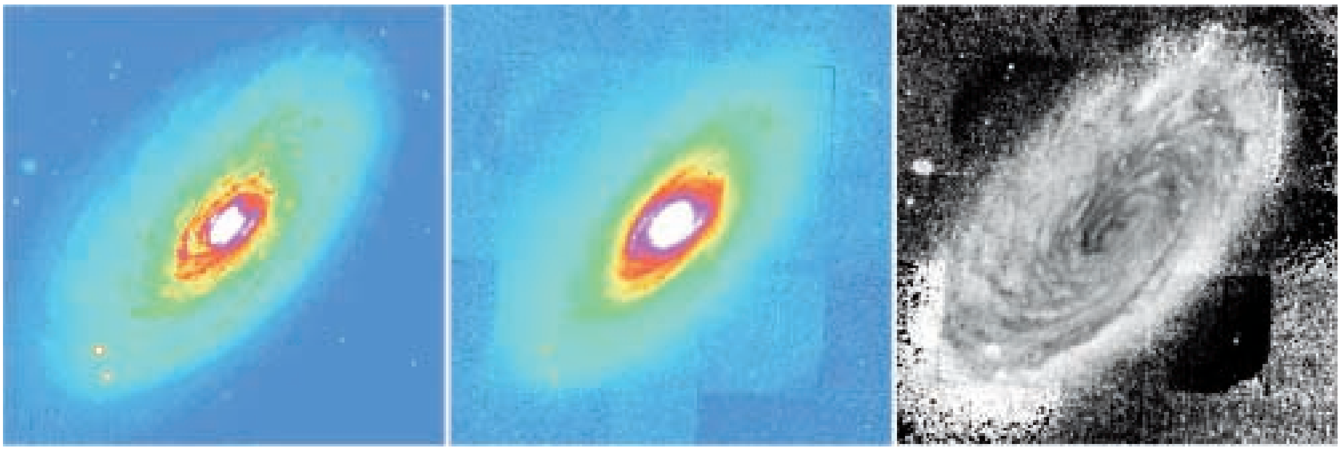

*Figure 1. V, $K_s$, and $V\!-\!K_s$ colour index images of the SA(rs)b galaxy Messier 88 (NGC 4501), as obtained with INGRID on the WHT and with the JKT. The field of view of the images is ~7 arcmin, but only the central 4 arcmin is shown here.*

ellipticity or axis ratio) also have the highest bar torques or strengths, the spread in $Q_b$ for each axis ratio is very large, and in fact large enough as to invalidate any claims that bar ellipticity is a reliable bar strength estimator. For example, bars with moderate ellipticity (axis ratios of 0.4–0.5) span the entire range of bar strengths $Q_b$ and their ellipticities are thus completely useless to discriminate strong from weak bars. It is only at the very extreme ends of the bar axis ratio range that such a discrimination might have a chance of success. Laurikainen, Salo & Rautiainen (2002) derive $Q_b$ using a slightly different method, and compare their values with bar ellipticities. They find a better correlation between $Q_b$ and bar axis ratio than we do, possibly due to the fact that the latter were derived from NIR images, whereas Martin (1995) used blue light photographs.

In Figure 5, we plot $Q_b$ for each galaxy against its classification from de Vaucouleurs (1963), who classified galaxies as un-barred (SA), barred (SB) or intermediate (SAB, often referred to as weakly barred though this may not be correct in all cases). A clear trend is seen where the SB galaxies have higher bar strengths $Q_b$ than SA or SAB galaxies, but more interesting is the considerable overlap in $Q_b$ values between the SA, SAB and SB classes. This implies that many of the galaxies classed as SAB in fact have stronger bars than many classed SB, and even that a considerable number of SAB galaxies have weaker bars than others classed as un-barred! In addition, Figure 5 shows clearly that the effect of overlapping bar strength is not due to either early- or late-type galaxies, but is present equally for all sub-types. Massive bulges, which will dilute bar strength, are thus not the cause of the observed effect. Apparently, the relative bar strength comes from a complex mixture of bar amplitude, radial profile and relative length, combined with the bulge strength. The resulting spread of $Q_b$ for each Hubble subtype is due to the different ways in which these quantities vary along the Hubble sequence. How exactly this affects

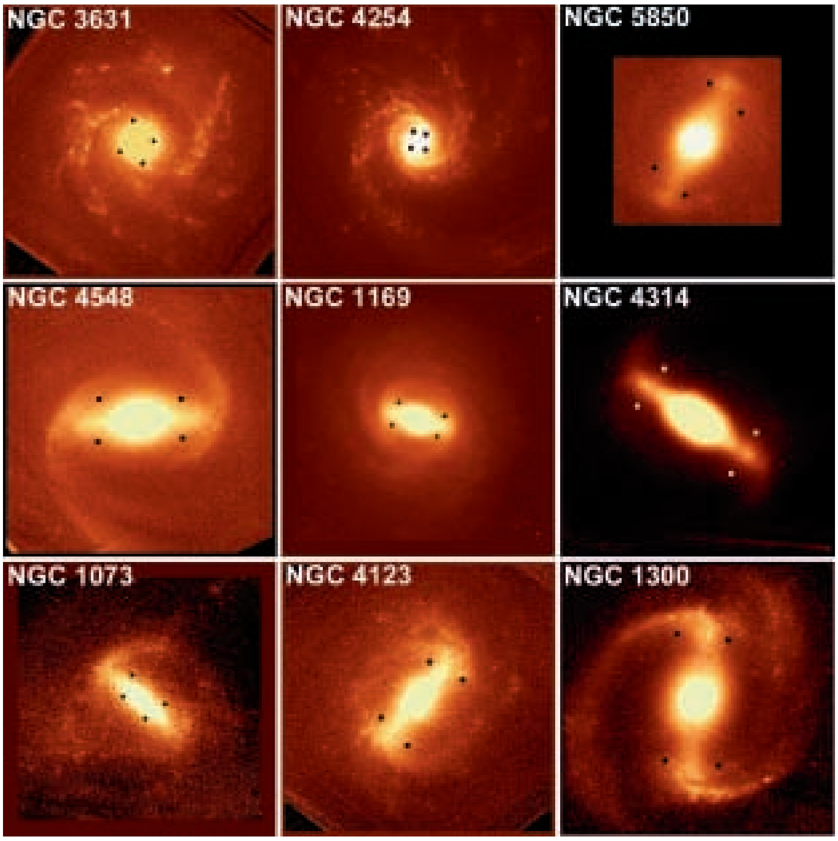


*Figure 2. Deprojected $K_s$ images of nine galaxies observed with the 4.2-m WHT, ranked in terms of increasing bar strength, or torque. The four filled black or yellow dots indicate the locations where the ratio of the tangential force to the mean axisymmetric radial force reaches a maximum. From Block et al. (2001).*

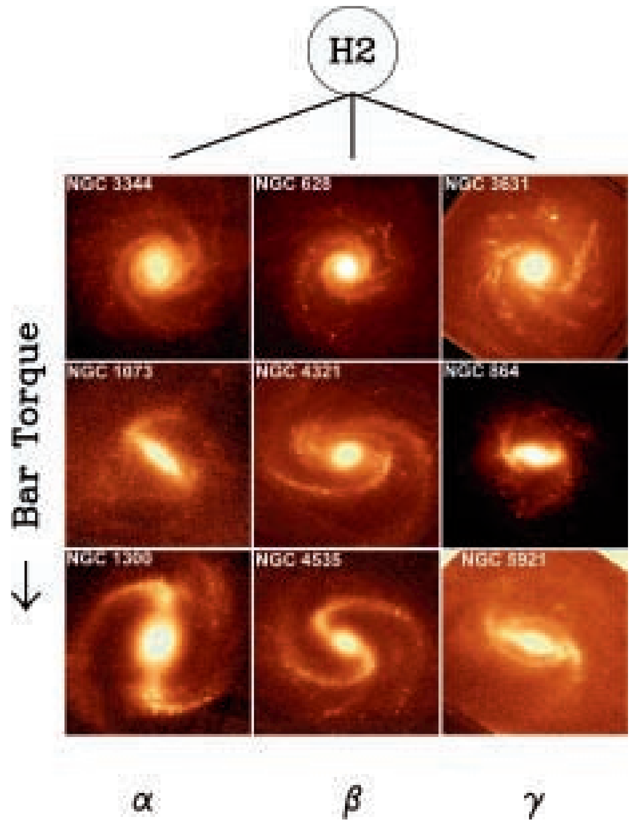


*Figure 3. Montage of 9 $K_s$ images of two-armed spirals, which have been ranked vertically in terms of bar torque, where the strongest bars are seen in the lower panels, and horizontally in terms of pitch angle class, where class $\alpha$ contains the most tightly wound spirals. From Block et al. (2001).*

the bar parameters, and the influence the bar has on its surroundings, is not clear, and is the subject of our further exploration, partly aided by INGRID imaging.

## 5. Summary

In this short paper, we illustrate the power of the INGRID NIR camera on the WHT in obtaining deep, wide-field, imaging of nearby spiral galaxies. We describe results from our study of bar torques, or bar strengths, in a large sample of galaxies which we imaged with INGRID, and show that this bar strengths only very weakly correlates with de Vaucouleurs bar type, or with bar axis ratio.

References:

Block, D. L. & Wainscoat, R. J., 1991, *Nature*, **353**, 48.

Block, D. L., Bertin, G., Stockton, A., Grosbol, P., Moorwood, A. F. M., Peletier, R. F., 1994, *A&A*, **288**, 365.

Block, D. L., Puerari, I., Knapen, J. H., Elmegreen, D. M., Buta, R., Stedman, S., Elmegreen, D. M., 2001, *A&A*, **375**, 361.

Buta, R. & Block, D. L., 2001, *ApJ*, **550**, 243.

Combes, F. & Sanders, R. H., 1981, *A&A*, **96**, 164.

de Vaucouleurs, G., 1963, *ApJS*, **8**, 31.

Elmegreen, D. M. & Elmegreen, B. G., 1987, *ApJ*, **314**, 3.

Eskridge, P. B. et al., 2000, *AJ*, **119**, 536.

Knapen, J. H., 1999, in The Evolution of Galaxies on Cosmological Timescales, J. E. Beckman & T. J. Mahoney, Eds., *ASP Conf. Ser.*, **187**, 72.

Knapen, J. H., Shlosman, I. & Peletier, R. F., 2000, *ApJ*, **529**, 93.

Laurikainen, E., Salo, H. & Rautiainen, P., 2002, *MNRAS*, in press (astro-ph/0111376).

Martin, P., 1995, *AJ*, **109**, 2428.

Mulchaey, J. S., & Regan, M. W., 1997, *ApJ*, **482**, L135.

Sellwood, J. A. & Wilkinson, A., 1993, *Rep. Prog. Phys.*, **56**, 173. ¤

Johan Knapen (knapen@star.herts.ac.uk)

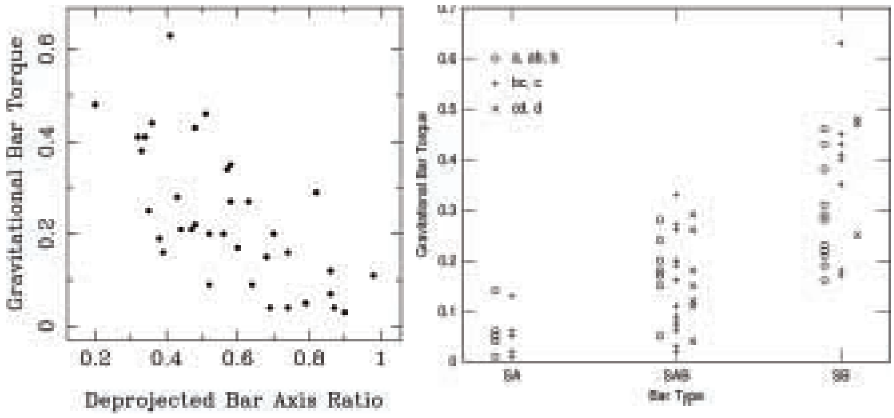


*Figure 4 (left). Bar strength plotted as a function of deprojected bar ellipticity, or bar axis ratio. From Block et al. (2001). Figure 5 (right). Bar strength plotted as a function of Hubble type for our sample galaxies. From Block et al. (2001).*

# Searching for Obscured Supernovae in Nearby Starburst Galaxies

Seppo Mattila (Imperial College), Robert Greimel (ING), Peter Meikle (Imperial College), Nicholas A. Walton (IoA), Stuart Ryder (AAO), Robert D. Joseph (IfA)

We are currently carrying out a $K_s$ band survey for core-collapse supernovae (CCSNe) in the nuclear (central kpc) regions of nearby starburst galaxies with the INGRID near-IR camera at the WHT. In this article we concentrate on describing mainly the observations and the real time processing of the SN search data, which makes use of the ING's integrated data flow system.

Very little is currently known about the behaviour of SNe in a starburst environment. The enhanced metallicity in starburst regions is expected to result in large mass-loss rates (Vink et al., 2001) for the SN progenitor stars. In addition, many of these events are expected to occur within molecular clouds (Chevalier & Fransson, 2001), adding further to the density of material surrounding the SN. Therefore, nuclear SNe can be expected to explode within a dense circumstellar medium. In general, a dense (but non-nuclear) circumstellar environment has been observed to produce bright CCSNe with slow near-IR light decline rates (e.g. SN 1998S, Fassia et al., 2000). However, the behaviour of SNe in nuclear starburst regions may be much more extreme (Terlevich et al., 1992). The high-$z$ CCSN surveys with the VLT, HST and NGST (e.g., Dahlen & Fransson, 1999; Sullivan et al., 2000) will use SNe to probe the cosmic star formation rate. For this, it is important to determine (i) a better estimate of the *complete* local CCSN rate (cf. Sullivan et al., 2000), (ii) a proper understanding of the behaviour of SNe within the dusty, high-density starburst environment and (iii) the extinction towards these events.

Most of the CCSNe in young starbursts like M 82 (Figure 1; Mattila & Meikle, 2001, 2002) are expected to be heavily obscured by dust, and therefore remain undiscovered by current SN search programmes working at optical wavelengths. However, in the near-IR $K_s$-band the extinction is greatly reduced and the sensitivity of ground-based observations is still good. That is why we are using INGRID to carry out an imaging survey of the

~40 most luminous nearby ($d < 45$ Mpc) starburst galaxies visible in the northern hemisphere. These galaxies have been selected to have far-IR luminosities greater than or comparable to those of the two prototypical starbursts, M 82 and NGC 253, but excluding galaxies whose far-IR luminosity is powered by a population of old stars or an AGN. The expected CCSN rates in these galaxies (Mattila & Meikle, 2001) range from around 0.05 yr$^{-1}$ in NGC 253 ($L_{\rm FIR} \sim 10^{10.3} L_{\odot}$ and 0.2 yr$^{-1}$ in NGC 4038/39 ($L_{\rm FIR} \sim 10^{10.8} L_{\odot}$) to around 1–2 CCSNe per year in Arp 299 ($L_{\rm FIR} \sim 10^{11.8} L_{\odot}$).

Since the average distance to our targets is ~30 Mpc, most of them fit well within one quadrant of the INGRID detector (2 arcmin × 2 arcmin). This enables us to observe most of the target galaxies using the *quadrant jitter* method in which the galaxy nucleus is placed in the middle of each quadrant of the array in turn. As the three other quadrants contain "empty" sky, the actual target frames can be used to create a sky frame for each of the galaxies and a sky flat field frame for the whole night. Thus, there is generally no need for offset sky images. This improves the observing efficiency allowing 2–3 galaxies to be observed per hour (with 10–20 minutes on-source exposure time each). The catch of a clear night is therefore 20–30 galaxy images in which nuclear CCSNe might be hiding. In Figure 2 we show four individual frames and the final combined frame of Arp 299, a luminous infrared galaxy at a distance of 45 Mpc, as an example of a *quadrant jitter* observation. In Figure 3 the $K_s$ image of another sample galaxy is shown, NGC 4038/39 (the Antennae, distance 20 Mpc). In general, to increase the number of frames and thus the total on-source exposure time per galaxy we perform a 4-point dither on each of the quadrants in turn. Therefore, a full quadrant jittering cycle produces typically 16 frames per galaxy, all with different offsets. When creating a sky frame the quadrants in which the galaxy is known to be are masked out. Thus the number of pixels which are median-combined to form a sky frame is 12. The observing procedure is simplified by the use of scripts which control the telescope/data acquisition sequence. The target quadrant identification is encoded into the object string in the image header, for subsequent use by the data pipeline.

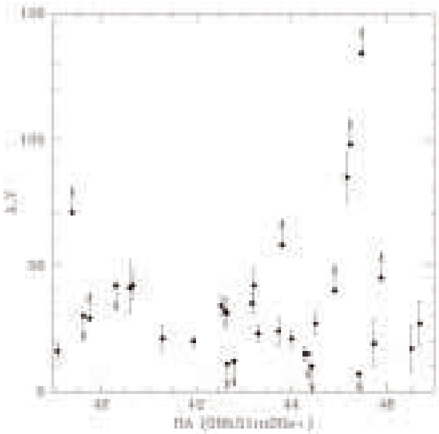

*Figure 1. Extinctions ($A_V$) towards 33 SNRs in M 82 (from Mattila & Meikle, 2001, 2002).*

*Figure 2. $K_s$ band images of Apr 299 (North is up and East to the left) obtained with INGRID at the WHT on January 2nd, 2002. Four quadrant jitter frames with 10×6 sec. exposure time are shown on the left, and the combined frame formed from 32 individual frames (32 minutes total exposure time) on the right. The intensity in the combined frame has a square root scaling.*

The full sampling of the seeing disk (FWHM ~ 0.7") by INGRID (0.24"/pixel) allows us to compare the reduced galaxy images to reference frames obtained earlier, using image subtraction. For this we use the Optimal Image Subtraction method (Alard & Lupton, 1998; Alard, 2000) which derives a convolution kernel to match the better seeing image to the image with the poorer seeing. It also matches the background differences. In Figure 4 we show an example of image subtraction using a pair of images of NGC 253 (distance ~3 Mpc) observed under different seeing and photometric conditions in August 2001 (FWHM = 0.9") and January 2002 (FWHM = 1.1"). Here, 21 different 5.7"×5.7" regions automatically selected by the image subtraction program were used for deriving the convolution kernel. The spatial variations of the INGRID PSF were modelled with a 2nd order polynomial and the differential background variations with a 1st order polynomial. The subtraction residuals are very small except for the two bright stars visible in the north-east and south-west from the nucleus. When the image subtraction is carried out with a constant kernel solution using just one

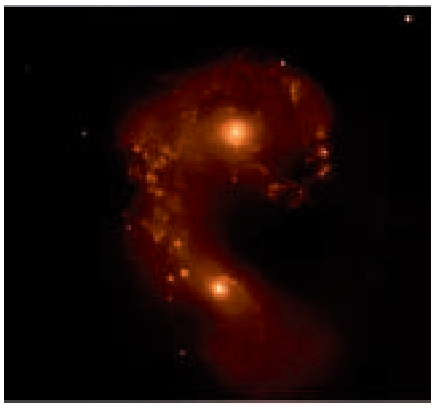

*Figure 3. $K_s$ band image of the Antennae, NGC 4038/39 (North is up and East to the left) obtained with INGRID at the WHT on January 2nd, 2002 (640 second exposure time).*

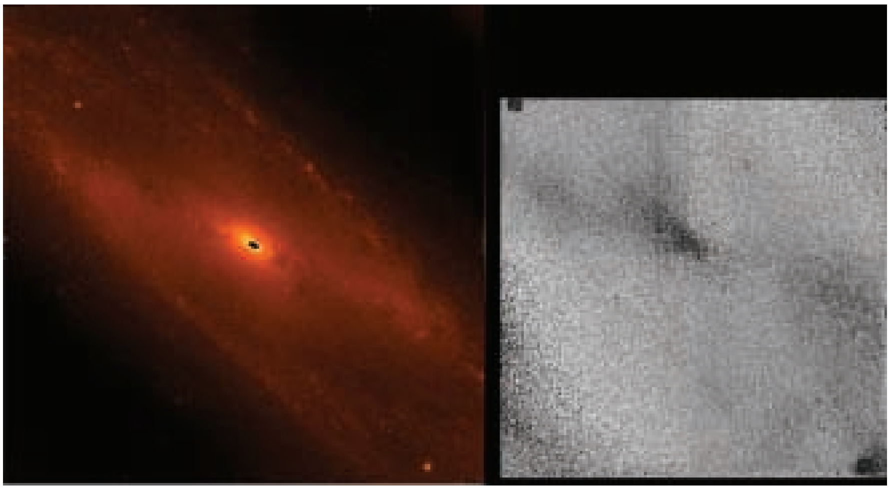

Figure 4. $K_s$ band image of NGC 253 (North is up and East to the left) obtained with INGRID at the WHT on August 31st, 2001 (300 second exposure time) is shown with a square root intensity scaling on the left. The result of image matching and subtraction is shown on the right.

region centred on the galaxy nucleus for deriving the kernel, a slight PSF variation between the frames over the INGRID field of view (4 arcmin× 4 arcmin) is visible. Such relative PSF variations can be caused by e.g. differential rotation between the two frames (Alard, 2000) as a result of imperfect image registration. More image subtraction examples and starburst galaxy images can be found at `http://astro.ic.ac.uk/nSN.html`.

The quick, effective reduction and analysis of the SN search data is essential for this programme to succeed. Therefore, the INGRID data taken in this project are pipeline-processed in near-real time at the telescope (see Figure 5). The IRAF-based pipeline runs on one of the Beowulf clusters at the telescope (Greimel et al., 2001). At the beginning of the observing run, calibration data is taken to generate a bad pixel mask and a dome flat field for the image processing. When a new image is taken by the Data Acquisition System it is automatically copied to the cluster and the post-pre image subtraction is done. An image grouping task then waits until all the exposures for a given galaxy have been taken before feeding the list of exposures to the next step. Once all the images for one object are on the cluster they are combined to give an initial sky frame. The images and the initial sky frame are then fed into a modified de-dithering routine (`idedither_qd`) from the INGRID quicklook package (`ingrid_ql`) in which the images are registered on a user defined star (this will be automated in future); a final sky image is created based on quadrant masking; then every image is sky subtracted, bad pixel masked and flat fielded; and the processed images are finally combined. The last processing step is to apply a World Coordinate System (WCS) solution based on the USNO catalogue to the combined image. At this point a data analysis task takes over. The new image of the object is compared with an archived image from previous runs. The rotation, shift and scaling are calculated for the image, based on user-selected stars. In the future this will be automatically done based on the WCS solution. The final step in the data analysis is the image subtraction using the Optimal Image subtraction software (ISIS) as described above. The subtracted images are then inspected by eye. In addition, the fully reduced search images are compared to the existing reference images by blinking. Apart from automating the various pipeline steps, we are also working on the implementation of a web-based interface for the pipeline which will allow easy steering of the pipeline as well as immediate access to the data by off-site collaborators. Having acquired a complete set of INGRID reference images we estimate a probable discovery rate of between 0.4 and 0.8 SNe in each clear night's observations (see Mattila & Meikle, 2001, 2002). The newly developed data processing pipeline for the on-going nuclear CCSN search on the WHT enables an easy real-time analysis of the search data. This is essential for the rapid follow-up observations of discovered SNe, in order to determine the nature of these events. Near-IR (*JHK*) photometry and spectra will probe both the conditions in the immediate circumstellar/interstellar environment of the SN and the line-of-sight extinction towards the SN. A large amount of near-IR imaging data still needs to be collected if we are to detect a sufficient number of obscured SNe to derive a statistically significant SN rate in nearby starburst galaxies. Therefore, we invite any observers who will be acquiring or have recently acquired *K*-band data of luminous nearby starburst galaxies to take part in the Nuclear SN search. Full details of this, and contact information, are given on the 'Nuclear SN Search' pages at `http://astro.ic.ac.uk/nSN.html`

We thank Johan Knapen and Petri Väisänen for advice and discussions on the observing technique. ¤

References:

Alard C., Lupton R. H., 1998, *ApJ*, **503**, 325.

Alard C., 2000, *A&AS*, **144**, 363.

Chevalier R. A. & Fransson C., 2001, *ApJ*, **558**, 27.

Dahlen T. & Fransson C., 1999, *A&A*, **350**, 349.

Fassia A. et al., 2000, *MNRAS*, **318**, 1093.

Greimel R., Lewis J. R., Walton N. A., 2001, *ING Newsl*, **4**, 9.

Mattila S., Meikle W. P. S., 2001, *MNRAS*, **324**, 325.

Mattila S., Meikle W. P. S., 2002, in The central kpc of starbursts and AGN: the La Palma connection, eds. J. H. Knapen, J. E. Beckman, I. Shlosman and T. J. Mahoney, *ASP Conf. Ser.*, **249**, 569.

Terlevich R., Tenorio-Tagle G., Franco J., Melnick J., 1992, *MNRAS*, **255**, 713.

Sullivan M., Ellis R., Nugent P., Smail I., Madau P., 2000, *MNRAS*, **319**, 549.

Vink J., de Koter A., Lamers H. J. G. L. M., 2001, *A&A*, **369**, 574.

Seppo Mattila (s.mattila@ic.ac.uk)

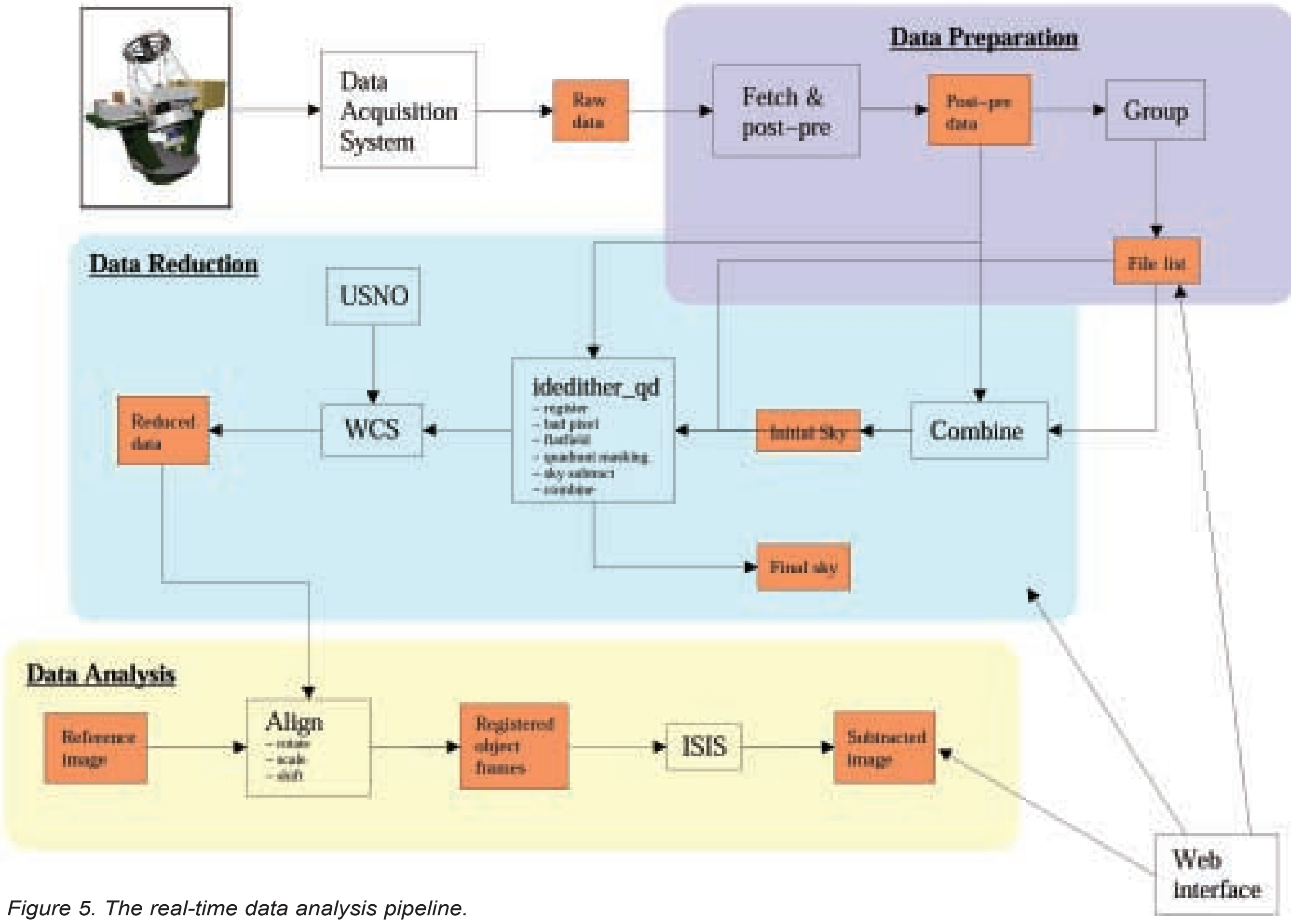


*Figure 5. The real-time data analysis pipeline.*

# The INGRID MDS ERO Survey

David Gilbank (University of Durham), Ian Smail (University of Durham), Rob Ivison (Astronomy Technology Centre), Chris Packham (University of Florida), Richard Bower (University of Durham)

We are taking advantage of the wide-field near-infrared imaging capabilities of INGRID on the WHT to construct a deep, wide area survey for Extremely Red Objects (EROs) in archival Hubble Space Telescope Medium Deep Survey (MDS) fields.

The last five years have seen a growing appreciation of the diversity of galaxy properties at $z \gtrsim 1-2$. In part this has come about from an impressive growth in our observational knowledge of galaxies at these redshifts —driven by the availability of powerful new instruments on 4- and 8-m class telescopes. However, an equal role has been played by the realisation of the necessity of a multi-wavelength approach to studies of galaxy evolution at $z \gtrsim 1$. Thus a range of surveys spanning wavebands from the X-ray, near- and mid-infrared, submillimeter and out to the radio, have complimented the traditional view based on UV/optical observations. These new studies have all tended to stress the role of dust obscuration in censuring our view of the galaxy population at high redshifts, and especially in disguising the extent of activity in the most active environments, both AGN and star-forming systems. This is much more of a concern due to the very strong evolution seen in obscured populations, which result in them dominating the bolometric emission at high redshifts (e.g. Haarsma et al., 2000; Smail et al., 2002).

One of the most striking themes to arise from this new multi-wavelength view of galaxy formation is the ubiquity of optically-faint, but bright near-infrared counterparts to sources identified in many wavebands: in the X-ray (Cowie et al., 2001; Page et al., 2001), the mid-infrared (Pierre et al., 2001; Smith et al., 2001), submillimeter (Smail et al., 1999; Lutz et al., 2001) and radio (Richards, 1999; Chapman et al., 2002). This has resulted in a renaissance in interest in such Extremely Red Objects —a class of galaxies which had previously been

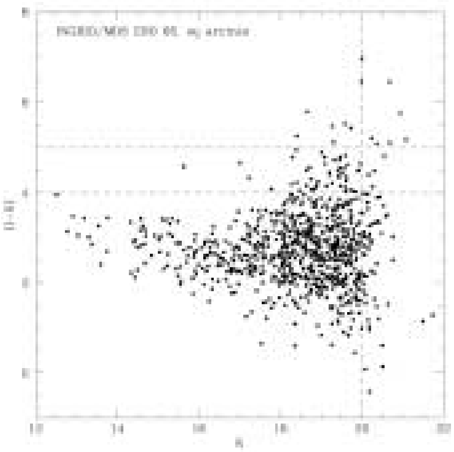

*Figure 1 (left). Preliminary I–K, K colour-magnitude diagram from 85 sq. arcmins of data from our survey. These data cover 17 HST WFPC2 fields — with typical integration times of 6.0 ks in the I (F814W) passband and 3.0 ks in the K-band with INGRID. The INGRID data for this survey was taken in typically good conditions, 0.5–0.9" FWHM, while the HST imaging has nominally 0.1" resolution, although poor signal to noise for the reddest galaxies targeted here, I-K$\gtrsim$4–5. We catalogue a total of 55 galaxies brighter than K=20 and redder than I–K=4, of which 7 are redder than I–K=5. The equivalent sample for the full survey will have around 170 and 20 respectively. Figure 2 (right). A "true colour" I/$K_S$ image of one of our fields. An extreme ERO, I–K>5, is visible to the south-east of the brightest star. Other (I–K>4) EROs are indicated by arrows. The unusual shape of the image arises from the coverage of the WFPC2 image. The field is ~4' in diameter — meaning that the WFPC2 field is completely covered by INGRID, irrespective of the roll angle of HST when the observations were taken. The image reaches 5σ point source sensitivities of K~20 and I~26.*

viewed as a curiosity with little relevance to our understanding of galaxy formation and evolution — comprising a mere 5–10 % of the population down to $K$=20.

The ERO class is photometrically-defined — one frequently used definition is $I–K \geq 4$ (or a more extreme selection of $I–K \geq 5$). This very red optical-near-infrared colour is intended to effectively isolate two broad populations of galaxies at $z \gtrsim 1$: those which are red by virtue of the presence of large amounts of dust (resulting from active star formation), as well as passive systems whose red colours arise from the dominance of old, evolved stars in their stellar populations. The very different nature of these two sub-classes, dusty starbursts and evolved ellipticals, has prompted efforts to disentangle their relative proportions (Pozzetti & Mannucci, 2000) so that well-defined samples can be used to test galaxy formation models (Daddi et al., 2000; Smith et al., 2002; Firth et al., 2002).

One particularly powerful approach is to use the morphology of the ERO to distinguish regular, relaxed ellipticals from disturbed and dusty starbursts.

A common misconception is that the key to a successful ERO survey is to obtain deep NIR imaging — in fact, the observationally most demanding aspect is achieving the necessary depth in the optical to identify that a galaxy is an ERO. For this reason, we have chosen to concentrate our survey on fields for which deep, high-quality archival optical imaging already exists. These fields come from the Medium Deep Survey (Griffiths et al., 1994) who have amassed over 500 deep HST/WFPC2 images of intermediate/high-Galactic latitude blank fields. These represent high-resolution (0.1") and very deep ($I$~27) images of random areas of extragalactic sky. Using a sample taken from the 100 deepest $I$-band MDS fields (covering an effective area of 500 sq. arcmin) we are able to obtain morphological information (sufficient to distinguish compact, regular evolved early-type galaxies from the more distorted starbursts) for galaxies as faint as $I$=25. Six nights of INGRID time in November 2000 and a further six in May 2001 have resulted in over 50 MDS fields being imaged in $K_s$ and more than 30 of these also in $J$, to 5σ limiting magnitudes of $K_s$=20 and $J$=22.5. It is thanks to the generous field of view of INGRID that such a survey is possible in a reasonable amount of telescope time. In contrast UFTI on UKIRT would take a factor of 3–4 longer to tile each MDS field. These data will form the basis of a sample of EROs with which we can undertake NIR spectroscopy on 8-m class telescopes, selected from an area an order of magnitude larger than the Cimatti et al. (2000) survey.

Preliminary results are shown in Figure 1. From 85 square arcmins, 55 EROs are found with $I–K \geq 4$ and 7 with $I–K \geq 5$. The samples from the full survey of 260 sq. arcmin will be 170 and 20 respectively. A colour image of one field made from INGRID data is illustrated in Figure 2. This survey is supported by the Leverhulme Trust. ¤

References:


Chapman, S. C., Lewis, G. F., Scott, D., Borys, C., Richards, E., 2002, *ApJ*, **570**, 557.

Cimatti, A., Villani, D., Pozzetti, L., di Serego Alighieri, S., 2000, *MNRAS*, **318**, 453.

Cowie, L. L., et al., 2001, *ApJ*, **551**, L9.

Daddi, E., Cimatti, A., Renzini,A., 2000, *A&A*, **362**, L45.

Firth, A. E., et al., 2002, *MNRAS*, **332**, 617.

Griffiths, R. E., et al., 1994, *ApJ*, **435**, L19.

Haarsma, D. B., Partridge, R. B., Windhorst, R. A., Richards, E. A., 2002, *ApJ*, **544**, 641.

Lutz, D., et al., 2001, *A&A*, **378**, 70.

Page, M. J., Mittaz, J. P. D., Carrera, F. J., 2001, *MNRAS*, **325**, 575.

Pierre, M., et al., 2001, *A&A*, **372**, L45.

Pozzetti, L., Mannucci, F., 2000, *MNRAS*, **317**, L17.

Richards, E. A., 1999, *ApJ*, **513**, L9.

Smail, I., et al., 1999, *MNRAS*, **308**, 1061.

Smail, I., Ivison, R. J., Blain, A. W., Kneib, J.-P., 2002, *MNRAS*, **331**, 495.

Smith, G. P., et al., 2001, *ApJ*, **562**, 635.

Smith, G. P., Smail, I., Kneib, J.-P., Davis, C. J., Takamiya, M., Ebling, H., Czoske, O., 2002, *MNRAS*, **333**, L16.


David Gilbank (D.G.Gilbank@durham.ac.uk)

# The COSMOS NIR Survey with INGRID

Marc Balcells, David Cristóbal-Hornillos, Mercedes Prieto (Instituto de Astrofísica de Canarias), Rafael Guzmán (University of Florida), Jesús Gallego, Angel Serrano, Nicolás Cardiel (Universidad Complutense de Madrid), Roser Pelló (Obervatoire Midi-Pyrenées)

Towards the end of the last decade, the international astronomical community realised that exploitation of the new generation of 8–10-m class telescopes would be hampered unless surveys of the sky with suitable depth were carried out. Spurred by this realisation, several observatories and research groups planned and established survey programs. Examples are the NOAO Deep Wide-Field Survey (`http://www.noao.edu/noao/noaodeep/`), the ING Wide Field Imaging Survey (`http://www.ing.iac.es/WFS/`), the DEEP project (`http://deep.ucolick.org/`), the CADIS survey (`http://www.mpia-hd.de/GALAXIES/CADIS/science_index.html`) and many others. Deep surveys aimed at the study of distant galaxies require NIR imaging in order to cope with the cosmological redshift of the galaxy spectral energy distributions (SEDs). In 2000 our group started a deep survey in the $K_s$-band using INGRID on the WHT and Omega Prime on the CAHA 3.5-m telescope. Our goal is to cover 0.5 square degrees of high-galactic latitude sky. Our target depth is $K_s=22$ in AB magnitudes. Good La Palma seeing and better noise behaviour allows us to reach this depth in 2 hr exposures with INGRID, the CAHA/Omega data being about 1 mag. shallower for equal exposure times. On the other hand, the wider field of Omega allows a faster coverage of sky area. Our survey, deemed the COSMOS Survey, thus has two depth regimes, $K_{AB}=21$ on a wide area and $K_{AB}=22$ on the deeper areas mapped with INGRID. This depth allows us to map luminous blue compact galaxies (LBCGs) with $M_B=-21.4$ out to $z=2.4$ ($H_0=70$) (Cristóbal et al., 2000).

Foremost in the science motivation for the COSMOS survey is to produce a database of distant galaxies for study with EMIR, the NIR multi-object spectrograph now in construction for the upcoming 10-m GTC on the ORM. EMIR is described in Balcells (1999 and 2000). Up-to-date information on the instrument is posted at `http://www.ucm.es/info/emir/`. Operating at cryogenic temperatures, EMIR will be one of the first spectrographs capable of performing multi-object spectroscopy in the 2.2-µm *K*-band. EMIR will allow us to efficiently obtain rest-frame visible spectra of large samples of galaxies at redshifts above 2, thus allowing the analysis of all the emission lines that have traditionally provided us with diagnostics on the excitation, extinction, star formation rates, metallicities, etc. of nearby galaxies.

Because of the $(1+z)^4$ cosmological surface brightness dimming, high-$z$ sources in the COSMOS survey will predominantly be luminous, compact, i.e. high surface brightness galaxies. Best known among these are star-forming galaxies for the ease with which they can be identified via *U*-band dropout and related techniques (Steidel et al., 1996). Such galaxies at $z\sim2$ will remain keys to understanding the rate of cosmic star formation when EMIR comes into operation. Of special interest is the possible connection of LBGs and other $z=3$ compact galaxies (Lowenthal et al., 1997) to luminous blue compact galaxies (LBCGs) found at $0.5<z<1$ (Guzmán et al., 1997). The COSMOS survey should also break ground in cataloguing galaxies without the strong star formation rates of Lyman-break galaxies. At $2<z<3$, current surveys, selected in the visible, sample the UV continuum and are biased toward actively star-forming galaxies. COSMOS is mapping rest-frame *R*, which is sensitive not only to luminous star-forming galaxies but also to luminous, massive galaxies harbouring old populations.

For galaxy selection, photometric redshifts and photometric characterisation of the sources we plan to use complementary data at visible wavelengths, which we are gathering via our own parallel surveys and via collaborative agreements with other groups.

Survey fields were selected for their high-galactic latitude, low cirrus emission, lack of bright stars, and perhaps most importantly for the availability of complementary data from HST and at other wavelengths. Our fields now include: the Groth field, including a strip of 28 deep, two-band, HST/WFPC2 pointings and its flanking fields; the Coppi field, containing a deep exposure with the Chandra X-ray satellite; one of the SIRTF First-Look Survey fields, and the Koo-Kron SA68 field. COSMOS will also observe equatorial fields such as the NOAO Deep Survey 2-hr field, to make use of existing public multi-band databases, and to allow spectroscopic studies with VLT and Gemini-S in addition to the GTC.

To date, data was obtained on runs in April 2000, October 2000 and June 2001. Our first run was part of the first science run of INGRID, soon after the camera commissioning. We are pleased to acknowledge a lack of technical problems, a smooth camera operation, and the high cosmetic quality of the images — not to mention the 0.7" FWHM seeing we obtained in the first 2-hr coadded images. We were then operating with the temporary collimator which gave reduced throughput, and, in the excellent seeing, gave a slightly non-circular PSF. These problems disappeared in 2001 using the definitive INGRID collimator. We were pleased by the ease with which the camera operation could be programmed using UNIX scripts, allowing us to prepare custom-made dithering patterns tailored to the geometry of our fields, or to readily program and execute long linearity calibration exposure sets. We note a single technical problem, which was eventually clarified with the ING staff: an inaccuracy (an offset of a fraction of a second) in the exposure times recorded in the headers during the first months of operation.

Data reduction for the Survey was carried out using IRAF. For sky subtraction, we found the `dimsum` task (Stanford, Eisenhard & Dickinson, 1998) particularly adequate. Our pipeline, while not fully automated, allows now for streamlined reduction of long observing runs, reaching flat-field accuracies of $6\times10^{-5}$ (peak-to-peak in the uniformly exposed areas). Our photometric calibration accuracy, in good atmospheric conditions, is typically 0.03 mag.

With INGRID, we have mapped the Groth strip, the Coppi field and a fraction of the SA68 field, for a total of 303 arcmin$^2$. Figure 1 shows a sample image from the Groth strip, together with the same field imaged in F606W with HST. The HST Groth images were obtained from the HST archive. We have performed source count and photometry using SExtractor (Bertin & Arnouts, 1996). Essential for deep galaxy photometry is to obtain reliable estimates of detection efficiency and spurious fraction (detection reliability). For the latter, we have developed a test, inspired on that used by Bershady et al. (1998), which we found more robust than tests based on injecting synthetic sources from eg. `artdata.mkobject` in IRAF. Our test relies on comparing photometry performed on two disjoint sets of co-added frames, each corresponding to half the total exposure time. Good detection of a given source in the two half-time images provides reliability that the source is real. A spurious source, in contrast, must come from a noise peak and therefore be detected on one of the two half-time images only. With this assumption, we deem spurious any detection in which the photometry in any one of the two half-time images is below a given $SN_{lim}$. To determine the value of $SN_{lim}$ that isolates truly spurious sources, we construct the histogram of magnitude differences between the measurements in the two half images. Values of $SN_{lim}$ that isolate spurious sources lead to a double-peaked histogram of magnitude differences, while values which do not, i.e. which include real sources, yield a histogram of magnitude differences with a single peak at $m_1-m_2=0$. Examples of magnitude difference histograms are shown in Figure 2.

Differential number counts in a 71 arcmin$^2$ area of Groth are shown in Figure 3. The area comes from six INGRID pointings, from which the edge areas with lower exposure time have been excluded. Similar counts were obtained for the 47 arcmin$^2$ mapped in the Coppi field. Our Groth counts bridge over the magnitude range between shallow, wide- area surveys, eg. Martini (2001) and deeper, pencil-beam surveys such as the one by Bershady, Lowenthal & Koo (1998). There is good continuity between the three sets of counts. Our counts in Coppi and Groth are quite close to each other. The counts stress earlier results that no-evolution models are inconsistent with the counts. At these depths, and for this cosmology, pure luminosity evolution (PLE) models provide a good fit to the counts. We reproduce a moderate excess at intermediate magnitudes over the PLE models, as found by Martini (2001).

Subsequent work on the COSMOS Survey includes covering a wider area until the target 0.5 degree$^2$ is reached. Progress on COSMOS may be followed at the EMIR web site, `http://www.ucm.es/info/emir/`. ¤

References:

Balcells, M., 1999, *Ap. Sp. Sc.*, **263**, 361.

Balcells, M. et al., 2000, *SPIE*, **4008**, 797.

Bershady, M. A., Lowenthal, J. D., Koo, D. 1998, *ApJ*, **505**, 50.

Bertin, E., Arnouts, S., 1996, *A&A*, **117**, 393.

Cristóbal-Hornillos, D. , Balcells, M., Prieto, M., Guzmán, R., 2001, *Astrophysics and Space Science Supplement*, **277**, 577.

Guzmán, R., Gallego, J., Koo, D. C., Phillips, A. C., Lowenthal, J. D., Faber, S. M., Illingworth, G. D., & Vogt, N. P., 1997, *ApJ*, **489**, 559.

Gardner, J. P., 1998, *PASP*, **110**, 291.

Martini, P., 2001, *AJ*, **121**, 598.

Stanford, S. A., Eisenhardt, P. R. M., Dickinson, M. E., 1998, *ApJ*, **492**, 261.

Steidel, C. C., et al., 1996, *ApJ*, **462**, L17.

Marc Balcells (balcells@ll.iac.es)

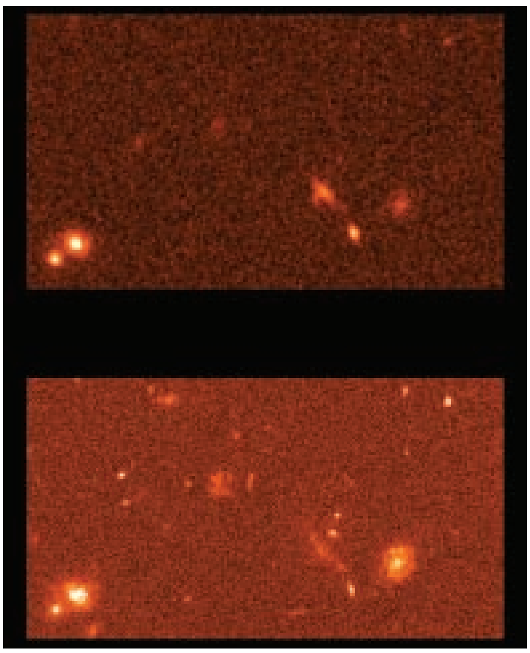

*Figure 1. An 11.4"x 5" field in the Groth stirp, imaged in the $K_s$ NIR band by INGRID (top) and in the F606W filter by HST/WFPC2. The INGRID exposure was 1.5 hr on-target integration. Seeing was 0.65" FWHM in the coadded image (pixel size 0.24 arcsec). On such images, we reach 50% detection efficiency at K~20.8. The low-inclination spiral in the lower left is clearly blue, while, next to it, an elongated object, seemingly another spiral, has pronounced redder colours.*

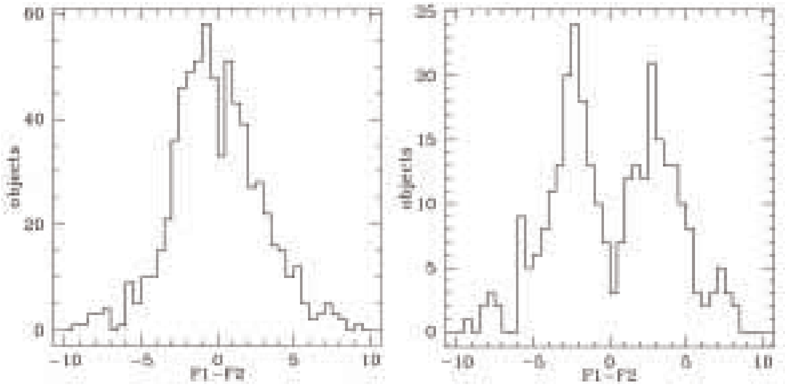


*Figure 2. Histograms used in identifying spurious sources. After `SExtractor` has produced a source catalogue from the total-exposure image, we perform photometry at the same source positions on two independent images, each from a coadd totalling half the total exposure time. We select sources for which the SN in any one of the two half-time measurements is lower than a given $SN_{lim}$, and plot the histogram of magnitude differences $m_1 - m_2$. The first histogram used $SN_{lim}=2.8$; the single peak indicates that the $SN_{lim}=2.8$ cutoff selects many sources for which $m_1 - m_2 \sim 0$, two independent measurements consistent with each other which indicate that the sources are real. The second histogram used $SN_{lim}=1.6$; the double peak indicates that $SN_{lim}=1.6$ correctly isolates spurious sources.*

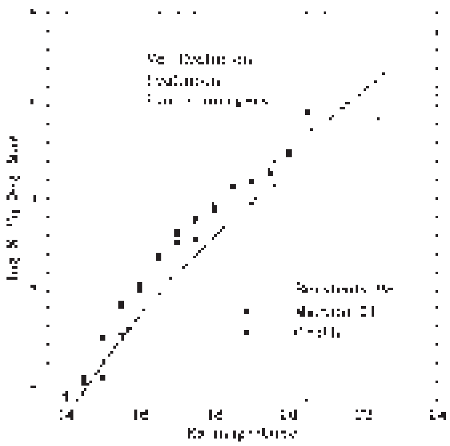

*Figure 3. Number counts obtained on the Groth strip. The figure gives number of galaxies per square degree per magnitude interval. Counts are corrected for efficiency and for spurious sources. Efficiency correction is performed only for magnitude bins with a detection efficiency above 50%. Error bars are 1-σ upper- and lower-confidence intervals (84.13% confidence level). Superimposed on the counts are three reference number count predictions, which we derive using `ncmod` (Gardner, 1998).*

# Satellites and Tidal Streams Conference

We are pleased to announce the conference “Satellites and Tidal Streams”, organised by the Isaac Newton Group of Telescopes (ING) and the Instituto de Astrofísica de Canarias (IAC), to be held on the island of La Palma on May 26–30, 2003.

Current cosmological models predict that galaxies form through the merging of smaller substructures. Satellites and tidal streams might then represent the visible remains of the building blocks of giant galaxies. They therefore provide important information on the merging history and galaxy formation in the Universe. In this conference the observational evidence for substructures, their internal structure and their dynamical evolution and disruption within the tidal field of the host galaxy will be discussed and confronted with theoretical cosmological predictions of hierarchical merging and galaxy formation. Topics that will be discussed include: satellites of galaxies: bright and dark, the dark matter content of dSph and LSB galaxies, tidal streams: probes of the structure and formation of the Milky Way and other Nearby Large Galaxies, predictions of Cold Dark Matter models on small scales, compact HVCs and galactic substructure and mass substructure from gravitational lensing.

To achieve these goals, invited reviews and talks given by leading scientists in all the fields above are planned, as well as a number of contributed talks and posters presenting the recent results from the relevant fields. A preliminary list of invited speakers is: R. Braun (NFRA, The Netherlands), A. Burkert (MPIA, Germany), E. Grebel (MPIA, Germany), R. Ibata (Observatoire de Strasbourg, France), M. Irwin (IoA, UK), K. Johnston (Wesleyan University, USA), A. Klypin (NMSU, USA), D. Lynden-Bell (IoA, UK), S. Majewski (University of Virginia, USA), M. Mateo (University of Michigan, USA), B. Moore (University of Zurich, USA), J. Primack (University of California at Santa Cruz, USA), P. Schneider (Bonn University, Germany), S. White (MPA, Germany), R. Zinn (Yale University, USA).

You will find more information on the conference web site at: `http://www.iac.es/proyect/sattail/`

Registration opens on Thursday November 14th. The deadline for registration is April 1, 2003. The list of speakers, posters, etc. will be finalized after this deadline. Note that the total number of participants will be limited to 120. ¤

Francisco Prada and David Martínez-Delgado, *Co-chairs SOC* (sattail@iac.es)

SCIENCE

# Quasar Redshifts from S-CAM Observations: Direct Colour Determination of ~12 Gyr-Old Photons

Jos H. J. de Bruijne[1], A. P. Reynolds[1], M. A. C. Perryman[1,2], A. Peacock[1], F. Favata[1], N. Rando[1], D. Martin[1], P. Verhoeve[1], N. Christlieb[3]

*1: Research and Scientific Support Department of the European Space Agency. 2: Sterrewacht Leiden. 3: Hamburger Sternwarte*

CCDs have revolutionised astronomy in the last quarter of the 20th century, yet measuring energy distributions of celestial objects still requires the indirect methods of filter photometry or dispersive spectroscopy. The development of superconducting tunnel junction (STJ) detectors (Perryman et al., 1993; Peacock et al., 1996, 1997) has opened up the possibility of measuring individual optical photon energies directly. The first time-and spectrally-resolved observations of cataclysmic variables and pulsars using these techniques have been reported (e.g., Perryman et al., 1999, 2001; Bridge et al., 2002), and the first direct measurements of the redshifts of quasars using an imaging detector with intrinsic energy resolution were published early this year (de Bruijne et al., 2002; cf. `http://astro.esa.int/SA-general//Research/Detectors_and_optics/`).

## Observations

We observed 11 Lyman-limit quasars, selected from the literature in the range $z=2.2-4.1$, using S-Cam2 (Rando et al., 2000) on the William Herschel Telescope in October 2000. S-Cam 2 is a 6×6 imaging array of $25{\times}25\,\mu\text{m}^2$ ($0.6{\times}0.6$ arcsec$^2$) tantalum junctions, providing individual photon arrival times to ~5 µs, a resolving power of $\Re\sim 8$ at 500 nm, and a high sensitivity from the atmospheric cutoff to ~720 nm (this cutoff is currently set by long-wavelength filters which reduce thermal noise photons). All targets show strong Ly-α and CIV emission lines which, at redshifts ~2–4, fall in our wavelength response range.

Information on each detected photon consists of arrival time, coordinates of the junction, and an energy channel $E$ in the range 0–255. Laboratory measurements have confirmed that all junctions have a highly linear energy response, so that an incident photon of energy $E_p$ is assigned to an energy channel $E \sim 42.5 \cdot E_p[\text{eV}] - 2.0$ (de Bruijne et al., 2002).

## Results

We determined quasar redshifts $z$ by fitting the calibrated observed energy distributions with a single template HST quasar spectrum, i.e., by minimising the function $\chi^2(z)$ (de Bruijne et al., 2002). Examples of observed and modelled spectra are shown in Figure 1. The overall shape of these spectra, in particular the falloff at low energy channels (long wavelengths), is due to the combined response of the instrument and telescope. In practice, the Ly-α line and the associated break at shorter wavelengths contribute most to the redshift determination.

Figure 2 compares the best-fit redshifts with the literature values. QSO 0127+059 is our single prominent outlier. It was discovered in a thin prism survey, classified as a possible quasar, and tentatively assigned a redshift of $z\approx 2.30$ with a questionable line identification. Our fit provides a good representation of the data (Figure 1), yet the derived redshift, $z=2.976$, differs significantly from the literature value. We therefore obtained a spectrum of this object with the Siding Spring Observatory 2.3-m telescope, from which a redshift $z=3.04$ was deduced, in excellent agreement with our estimate!

As all fits have reduced $\chi^2 \gg 1$, none of them is formally acceptable. The general consistency between the models and the observations, combined with the pronounced, deep and narrow, minima in all $\chi^2(z)$ plots, nonetheless indicates that our model fits the data well. Small systematic errors related to, e.g., template mismatch, are, although largely hidden due to the limited detector resolution, the key to this paradox (de Bruijne et al., 2002).

## Discussion

Pronounced $\chi^2(z)$ minima are already present in our data truncated *a posteriori* to observation times as small as, e.g., 10–20s for QSO 0000–263 ($z=4.1$; $V$=17.5 mag), where ~350 source photons s$^{-1}$ were recorded (Figure 3). We therefore conclude that efficient low-resolution spectroscopy of faint extragalactic sources is possible with STJ devices, enabling the determination of redshift. Extraction of detailed physical information from the spectra presented here is limited by the modest resolving power of S-Cam2 ($\Re\sim 8$). A significant improvement in energy resolution is,

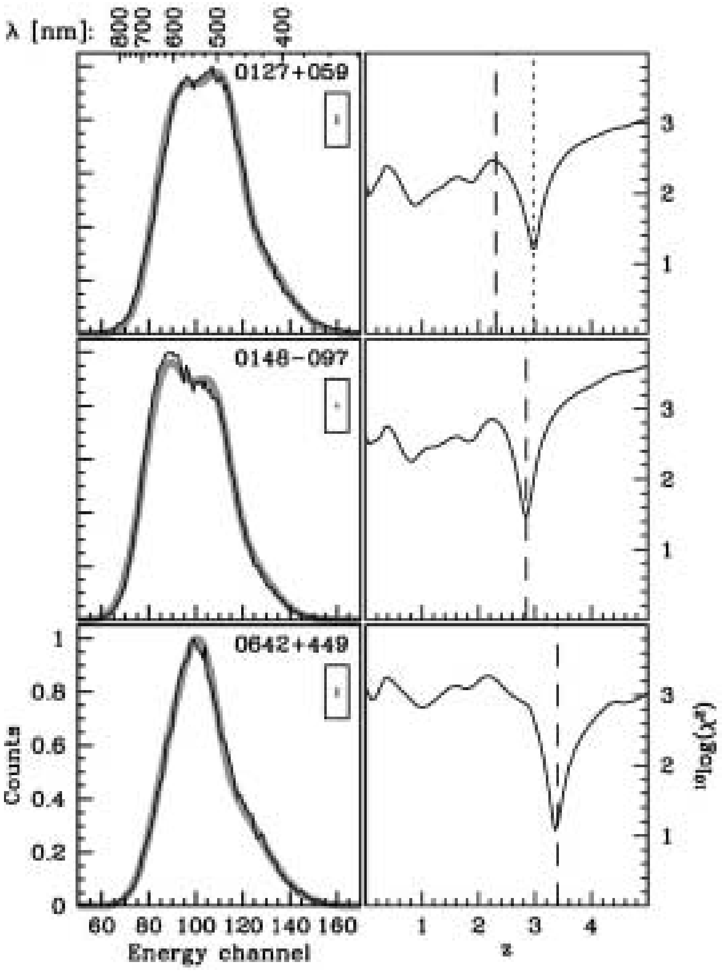


*Figure 1. Results for QSO 0127+059, 0148−097, and 0642+449. Left: observed (black) and modelled (grey) energy channel distributions (arbitrary units). Our model is based on a single template HST quasar spectrum. Insets indicate the Poisson noise. Numbers above the top left panel show the mapping between energy channel and wavelength. Right: the corresponding dependence of $\chi^2$ on z. Vertical dashed lines indicate the literature redshifts; the dotted line for QSO 0127+059 indicates z = 3.04 (see text).*

however, foreseen in the future (e.g., Rando et al., 2000), promising enhanced physical diagnostic capabilities. It has, for example, been shown that an STJ detector with $\Re \sim 20$ would allow the determination of galaxy morphological type and perhaps emission and absorption line ratios (Jakobsen, 1999; Mazin & Brunner, 2000).

STJ instrument development within ESA is currently also aimed at producing larger format arrays, to facilitate sky subtraction and possibly allow for multi-object spectroscopy, and at extending the wavelength response further to the red. The latter objective, which is consistent with the fundamental device response characteristics, would open up a larger accessible redshift range.

## Acknowledgments

We acknowledge the ING staff for their excellent support during the S-Cam observing campaigns. ¤

References:

Bridge, C. M., et al., 2002, *MNRAS*, submitted.

de Bruijne, J. H. J., et al., 2002, *A&A*, **381**, L57.

Jakobsen, P., 1999, in *ASP Conf. Ser.*, **164**, 397.

Mazin, B. A., Brunner, R. J., 2000, *AJ*, **120**, 2721.

Peacock, A., et al., 1996, *Nature*, **381**, 135.

Peacock, A., et al., 1997, *A&AS*, **123**, 581.

Perryman, M. A. C., et al., 1993, *Nuc. Inst. Meth. A*, **325**, 319.

Perryman, M. A. C., et al., 1999, *A&A*, **346**, L30.

Perryman, M. A. C., et al., 2001, *MNRAS*, **324**, 899.

Rando, N., et al., 2000, in *SPIE Proc.*, **4008**, 646.

Jos de Bruijne (Jos.de.Bruijne@esa.int)

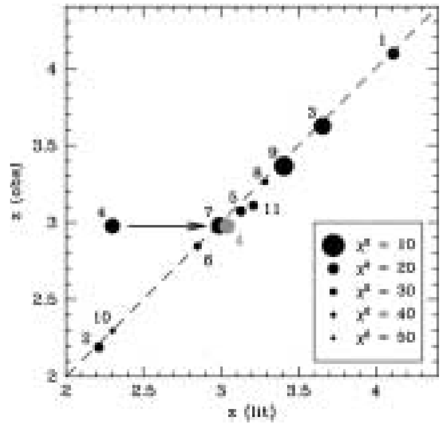

*Figure 2. Observed versus literature redshifts. Numbers refer to the objects (de Bruijne et al., 2002). Symbol sizes correspond to $\chi^2$; smaller symbols indicate a poorer fit. QSO 0127+059 has an incorrect literature redshift of 2.30; follow-up spectroscopy has yielded z = 3.04, moving the point to the position shown in grey. The dashed line shows the 1:1 correlation.*

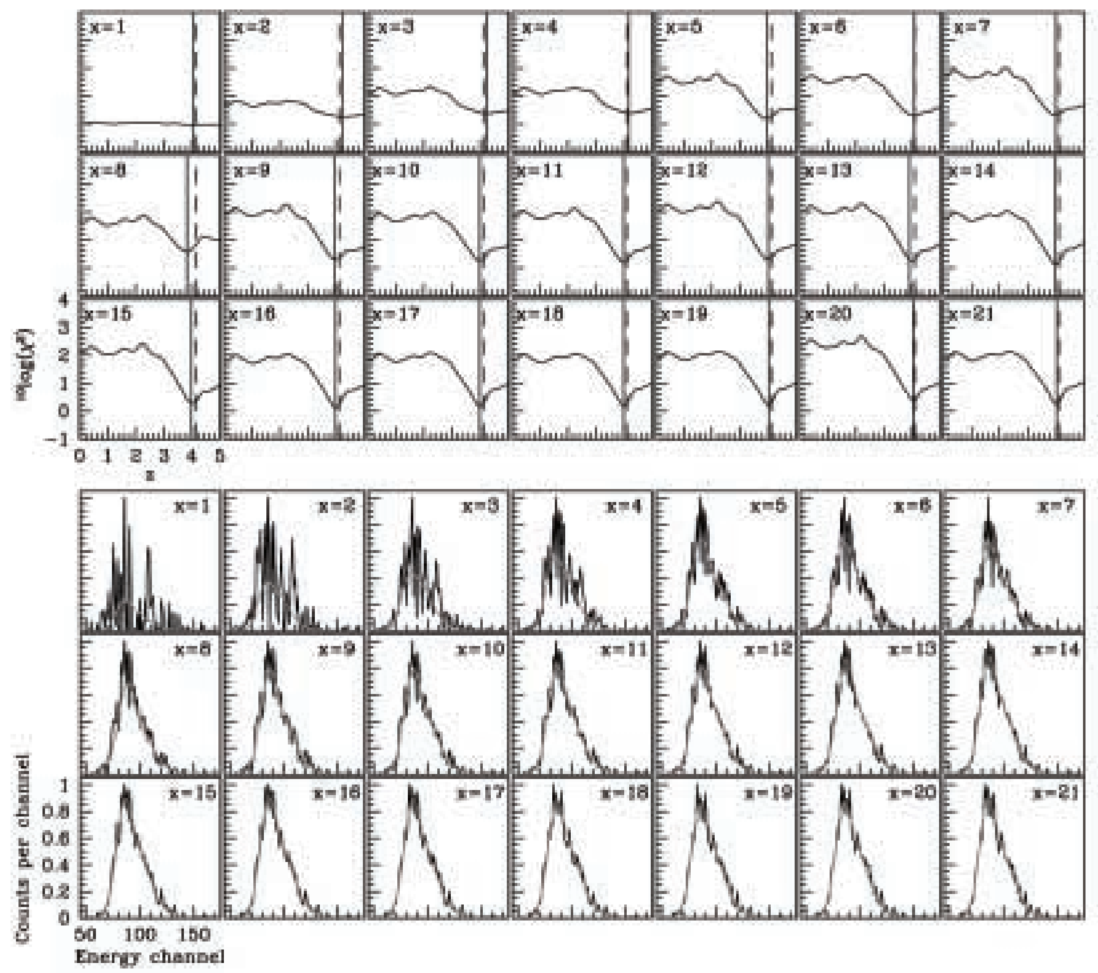


*Figure 3. Top: $\chi^2(z)$ using the first $x = 1,...,21$ seconds of data of QSO 0000−263 ($z = 4.1$). The dashed and solid lines indicate the literature and best-fit redshifts, respectively. Bottom: as top panels, but showing the observed QSO spectra (black) and best-fit models (grey). Panels have differing vertical scales.*

# The CIRSI-INT IR Survey

R. G. Sharp, R. G. McMahon, S. Hodgkin and C. D. Mackay (Institute of Astronomy, University of Cambridge)

*Note from the editor: article received in March 2002*

The Isaac Newton Telescope has been used in conjunction with the Cambridge InfraRed Survey Instrument (CIRSI), to undertake a wide area deep IR survey in the *J* and *H* bands. This article gives a brief introduction to the survey and presents some initial results. In the spirit of the INT Wide Field Camera Survey program (Walton et al., 2001; `http://www.ing.iac.es/Astronomy/science/wfs/`; `http://www.ast.cam.ac.uk/~wfcsur/`) we are making reduced data products publicly available. A preliminary data release is planned for April 2002 with a complete release planned in the Summer 2002. The survey observations have been used in conjunction with optical CCD data from the INT Wide Angle Survey to undertake a survey for low and intermediate redshift quasars ($z < 3$) free from the potential biasing effect of dust absorption. The results of these observations are reported to illustrate the utility of the survey data for combined optical-IR survey projects.

## CIRSI-INT IR Survey

With a field of 4×7.80'×7.80' at the prime focus of the 2.5m Isaac Newton Telescope, the Cambridge InfraRed Survey Instrument, CIRSI (Mackay et al., 2000), is currently the largest field of view IR imager in operation. The camera, a mosaic of 4 Rockwell HgCdTe HAWAII IR arrays, is capable of observing in the *J* and *H* bands at the INT. The physical construction of the detector arrays prevents them being butted together

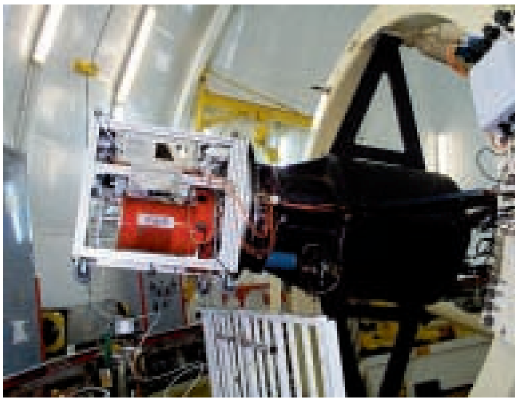
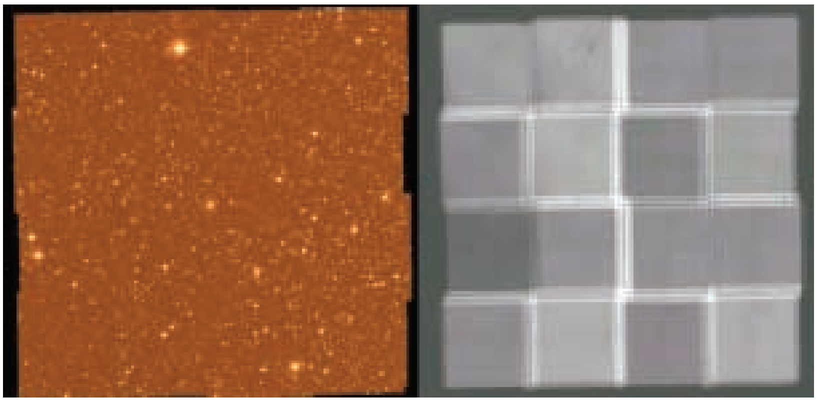

*Figure 1 (left). CIRSI at the prime focus of the 2.5m INT. Figure 2 (right). The image to the left is a 29.6'×29.6' mosaic of four poinitngs of the CIRSI camera. To the right the weight map associated with the mosaic is shown.*

in close proximity as is normal for optical CCD mosaic cameras. There is a 90% spacing between the elements of the mosaic. Sequential observations are offset to fill the gaps in the mosaic. A 4 pointing tile of observations covers an area of 29.6'×29.6'. Figure 2 demonstrates the camera layout.

The nominal survey depths attained are $J$<20.0, $H$<19.0 roughly three magnitudes deeper than the level attained by the 2MASS project. Details of the fields observed are given in Table 1. The survey observing strategy consists of ~350 sec exposures. Depending on sky brightness conditions during observations the exposure is built up from a sequence of 4 (or 5) dither positions with 4 (or 3) exposures of 22 s (or 30 s) duration at each position. Approximately 5 Gb of data are obtained a night. Data processing is performed using pipeline processing software developed in Cambridge (Sabbey et al., 2001).

| Field | RA Dec (J2000) | Depth | Extent |
|---|---|---|---|
| INT WAS ISO ELAIS N1 | 16:10 +54:30 | J<20.0, H<19.0 | 7 deg$^2$ |
| INT WAS ISO ELAIS N2 | 16:37 +41:16 | J<20.0, H<19.0 | 7 deg$^2$ |
| INT WAS NGC | 14:52–14:58 +00:00 | J<20.0 | 3 deg$^2$ |
| INT WAS SGC | 22:00–22:16 +00:00 | J<20.0 | 2 deg$^2$ |

*Table 1. Survey regions and observational data available. The North and South Galactic Cap regions (NGC/SGC) are coincident with the recently released SDSS zero declination strip observations.*

## INT WAS Data

The fields targeted by the CIRSI-INT survey program are chosen to be coincident with observations from the INT Wide Angle Survey project (McMahon et al., 2001). The INT WAS fields surrounding the ISO ELAIS N1 and N2 fields at 1610+54 and 1637+41 have been extensively observed in the $J$ and $H$ bands and observations have also been undertaken in the $J$ band of the zero declination strips at RAs of 14:55 and 22:08, coincident with the recent data release from the Sloan Digital Sky Survey (SDSS).

## Example Science: Reddening Independent Quasar Selection

It has long been known that absorption by dust, if present either along the line of sight to quasars or within the quasar host galaxies themselves, could bias samples of quasars selected primarily on the bases of ultraviolet excess (UVX). Figure 3 demonstrates the predicted effects of dust reddening on UVX selection of quasars. Two of the quasars identified in the CIRSI-INT sample for which $U$ band observations are currently available do not show a UV excess. There are a number of reasons to endeavor to construct a quasar sample free from a bias against dusty quasars. Two examples are the following:

– There is an apparent lack of high column density ($\log N(HI) > 21 cm^{-2}$) damped Lyman-α (DLA) quasar absorption systems observed with high metallicity (Boisse et al., 1998). If the dust within DLA absorption systems themselves is responsible for reddening quasars then more evolved DLA hosts with higher metallicities could well be expected to exhibit higher dust content and greater dust obscuration of the background quasar, preventing the most evolved DLA systems from being discovered.

– Dust may bias quasar lensing statistics (Kochanek, 1996). If the identification of quasars is biased against objects lensed by dusty lenses then any model associated with the population of lensed quasars is also biased. Recently multiply imaged lensed quasars have been used to study the structure of distant galaxies by detailed studies of quasar absorption line systems. If lensed quasar samples are biased against dusty lens then these studies will only investigate systems with little dust.

Figure 4 illustrates the principle of the $gzH$ colour selection technique developed for defining quasar candidates. The principle is similar to the $VJK$ selection method proposed

| | |
|---|---|
| Pixel scale (arcsec/pixel) | 0.46 |
| FOV per chip | 7.8' × 7.8' |
| FOV for 2×2 mosaic | 29.6' × 29.6' |
| Frames/deg$^2$ | 16 |
| J, 5min 5σ in 1.2" seeing | 20.0 |
| H, 5min 5σ in 1.2" seeing | 19.0 |

*Table 2. CIRSI Characteristics on 2.5-m Isaac Newton Telescope.*

by Warren, Hewett & Foltz (2000), however, observations are required in only one *IR* band. A preliminary quasar identification has been undertaken by Sharp et al. (2002). 68 candidate quasar are identified in data taken from a subset of 0.7 deg$^2$ of the available survey area. Spectroscopic observations of 32 targets have been obtained confirming 22 quasars, a success rate of 65%. Observations are currently available across the *ugrizJ* and *H* bands for a sub set of the quasars identified. The *ugr* colour diagram, analogous to the traditional UVX quasar colour selection scheme, is shown in Figure 3. Two of the newly discovered quasars show no UV excess at all. ¤

References:


Boisse, P., Le Brun, V., Bergeron, J., Deharveng, J., 1998, *A&A*, **333**, 841.

Boyle, B. J., Shanks, T., Croom, S. M, Smith, R. J., Miller, L., Loaring, N., Heymans, C., 2000, *MNRAS*, **317**, 1014.

Kochanek, C. S., 1996, *ApJ*, **466**, 638.

Mackay, C. D., McMahon R. G., Beckett, M. G., Gray, M., Ellis, R. S., Firth, A. E., Hoenig, M., Lewis, J. R., Medlen, S. R., Parry, I. R., Pritchard, J. M., Sabbey, C. S., 2000, *SPIE*, **4008**, 1317.

McMahon, R. G., Walton, N. A., Irwin, M. J., Lewis, J. R., Bunclark, P. S., Jones, D. H., 2001, *NewAR*, **45**, 97.

Sabbey, C. N., McMahon, R. G., Lewis, J. R., Irwin, M. J., 2001, *ASP Conf. Ser.* , **238**, 317.

Sharp, R. G., McMahon, R. G., Irwin, M. J., Hodgkin, S. T., 2001, *MNRAS*, **326**, L45.

Sharp, R. G., Sabbey, C. N., Vivas, A. K., Oemler, A. Jr., McMahon, R. G., Hodgkin, S. T. and Coppi, P. S., 2002, *MNRAS*, submitted.

Walton, N. A., Lennon, D. J., Irwin, M. J., McMahon, R. G., 2001, *ING Newsl.*, **4**, 3.

Warren, Hewett & Foltz, 2000, MNRAS, 312, 827.


Robert Sharp (rgs@ast.cam.ac.uk)

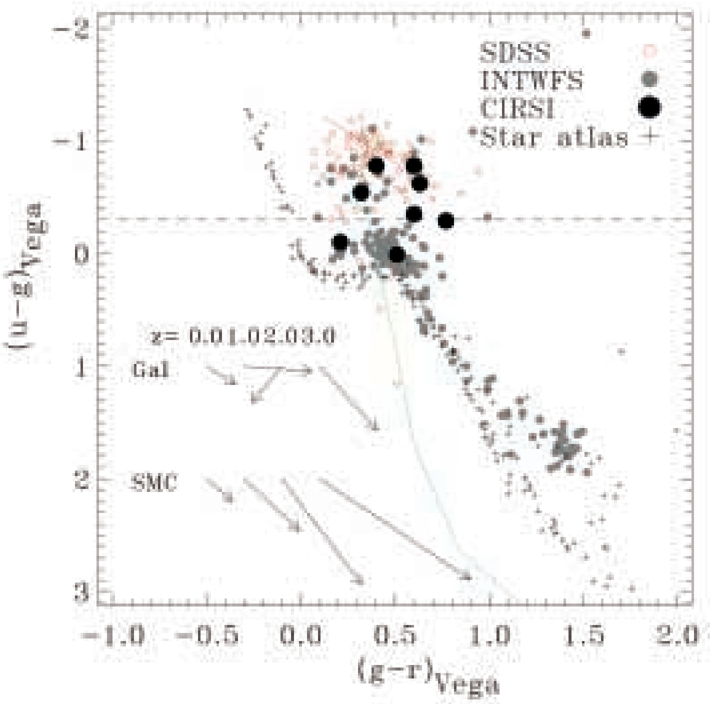


*Figure 3. A comparison is shown of a sample of previously known quasars identified in the SDSS. The new quasars identified by gzH selection for which ugr data is available from the INT WAS are marked with filled circles. The horizontal line at $u-g=-0.3$ represents a UVX selection boundary analogous to that used in the 2dF quasar survey (2QZ Boyle et al., 2000). The stellar locus, computed from a spectral atlas, is shown along with stellar objects from a field of the INT WAS. The locus of quasar colour as a function of redshift is indicated by the solid line. The onset of absorption in the g band, due to the Lyman-α forest, is evident for quasars with $z>3$. Reddening vectors for dust models based on the Galaxy and the Small Magellanic Cloud are shown over a range of redshifts. The 2175Å feature in the galactic law passes through the g band over the range $1<z<2$.*

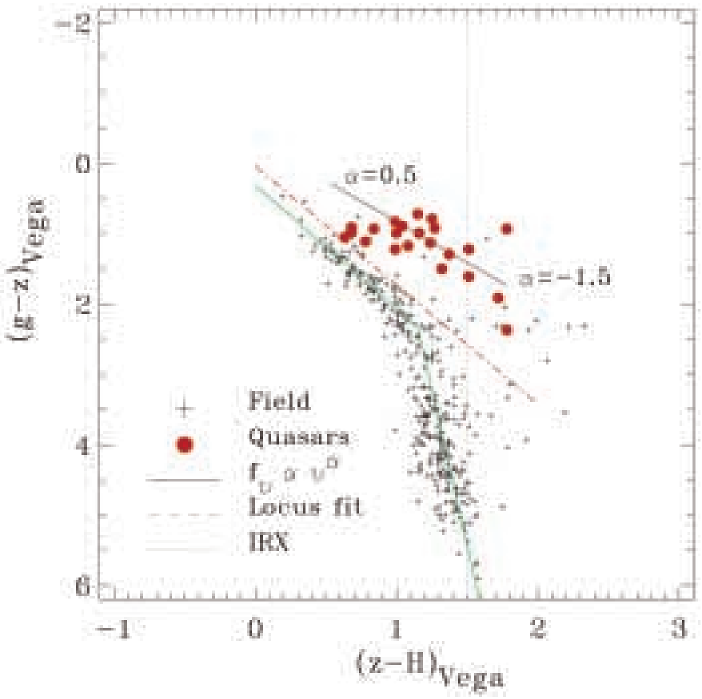


*Figure 4. The candidate selection diagram for a 0.17deg$^2$ region of the survey is shown with the full quasar sample overlaid. The selection boundary, chosen based on model quasar colours, is indicated by the broken line offset from the linear fit to the stellar locus.*

# TELESCOPES AND INSTRUMENTATION

## The ING Telescopes in a Changing Landscape

René G. M. Rutten (Director, ING)

Landscapes in geological terms tend to change slowly, unless there is a land slide. With the UK joining ESO the focus of UK ground-based astronomy will change in a dramatic way as well, strengthening its European focus. On December 5th 2001 PPARC Council took a number of important decisions related to the UK joining ESO. These decisions will have a profound impact on various existing facilities, including those of the ING. PPARC's way forward reflects the reality of the rapidly changing environment of ground-based astronomy, with the deployment of several 8-m class telescopes and the adhesion of the United Kingdom to the European Southern Observatory. Further reference to the Council's decision can be found in this PPARC press release `http://www.pparc.ac.uk/NW/ /ESOstars.asp`.

### Impact of Budget Reductions

It has been apparent for some time that the annual operating budget for ING would come under pressure, in particular as the UK has to free up funds to contribute towards the annual cost of joining ESO. Over the past year, plans have been developed on how ING could be operated within a reduced budget. Central in these plans is the improved collaboration with the Instituto de Astrofísica de Canarias. The ING Board has played a very active role in securing an agreement of principles of how in the future PPARC, NWO and the IAC could collaborate in the operation of the ING. The decision from PPARC Council is in line with these plans.

The key elements of the changes that these plans entail are presented here. Probably the most important change is presented by the fact that the Instituto de Astrofísica de Canarias will become a full partner in ING as of 2002. An agreement was reached, with strong support from the ING Board and the UK and NL funding agencies, on the terms under which the IAC would join in the operating costs of ING. This agreement significantly alleviates the impact of the budget reductions announced by PPARC and allows ING to remain a strong and vibrant organisation that can deliver quality service to its user community. The tight collaboration with the IAC is of strategic importance as this institute fulfills a pivotal role in the development of the observatory site, in particular with the construction of the 10-m GRANTECAN and its plans to create a European collaboration for observing facilities in the Northern hemisphere. Moreover, the IAC is developing a new observatory centre at sea level on La Palma, in which the ING will participate. But nevertheless, the future budget available to ING for the operation of the telescopes will reduce by more than 30%, in spite of the additional contribution of the IAC. The IAC's contribution will commence in 2002, and the Netherlands will leave its annual contribution largely unchanged. This large decrease in the operational budget and the change of balance between the international partners implies a number of important changes, that can be summarised as follows:

1. Balance of Observing Time

The balance of observing time will gradually change over the following years. The agreed percentage breakdown of observing time will be as follows (see Table 1).

2. Service Observations

The existing scheme of service observations that are carried out by observatory personnel will be discontinued on the JKT from the end of semester 02A and on the INT from the end of semester 03A. On the WHT service observation will remain available.

3. Use of the JKT and INT

The JKT will be taken out of normal service as of September 2003. Possibly this telescope will continue as a special-purpose telescope with external funding. But if no additional resources can be found the JKT will close. It is the intention to review the longer term future of the INT before the end of 2004. By that time various other telescopes will be carrying out imaging surveys and the Liverpool telescope will be well established, making it timely to review the scientific use of the INT. Until that time, operation of the INT will have to be carried out at a lower cost. Cost saving measures envisaged are to operate the INT with

| | 2001 | 2002 | 2003 | 2004 | 2005–9 |
|---|---|---|---|---|---|
| UK | 60.0 | 54.0 | 50.0 | 48.9 | 47.6 |
| NL | 15.0 | 15.0 | 15.9 | 17.0 | 18.3 |
| CAT Spanish additional time | 0.0 | 6.0 | 9.1 | 9.1 | 9.1 |
| CAT Spanish time | 20.0 | 20.0 | 20.0 | 20.0 | 20.0 |
| CCI international time | 5.0 | 5.0 | 5.0 | 5.0 | 5.0 |

*Table 1. Percentage breakdown of observing time.*

only the Wide Field Camera from some time in 2003 onwards, and at the same time fully withdraw telescope operator support from that telescope.

4. Use of the WHT

The focus of support and development will shift fully towards the WHT in order to keep that telescope as attractive as possible to the community. Although scheduling flexibility and instrument changes may have to be more strictly limited, the service delivered will be enhanced through the introduction of queue observing mode for up to 30% of the time on the WHT. Primarily queue observing will focus on adaptive optics observations.

5. A Common-User IR Imager and Spectrograph

As part of the agreement with the IAC, the LIRIS IR imager and spectrograph that is currently being developed at the IAC will be made available to the general user community for at least 3 years after commissioning and acceptance. Commissioning of LIRIS is anticipated to take place at the beginning of 2003. Given the popularity of ING's IR imager, we expect that this new instrument will attract much interest from the user community.

The changes mentioned above focus on the impact that the budget reductions will have on the use of the telescopes. Not mentioned here are the complex internal changes that will be implemented and cost saving measures in the way ING operates. It is our intention to minimise the disruption to normal day-to-day operation of the telescopes as much as possible, and ING remain dedicated to deliver the best possible service to our user community.

## Collaboration Between Observatories

In the European astronomical arena international collaborations are emerging between national facilities. These collaborations have been promoted and supported by the OPTICON European network, which combines astronomers from many European countries and is funded through the EU (see `http://www.astro-opticon.org`). An important driver for setting up collaborations between observatories is the wish to make the best instruments available to the wider community of astronomers for the advancements of our science, and to make the existing facilities work more efficiently in the process. Duplication of instrumentation with the consequential costs could be avoided, thus providing a better service to the community at a lower overall cost.

A few specific collaborations between the ING telescopes and other telescopes are being considered. One particular collaboration is to share observing time between the WHT and the Italian Galileo telescope, TNG, on La Palma. This collaboration centres on the use of the high-resolution spectrograph on that telescope, as the UES echelle spectrograph on the WHT will not be offered for some time.

Other collaborations currently under consideration are with the 3.5-m Calar-Alto telescope, with the Canada-France-Hawaii Telescope, and with the Nordic Optical Telescope. Discussions with these facilities are still at an early stage. In any case, for such collaborations to come into effect there must be a clear advantage for our community of telescope users. The above mentioned arrangement with the TNG is a good example, where without this arrangement the opportunity for high-resolution spectroscopy would have been lost.

## The Utrecht Echelle Spectrograph

The longer-term availability of a high-resolution spectroscopic facility is under study. The Nasmyth focal station currently occupied by the Utrecht Echelle Spectrograph will become a dedicated focus for adaptive optics instrumentations. For that reason the UES will be taken away from the telescope, but not necessarily be simply decommissioned. Apart from decommissioning there are currently two options. One option would be to enhance the instrument with an image slicer and fibre optics feed improving its spectral stability. The instrument would then be placed in a stable and controlled environment. The second option under study is the possibility to deploy UES on the 10-m GRANTECAN telescope, also fed by fibres.

Both options carry attractive possibilities, but first technical aspects will have to be explored. Apart from the technical and astronomical prospects, under the much tighter future operational budgetary regime aspects of operational efficiency and stream lining will become ever more important aspects for ING. ¤

René Rutten (rgmr@ing.iac.es)

*As part of the reestructuring plan, both the Jacobus Kapteyn Telescope (September 2003) and the Utrecht Echelle Spectrograph (July 2002) will be taken out of normal service.*

# NAOMI — Common-User Adaptive Optics at the WHT

C. R. Benn, S. Els, T. Gregory, R. Østensen, F. Prada (ING), R. Myers (University of Durham)

NAOMI, the WHT's adaptive-optics system, is now being used routinely with INGRID, the IR camera, to obtain near-diffraction-limited images at wavelengths 1–2.2 micron (*J*, *H*, *K*, and narrow-band filters). Time allocations are queue-scheduled to take advantage of the best seeing, but visiting observers are also welcome. The images reproduced here and on the front page are from the May 2002 commissioning run. With bright guide stars ($V$<11), NAOMI improves image FWHM from 0.7 to 0.2 arcsec in *J*, *H* and *K* bands. For $V$~12, the correction is typically from 0.7 to 0.3 arcsec, and useful correction has been obtained for guide stars down to $V$~13.5. An uncorrected seeing of 0.7 arcsec in *H* band corresponds to 0.9 arcsec in *V*, well above the median for the site (0.7 arcsec). A summary of measured performance (FWHM, FWHE, Strehl) can be found on the NAOMI web page: `http://www.ing.iac.es//Astronomy/instruments/naomi/`.

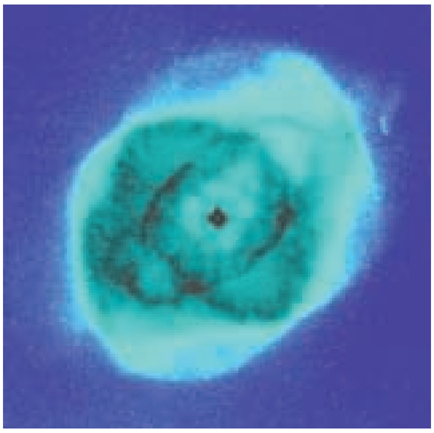

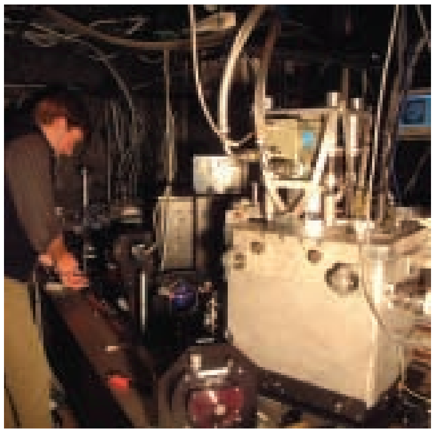

*Left: Figure 1. N6543 planetary nebula in Paschen beta, 600-sec integration, using central star (V=11) as a wavefront reference. Adaptive-optics correction from 0.7 to 0.3 arcsec. The finest structures visible in the nebula are ~0.3 arcsec across. Image is 30 arcsec top to bottom. Right: Figure 2. NAOMI in GHRIL. INGRID is in the foreground.*

Near Earth Asteroid 2002 NY40 was observed with NAOMI on the night 17 August 2002, just before its closest approach to earth. This is the first time an NEA has been imaged with an adaptive-optics system. The asteroid was only ~750000 km away during observation, and moving across the sky at about 5 arcsec per second. Despite the technical difficulties this introduced, H-band images were obtained with a resolution of 0.11 arcsec, close to the diffraction limit of the WHT. This sets an upper limit of 400 m on the projected size of the asteroid at the time of observation.

NAOMI's emissivity in *K*-band is still high (~100%), so programmes which can be observed in either *H* or *K* are probably best done in *H* until the emissivity has been reduced.

NAOMI's coronograph, OSCA, was successfully commissioned in May 2002, by Peter Doel and his team from UCL. OSCA offers 6 focal-plane stops with diameter ranging 0.2–2.0 arcsec. OSCA is offered to observers on a shared-risks basis in 2003A. For further information, see the OSCA web page: `http://www.ing.iac.es//Astronomy/instruments/osca/`.

At the end of 2002, NAOMI will move to a new purpose-built enclosure, GRACE, on the opposite Nasmyth platform (the platform formerly occupied by UES). NAOMI will stay in GRACE permanently, and will be joined by a second science instrument, OASIS, mid-2003. OASIS is the optical integral-field spectrograph formerly at CFHT. NAOMI will deliver significant adaptive-optics correction at optical wavelengths, permitting OASIS spectroscopy of galaxies (and other targets) at high spatial resolution.

The GHRIL enclosure will revert to its original function of hosting visiting instruments and experiments, including further tests by Durham University of wavefront correction using a Rayleigh laser beacon.

In support of future adaptive-optics observations, and in particular in preparation for extensive queue observing, a robotically-operated seeing monitor, RoboDIMM, has recently been brought into use. RoboDIMM (Augusteijn, T., 2001, *ING Newsl.*, **4**, 27), delivers a measurement of the seeing every few minutes, from a small telescope outside the WHT building. ¤

Chris Benn (crb@ing.iac.es)

*Figure 3. RoboDIMM tower, dome and telescope.*

# LIRIS: A Long-Slit Intermediate Resolution Infrared Spectrograph for the WHT

José Acosta-Pulido[1], E. Ballesteros[1], Mary Barreto[1] (Project Manager), Santiago Correa[1], José M. Delgado[1], Carlos Domínguez-Tagle[1], Elvio Hernández[1], Roberto López[1], Arturo Manchado[1] (Principal Investigator), Antonio Manescau[1], Heidy Moreno[1], Francisco Prada[2], Pablo Redondo[1], Vicente Sánchez[1], Fabio Tenegi[1].

*1: Instituto de Astrofísica de Canarias; 2: Isaac Newton Group of Telescopes*

*Note from the editor: article received in March 2002*

LIRIS is an Instituto de Astrofísica de Canarias (IAC) project that consists in a near-infrared (0.9–2.4 microns) intermediate resolution spectrograph, conceived as a common user instrument for the WHT.

LIRIS will have imaging, long-slit and multi-object spectroscopy observing modes ($\Re$~1000–3000). Coronography, and polarimetry capabilities will eventually be added. Image capability will allow easy target acquisition for spectroscopy.

| | |
|---|---|
| **Focal station** | Cassegrain |
| **Array format** | Rockwell Hawaii 1024×1024 HgCdTe |
| **Scales at detector** | 0.25 arcsec/pixel |
| **Observing modes** | Imaging, long-slit spectroscopy, multi-object spectroscopy, coronography with apodization masking and polarimetry |
| IMAGING MODE | |
| **Field of view** | 4.2×4.2 arcmin |
| **Sensitivity** | K=22.13, H=23.68, J=24.75, Z=25.24 for t=1h, S/N=3, 0.5” seeing |
| SPECTROSCOPY MODE | |
| **Available slits** | Long slit: (0.5, 0.75, 1, 2.5, and 5) arcsec×4.2 arcmin<br>Multi-object: 10 multislit masks available (up to 24 slits per mask) |
| **Spectral coverage and sensitivity*** | $\Re$=1000<br>Bands Z and J (0.887–1.531 mm). Limiting magnitudes J=21.3, Z=22.0<br>Bands H and K (1.388–2.419 mm). Limiting magnitudes K=18.6, H=19.9<br>$\Re$=3000<br>Bands Z (0.997 to 1.185 mm). Limiting magnitude Z=21.2<br>Bands J (1.178 to 1.403 mm). Limiting magnitude J=20.3<br>Bands H (1.451 to 1.733 mm). Limiting magnitude H=19.5<br>Bands K (2.005 to 2.371 mm). Limiting magnitude K=18.0<br>*In all cases for the continuum and t=1hr, S/N=3, FWHM=0.5" |

*Table 1. Instrument features.*

## 1. Scientific Drivers

Given its common-user status, it should be possible to use LIRIS for a wide range of astrophysical disciplines, including the areas of stellar, planetary, extragalactic and cosmological physics. We list below some of the most relevant potential scientific applications:

– Spectroscopy of proto-planetary nebulae.
– Detection of very low mass secondaries, planets and brown dwarfs.
– Spectroscopy of nearby and distant galaxies with massive star formation: nearby HII regions and distant starbursts.
– Stellar kinematics and populations in spiral galaxies.
– Physical conditions of the gas, and the stellar kinematics and populations of starburst galaxies and AGNs.
– Ultraluminous infrared galaxies.
– The fundamental plane of high-redshift elliptical and S0 galaxies.
– Redshift measurements of infrared sources.

## 2. General Description

The optical system is based on a classical collimator/camera design (Figures 1, 2 and 3). The expected throughput (averaged across the wavelength range) for the optics is 80% and 64% in imaging and spectroscopic modes, respectively. The total throughput including filters, grisms and detector is 35% and 30% in imaging and spectroscopic modes, respectively. Grisms are used as the dispersion elements (the grism transmission is assumed to be 80%). Low resolution grisms are manufactured in Corning 9754 (Figure 4) while medium resolution will be manufactured in ZnSe. A set of filters (broad band, $Z$, $J$, $H$, $K_s$ and narrow band Br-α, $K$-continuum, $H$-continuum, [FeII], $H_2$ (v=1–0), $H_2$ (v=2–1), $CH_4$ and HeI) have been acquired through a consortium headed by Alan Tokunaga.

The mechanical design is based on a modular concept, integrated by the following modules: the aperture

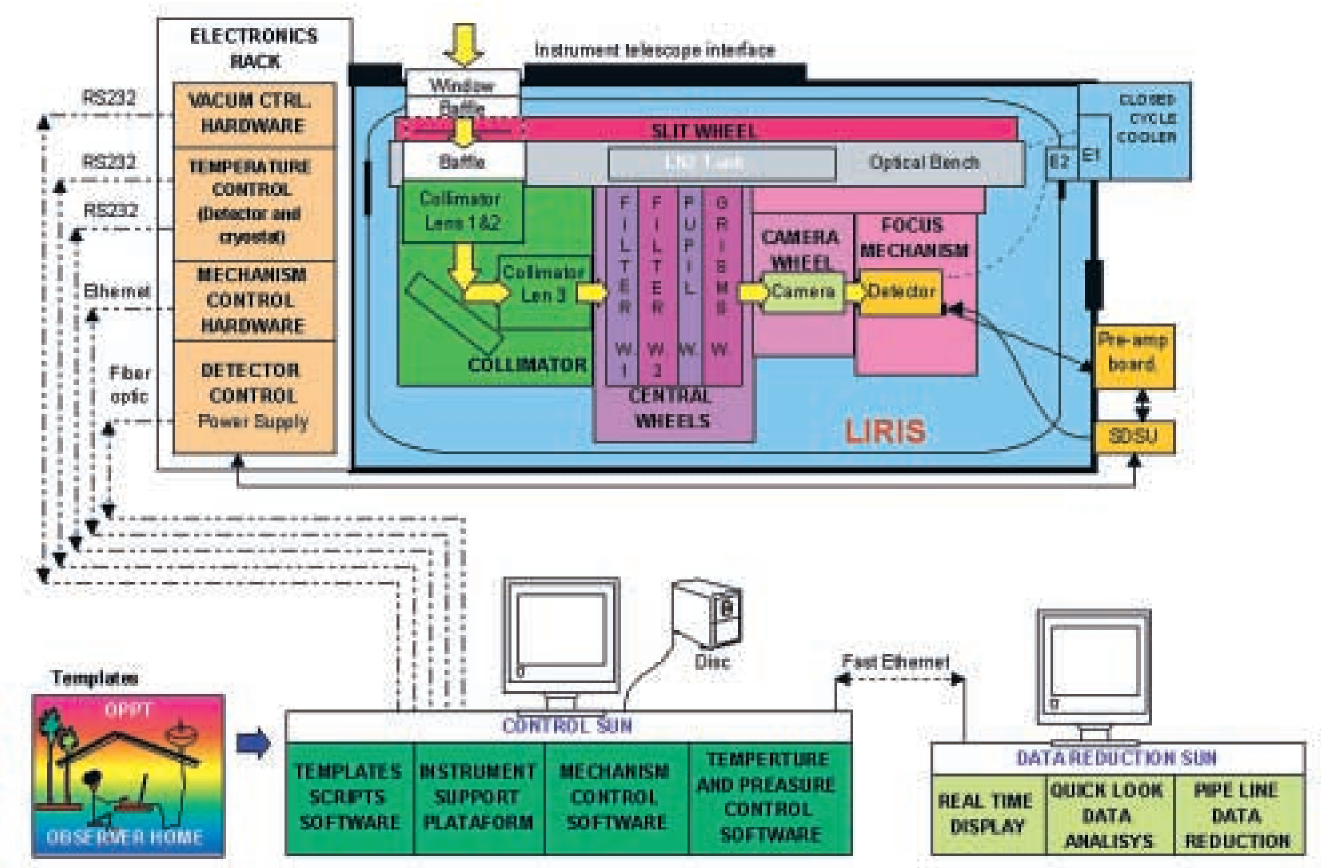


*Figure 1. LIRIS schematic representation.*

wheel (slit wheel), the collimator assembly, the central wheel assembly (formed by two filter wheels, the pupil wheel and the grism wheel), the camera wheel and finally the detector assembly with its focussing mechanism. The detector will be mounted in a cold translation mechanism to compensate for non-achromaticity along the observing spectral range.

The detail optical design and the conceptual mechanical design were subcontracted to the ROE (Royal Observatory of Edinburgh).

The slit wheel (Figure 5) contains 16 positions: one blank position, five long slits and ten multislit positions. The two filter wheels contain 12 positions each, and will hold the filters and the Wollaston prisms. The pupil wheel (Figure 6) contains 12 positions and will hold the pupil masks, plus an optional apodization mask with rotation mechanism for coronography capabilities. The grisms wheel has 10 positions for grisms. The camera wheel (Figure 7) has four positions and will carry the camera and the optics to re-image the pupil onto the detector plane, as well as an aperture and a black aperture. All mechanisms use Phytron cryogenic stepping motors and the control system is based on a VME system.

The instrument is pre-cooled with $LN_2$, and the cooling system is a two-stage closed-cycle refrigerator (Figure 8) (CTI model 1050C), which works on the Gifford-McMahon cycle.

The detector is a Hawaii 1024×1024 HgCdTe array using a SDSU controller, which communicates with the control computer (SUN workstation) using the SBUS card.

An agreement has been established between the IAC and the ING to develop jointly the detector control system and the Mechanism Control Software for the two infrared instruments (LIRIS/IAC and INGRID/ING).

The LIRIS Software system is being designed to be fully integrated in the observer environment available at the WHT. A common observer will have access to the following software packages: Instrument Simulator Software, Templates Generator Software, Instrument Support Platform User Interface, LIRIS Mechanism and Thermal Control Software, Real Time Display, Quick Look Data Analysis and Pipeline Data Reduction.

## 3. Current Status

At present LIRIS is in the calibration phase at IAC. Assembly, integration



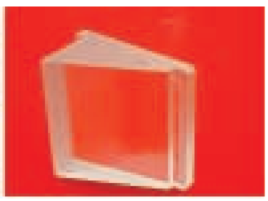

*From left to right: Figure 2. Collimator. Figure 3. Camera. Figure 4. Corning 9754 Gris.*

and verification phases were carried out in summer 2001.

The collimator, camera, slits wheel mechanism and the main central wheel (filter 1 and the pupil wheel) mechanism have been successfully tested at test cryostats (Figure 9) in cryogenic conditions. They have also been pre-integrated on LIRIS to check the interfaces (Figures 10, 11 and 12).

Test multi-slits masks have been manufactured by Electric Discharge Machining (EDM) and successfully tested achieving a roughness of 1.15±0.15 microns.

The engineering and the scientific detectors have been tested in cryogenic conditions on a purpose-built detector test bench (Figures 13 and 14). The main characteristics of the science degree array at 80 K are as follows: readout noise ~20 $e^-$, dark current 0.065 $e^- s^{-1}$, bad pixels <1.5% and the detector behaves linearly within 2% up to 50% of the full-well (175,000 $e^-$). The signal offset was found to vary 670 $e^-$/K with the detector temperature. The current temperature controller permits a stability of better than 0.005 K, which implies a signal offset variation of less than 4 $e^-$.

In November 2001 the LIRIS Cryostat integration was started (vacuum tank, optical bench, closed-cycle cooler, radiation shields, etc.) (Figures 15, 16, 17 and 18) and in December the first cool-down was successfully completed (Figures 19 and 20).

The following LIRIS cool-down took place in March and it included the slit wheel mechanism, collimator, central wheels mechanisms (two filter wheels, pupil and grisms wheels) and the camera mechanism. First light and commissioning at the telescope is expected at the beginning of 2003.

For on-line information about the LIRIS project, please visit our web site at:
`http://www.iac.es/proyect/LIRIS/`. ¤

Arturo Manchado (amt@ll.iac.es)



*From left to right: Figure 5. Slit wheel. Figure 6. Pupil wheel. Figure 7. Camera wheel integrated in the test cryostat (dummy on camera position).*

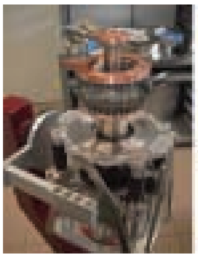


*Left: Figure 8. Closed-cycle refrigerator with the two-stage thermal links integrated. Right: Figure 9. Mechanism cryostat on the Mitutoyo during the functional verification of the main central wheels module.*

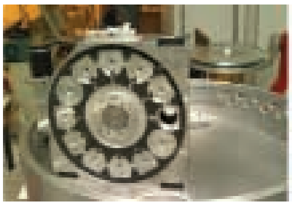

*From left to right: Figure 10. Main central wheel module (filter wheel side) pre-integrated on LIRIS. Figure 11. Bottom view of the slit wheel mechanism. Figure 12. Pre-integration of the slit wheel on the LIRIS optical bench.*


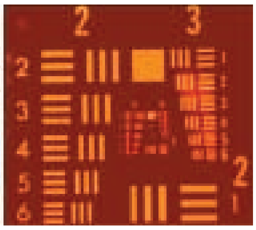

*Left: Figure 13. Internal view of the detector test cryostat. Right: Figure 14. Image of an USAFSR pattern taken with the scientific grade detector, through the H-band filter.*

*From top to bottom: Figures 15 and 16. Positioning the optical bench on the trusses in the vacuum tank central ring (cables provisionally fixed for this cycle). Figures 17 and 18. Optical bench with the collimator and reticules placed in specific positions to check their behaviour during the first cycle (these reticules were visible at all time through a very useful cryostat auxiliary window, see Figure 18). A simulation of the detector module was placed outside the beam line to test the detector thermal control system.*


*Left: Figure 19. LIRIS cryostat ready for the first cycle. Right: Figure 20. Pre-cooling with liquid $LN_2$.*

# ULTRACAM Successfully Commissioned on the WHT

Vik Dhillon (Univ. of Sheffield), Tom Marsh (Univ. of Southampton) and the ULTRACAM team*

**UKATC: Andy Vick, David Atkinson, Tully Peacocke, Steven Beard, Stewart McLay, David Lunney, Chris Tierney, Derek Ives; Southampton: Carolyn Brinkworth; Sheffield: Mark Stevenson, Paul Kerry, William Feline, John Kelly, Richard Nicholson, Richard French, Richard Pashley, Paul Kemp-Russell*

ULTRACAM was successfully commissioned on the WHT on 16 May 2002, over 3 months ahead of schedule and within budget. The instrument was funded by PPARC and designed and built by a consortium involving the Universities of Sheffield, Southampton and the UKATC, Edinburgh.

ULTRACAM is a high-speed, three-colour CCD camera designed to provide imaging photometry at high temporal resolutions. The instrument is highly portable and will be used at a number of large telescopes around the world. On the WHT, ULTRACAM mounts at the Cassegrain focus and provides a 5 arcminute field on its three 1024×1024 CCDs (i.e. 0.3 arcsec/pixel). Incident light is first collimated and then split into three different beams using a pair of dichroic beamsplitters. One beam is dedicated to the SDSS u' filter, another to the SDSS g' filter and the third to the SDSS r'/i'/z' filters, although it is possible to use different filters if required. By careful selection of glasses and coatings on the optics and chips, we have achieved an instrumental throughput of approximately 50% in the green and red arms of ULTRACAM and 30% in the blue arm. Combined with the fact that ULTRACAM mounts at Cassegrain, and hence telescope losses are minimal, we obtain a count rate of approximately 2,000 per second for a $V$=18 magnitude star in the $V$-band.

The CCDs in ULTRACAM are E2V 47-20 frame-transfer devices of exceptional cosmetic quality (grade 0) and quantum efficiency (97% at peak). The chips are Peltier and water-cooled to 233K, giving approximately 0.05 electrons/pixel/second dark current. This figure is much less than the faintest sky recordable with the WHT and hence dark current is an insignificant noise source with ULTRACAM. The readout noise of the chips is also remarkably low —just over 3 electrons when reading out at 10 microseconds/pixel and just under 6 electrons when reading out at 2 microsec/pixel.

There is a great deal of flexibility in the configuration of the ULTRACAM chips. It is possible to read the chips out in full-frame mode without clearing (for minimum dead-time), full-frame mode with clearing (for minimum exposure times), two-windowed mode, four-windowed mode, six-windowed mode and drift mode (for maximum frame rate). In each of these modes, it is possible to alter the size of the windows, the positions of the windows, the binning factors, the pixel digitisation speed, the gain and the clock speeds. Each image taken by ULTRACAM is also time-stamped using a dedicated GPS system to an accuracy of better than 0.1 millisec.

Because ULTRACAM employs frame-transfer chips, the dead-time between exposures depends only on the vertical clocking time and is hence negligible; for the full-frame and windowed modes the dead-time is typically 25 millisec and in drift mode it falls to a fraction of a millisecond. The maximum frame rate of ULTRACAM depends on the sizes of the windows being read out; using drift mode and two small windows it is possible to achieve frame rates of up to 300 Hz. To handle such huge data rates (up to 3.6 Mbytes/sec, i.e. up to 200 Gbytes/night), ULTRACAM uses a RAID array to store the data, a DDS4 drive to archive the data and, most importantly, a pipeline data reduction system to enable real-time assessment and full reduction of the light curves.

*Figure 1. Top: ULTRACAM mounted on the Cassegrain focus of the WHT. Bottom: The ULTRACAM commissioning team, from left-to-right: Mark Stevenson (Sheffield), Paul Kerry (Sheffield), Tom Marsh (Southampton), Marco Azzaro (ING), Vik Dhillon (Sheffield), Andy Vick (UKATC), David Atkinson (UKATC), Carolyn Brinkworth (Southampton).*

A key driver during the design of the instrument hardware and software has been simplicity, which ensures that the instrument is as reliable, portable and upgradeable as possible. Therefore, the instrument has no moving parts and the CCDs are read out using an SDSU controller (such as the ones used on the common-user instruments at the ING) connected to a linux PC via a PCI interface. Furthermore, the astronomer controls the CCD cameras using http requests sent via a standard web browser, enabling ULTRACAM to be operated remotely over the internet.

ULTRACAM has now been used for a total of 5 nights in May 2002 (1 night commissioning and 4 nights PATT science) and 13 nights in September 2002 (4 nights PATT science, 6 nights NL science and 3 nights CAT science). The instrument is working to specification and appears to be very reliable — we lost only 30 minutes in 13 nights in September 2002 to technical downtime, which was due to a faulty off-the-shelf ethernet card. The instrument has so far been used to observe a wide range of astrophysical targets at high temporal resolution, including pulsars, eclipsing binary stars, cataclysmic variables, black-hole X-ray binaries, neutron-star X-ray binaries and asteroseismology. Some of the initial results from these runs are presented in the accompanying figures. For more detailed information on ULTRACAM, including on-line signal-to-noise and frame-rate calculators, please consult the instrument web pages at `http://www.shef.ac.uk/~phys/people/vdhillon/ultracam`. If you are interested in using ULTRACAM on a collaborative basis, please contact Vik Dhillon (`vik.dhillon@shef.ac.uk`) or Tom Marsh (`trm@astro.soton.ac.uk`). ¤

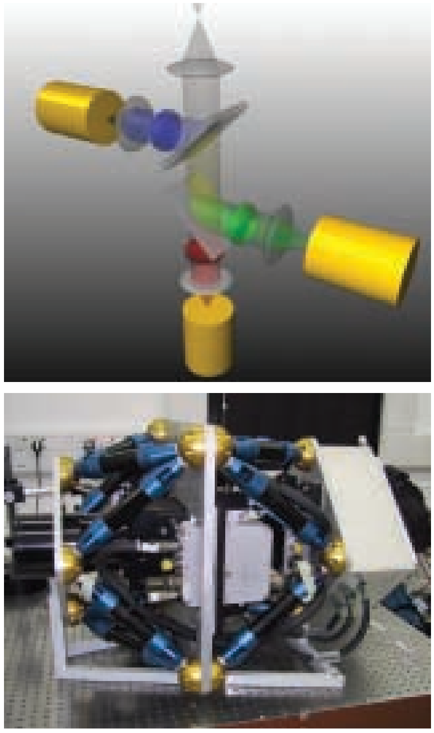

*Figure 2. Top: Schematic showing the light path through ULTRACAM. Bottom: ULTRACAM in the test focal station at the WHT, just prior to mounting on the telescope (courtesy Sue Worswick).*

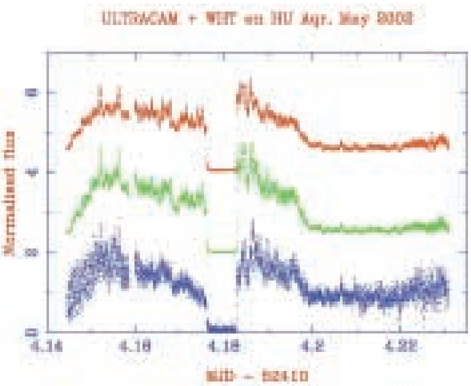


*Figure 3. Light curve of the eclipsing polar HU Aqr, which consists of a white dwarf accreting material onto its magnetic poles from a red dwarf companion star. The light curve shows intense flickering from the accreting poles and the eclipse of the poles (the 2-3 second transition into eclipse).*

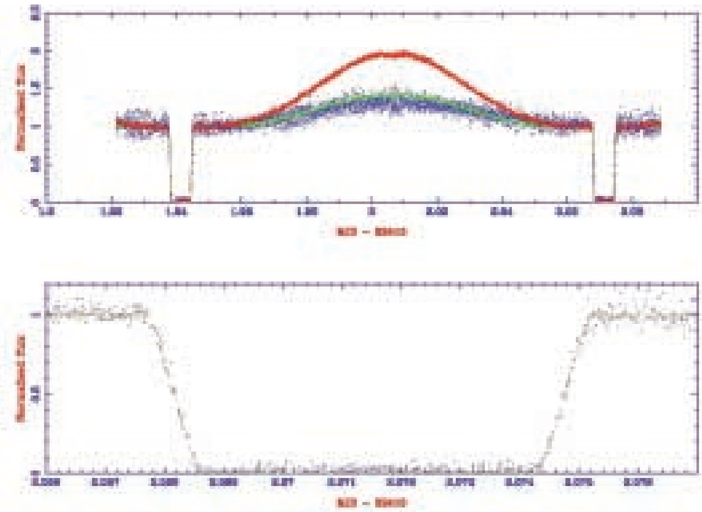

*Figure 4. Light curve of the eclipsing white-dwarf/red-dwarf binary NN Ser. Each point on the graph represents a 2 sec exposure. The upper panel shows the u', g' and r' flux versus time. The rise in the centre of the curve is due to a reflection effect, where the irradiated inner hemisphere of the cooler star comes into view. The lower panel is an expanded plot of the eclipse. The eclipse is due to the obscuration of the hot white dwarf by the cool red dwarf and will be used to measure the masses and radii of the two stars (using a full light curve fit) and the rate at which the orbital period of the binary is decreasing.*

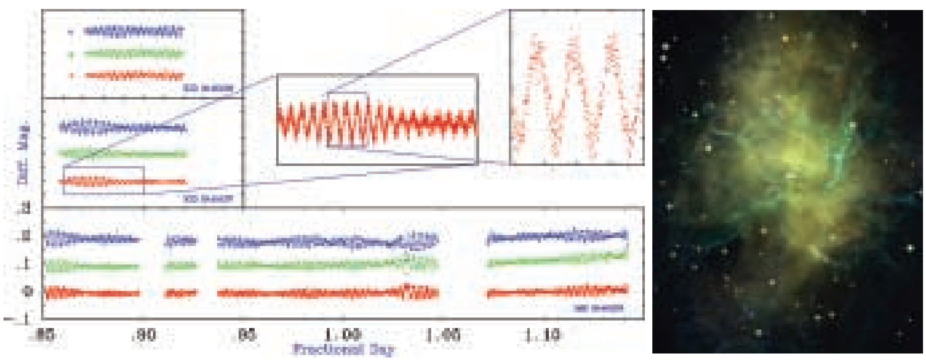


*Figure 5. Left: Light curve of the pulsating sdB star KPD2109+4401 obtained by Simon Jeffery (Armagh) for use in his ULTRACAM asteroseismology project. Right: Image of the Crab Nebula, obtained by combining the simultaneous u', g' and r' ULTRACAM images. Fast data on the Crab Pulsar at the centre of this image were obtained in order to calibrate the accuracy of the ULTRACAM GPS time-stamping.*

# A New Camera for WYFFOS

Gordon Talbot, Maarten Blanken, Romano Corradi, Begoña García (ING), Johan Pragt (ASTRON)

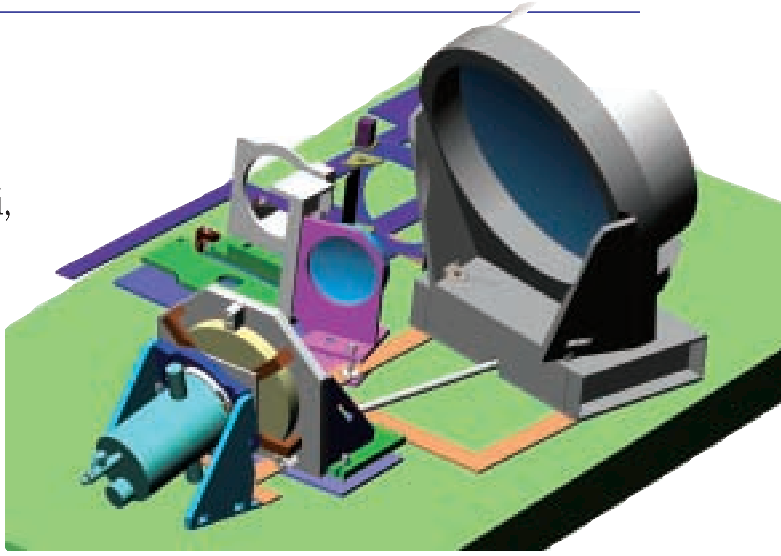

AutoFib2, the prime focus, multi-object spectrograph of the WHT, was recently upgraded with the installation of the Small Fibre Module. This allows to reach a fainter limiting magnitude and to observe a larger number of objects than with the previous large fibres.

With the new module, the image of each fibre (1.6 arcsec diameter in the sky) projected onto the CCD is presently undersampled with the present camera of WYFFOS, the Nasmyth spectrograph fed by AutoFib2. The projected full-width at half maximum of each fibre is in fact ~1.4 pixels both in the spectral and spatial direction.

As part of the upgrade of the instrument, a new camera for WYFFOS with a longer focal length (293 mm instead of 132 mm of the present camera) has therefore been designed. The new WYFFOS Long Camera will provide an adequate sampling of the fibres of AutoFib2, increasing the spectral resolving power up to 9500 with the Echelle grating presently available with WYFFOS.

The Long Camera, in combination with a large format CCD, will also allow further developments, such as introducing a larger number of fibres, or significantly increasing the spectral resolution by adopting smaller fibres in multi-object or integral-field spectrographs.

Beginning in the early nineties proposals for a new camera for WYFFOS were made by the RGO. The camera continued to be developed there until its closure in 1998. ING then took over project leadership and continued developing the concept culminating in 2001 in a definitive design.
In 2001 the optical design and construction of the WYFFOS Long Camera was contracted to ASTRON, based at Dwingeloo, The Netherlands. Just before last Christmas the design passed the Preliminary Design Review (PDR) held at ASTRON.

Some of the ASTRON team come originally from the Kapteyn Institute of Roden and some are relative young designers who together have recently worked on the instruments VISIR and MIDI for the VLT and VLTI. Those from Roden have a long relationship with ING, which is renewed with this project.

The preliminary design was made from ZEMAX optical data and tolerance calculations, to 3 dimensional file of optical lines generated by ZEMAX, copied into the drawing package pro-Engineer, into 3D dimensional principal sketches of the structure in pro-E. Also 3D strength and mostly stiffness calculations where done to prove the quality.

The accompanying illustration shows the camera (with the WYFFOS covers removed) looking from the cryostat end. The existing Hartmann shutter from the original camera will be reused in a new position. Light passes through a meniscus lens and is reflected from a folding flat onto a spherical mirror before passing to the detector through a cut-out in the flat. A field flattener lens is positioned just before the cryostat window.

The meniscus lens will be made out of N-BK7 material, the diametre will be 200 mm and the original optical design has been changed to use spherical surfaces, rather than the aspherical earlier design. The folding flat is made of Zerodur about 230 mm wide with a square hole in the middle.

What catches the eye is the large spherical mirror, again Zerodur, with a diameter of about 670 mm and a weight including structure of about 200 kg. This heavy mirror is the optical element that is the most sensitive for tolerances of the whole camera and is also very sensitive for temperature changes in position in respect to the flat mirror and detector. So the heaviest part will be adjustable in all its directions and will move in respect to the table to compensate for temperature expansion (see the thin, long, low-expansion rod) while the rest of the camera will be mostly non-adjustable optics.

Hereafter the light goes through the square hole in the middle of the flat and via a field flattener lens it will be projected into a standard ING cryostat.

The camera is optimised to use as a detector two MIT Lincoln Labs low-fringing, high-QE CCDs butted together as a two chip mosaic of 4K by 4K 15 micron pixels. These are being purchased by ING as part of a consortium of observatories and will be mounted in a standard cryostat and integrated with ING's Data Acquisition System (UltraDAS) using an SDSU-2 controller. This work will be carried out by ING on La Palma.

The final opto-mechanical design started early in January and is in full progress with commissioning planned for semester 2003A. ¤

Gordon Talbot (rgt@ing.iac.es)

# Upgrading the WHT Acquisition TV Cameras

Clive Jackman (ING)

Despite advances in solid state imaging devices over the last twenty years, the choice of a camera to replace the aging vacuum tube devices on the WHT telescope was not obvious. All ING telescopes originally had Westinghouse (Intensified Secondary Electron Conduction) ISEC TV cameras, which could be used at the standard 25 frame $s^{-1}$ TV rate, had an advantage of photon multiplication within an intensifier stage, and could be made to integrate charge at the photocathode. Being able to integrate for longer than a single TV frame made these cameras attractive in astronomical applications. The integrating facility works by inhibiting the electron beam from a thermionic cathode for an integer number of TV frames before reading off the two dimensional charge pattern with a single raster scan, the image is then held in a digital frame store until refreshed by the next scan but is presented to the observer on a TV monitor as a stationary image during the interscan period. The problem with ISEC cameras is that they can be damaged by over illumination and have poor geometric stability because image distortion is dependent among other factors on the linearity of the camera time-base oscillators. Furthermore these cameras are no longer supported by the manufacturer and obtaining or engineering around obsolete spares was starting to become a problem. Solid-state detectors offer excellent geometric stability are not damaged by over illumination and have a large dynamic range.

An important decision when retrofitting an acquisition camera to a telescope intended to operate with a camera such as the Westinghouse ISEC is whether to replace the reimaging optics and design a system utilising a smaller format imaging device. Small format devices are of course cheaper and several cameras are commercially available, many work at TV frame rates and some have thermoelectric cooling and can integrate for a few tens of seconds. A problem with many of these products is their poor quantum efficiency of the CCDs used and relatively high dark currents, these shortcomings combine to make it difficult to achieve the limiting magnitude of the ISEC cameras $\sim m_V=20$. A solution adopted at some observatories is to use an intensified CCD camera, generally a MCP ahead of a cooled CCD, but we wanted to avoid this solution partly because of the nuisance of managing the over illumination risk, but also to offer better photometric performance than the ISEC cameras. The performance requirements for future upgrades to ING acquisition cameras had previously been specified in a memo (Rutten and Barker, 1996) and these included features such as on-line bias subtraction, generation of FITS files and a minimum of 8 bit precision over the dynamic range of the detector. These requirements were easier to meet using commercially available cameras aimed at the university observatory market. Several suppliers offer cameras aimed at the university telescope niche but the Micro Luminetics Cryocam offered the possibility of remote PC operation over a single 50 ohm coaxial cable, whilst other contenders typically needed multicore cables of restricted length between the camera and PC. This cable limitation was an important factor in choosing the Cryocam although other observatories like the AAT have chosen to accept the cable restriction and have mounted the controlling PC on the telescope.

The Cryocam model presently operating at the Cassegrain focus of the WHT has a thinned back illuminated 1k square SITe chip with 24μ pixels. Replacing the original camera with a CCD having a similar format meant the acquisition FOV at Cassegrain has been retained and slightly increased in the y-direction, the possibility of interposing a focal reducer to change between a 1.5 arcmin and a 4 arcmin FOV remains along with the original camera filter wheel. The chip is operated at a temperature of 220 K and has a dark current better than 0.2 $e^{-}$ $\text{pixel}^{-1}$ $s^{-1}$ with a QE>80% between 600 to 750 nm. The Cryocam will operate in either fast readout 8 bit 'focus mode' when acquiring bright $\sim m_V=5-7$ calibrate stars or monitoring the position of a bright source on the ISIS slit or the 'normal mode' with 16 bit precision. Any shutter speed ≥200 ms is available in either mode giving the possibility of confirming the position of faint or extended objects on the ISIS slit without the need to trust a 'blind offset'. The camera is operated by the observer from the control room and the control and display application run on a PC under the Windows 98 operating system. The camera CCD does not operate in the frame transfer mode and requires a mechanical shutter to close during readout and the long term reliability of this component is an area of concern, with bright stars there is a temptation to use the minimum 200 ms integration time and a readout time of less than a second in focus mode implies several thousand shutter operations per hour. The recommendation is that in these circumstances it is preferable to integrate for longer and use a red filter, we have however operated a Cryocam at the Cassegrain focus for both direct and slit viewing since May 2001 and have not experienced any serious problems. The spare camera was recently tested with AF2 to manually guide utilising the recently upgraded coherent guide fibres and we are considering the purchase of enhanced Cryocam software so a Cryocam can be used for autoguiding AF2. ¤

Clive Jackman (cwmj@ing.iac.es)

# OTHER NEWS FROM ING

## A Workshop in Honour of Paul Murdin

René G. M. Rutten (Director, ING)

The creation of the Isaac Newton Group of Telescopes, and more generally of the Roque de los Muchachos Observatory, is intimately related with the relentless energy of Paul Murdin. In October 2001, after many years, Paul stepped down from the ING Board, and this was commemorated with a brief but interesting workshop with the title “Science from La Palma – Past, Present and Future.”

Various talks were given, showing the highlights as well as the unavoidable but entertaining anecdotes related to past discoveries, but, more importantly, talks were also given looking at the new developments at the observatory that point the way to the future.

Following an introduction on the planned developments at the ING, Carlos Frenk (Durham) beautifully reminded the audience how key developments and discoveries at the ING over the past decade have helped point the way towards the new generation of large telescopes. Vilppu Piirola (Tuorla) showed how the Nordic Optical Telescope exploits its excellent image quality, while Mike Bode (Liverpool) explained that the robotic Liverpool Telescope will open a new chapter in ground-based fast response astronomy. Michael Rowan Robinson complemented Carlos Frenk’s talk with examples of ING’s contribution to cosmology. The two final presentations by Eckart Lorenz (Munich) and José Miguel Rodríguez Espinosa (Tenerife), summarised the status of the two largest developments of facilities at the ORM, namely the MAGIC 17-m Cherenkov telescope, and the 10-m GRANTECAN telescope. Both these facilities will come into operation in the near future and lift the observatory as a whole to world class standards.

Of course at the end there was a lighter note to thank Paul for all these years of hard work that have helped shape the observatory in such a crucial way. Below, the top picture shows Francisco Sánchez presenting a gift to Paul. This celebration was a unique occasion to get four of the people together who have been at the helm of the ING. The picture in the middle shows, from left to right, Jasper Wall (Oxford), Paul Murdin (Cambridge), Jan Lub (Leiden) and René Rutten (ING).

The highlight of a buffet dinner in the evening was the performance of the Palmeran dancing group Echentive. The bottom picture shows Carlos Frenk having a good time on local Palmero rhythm. This formed the close of what had been an informative and entertaining event with many old friends of Paul and the observatory. ¤

### Other ING Publications and Information Services

**[INGNEWS]** is an important source of breaking news concerning current developments at the ING, especially with regard to instruments.

You can subscribe to this mailing list by sending an email to `majordomo@ing.iac.es` with the message *subscribe ingnews* in the body. Please leave the subject field and the rest of the body of the message empty.

Once subscribed, you can subscribe a colleague by sending to `majordomo@ing.iac.es` the command *subscribe ingnews your_colleague's_ address*. To unsubscribe from [INGNEWS] send to `majordomo@ing.iac.es` the command *unsubscribe ingnews*. More information on [INGNEWS] and all sent messages can be found on this web page: `http://www.ing.iac.es/Astronomy/ /science/bulletin/`.

A new **Technical Note** has been published recently: “No 127 The Definition of Dark, Grey and Bright Time at ING”, I. Skillen (ING), February 2002. This can be downloaded from `http://www.ing.iac.es/Astronomy/ /observing/manuals/man_tn.html`

Other ING publications are available on-line at the URLs below:
**In-house Research Publications**: `http://www.ing.iac.es/Astronomy/ /science/ingpub/`
**Annual Reports**: `http://www.ing.iac.es/PR/AR/`
**Press Releases**: `http://www.ing.iac.es/PR/press/`

# Real-Colour Images of Spiral Galaxies

Nik Szymanek (Univ. of Hertfordshire) and Johan H. Knapen (ING and Univ. of Hertfordshire)

The real-colour images of spiral galaxies reproduced in this Newsletter form part of a new series of such pictures, currently under construction. The original images used have all been obtained with the ING telescopes, mostly with the JKT, some with the INT, and an occasional (H-alpha) image with the WHT. We collected most of the images ourselves as part of a large PATT-supported science programme aimed at studying spiral arm structure, and the rest from the ING archive. For each galaxy, we have images in the $B$ and $I$ bands as well as in the near-IR $K_s$ band (see also article on page 3), and in H-alpha. Using a set of newly developed IRAF scripts we can produce series of images for each galaxy which are registered to a high accuracy, i.e., have the same pixel scale, orientation, resolution, and overall image size. This is not trivial, given the use of large amounts of archive data, taken with different cameras, detectors and even telescopes. Whereas the data sets are being produced for scientific work, they serve another purpose which is to show the beauty and the variety of spiral galaxies. Our sample consists of 57 galaxies of all spiral types, from flocculent (multi-armed) to grand-design (two-armed and symmetric), and with and without bars, circumnuclear structure, and rings.

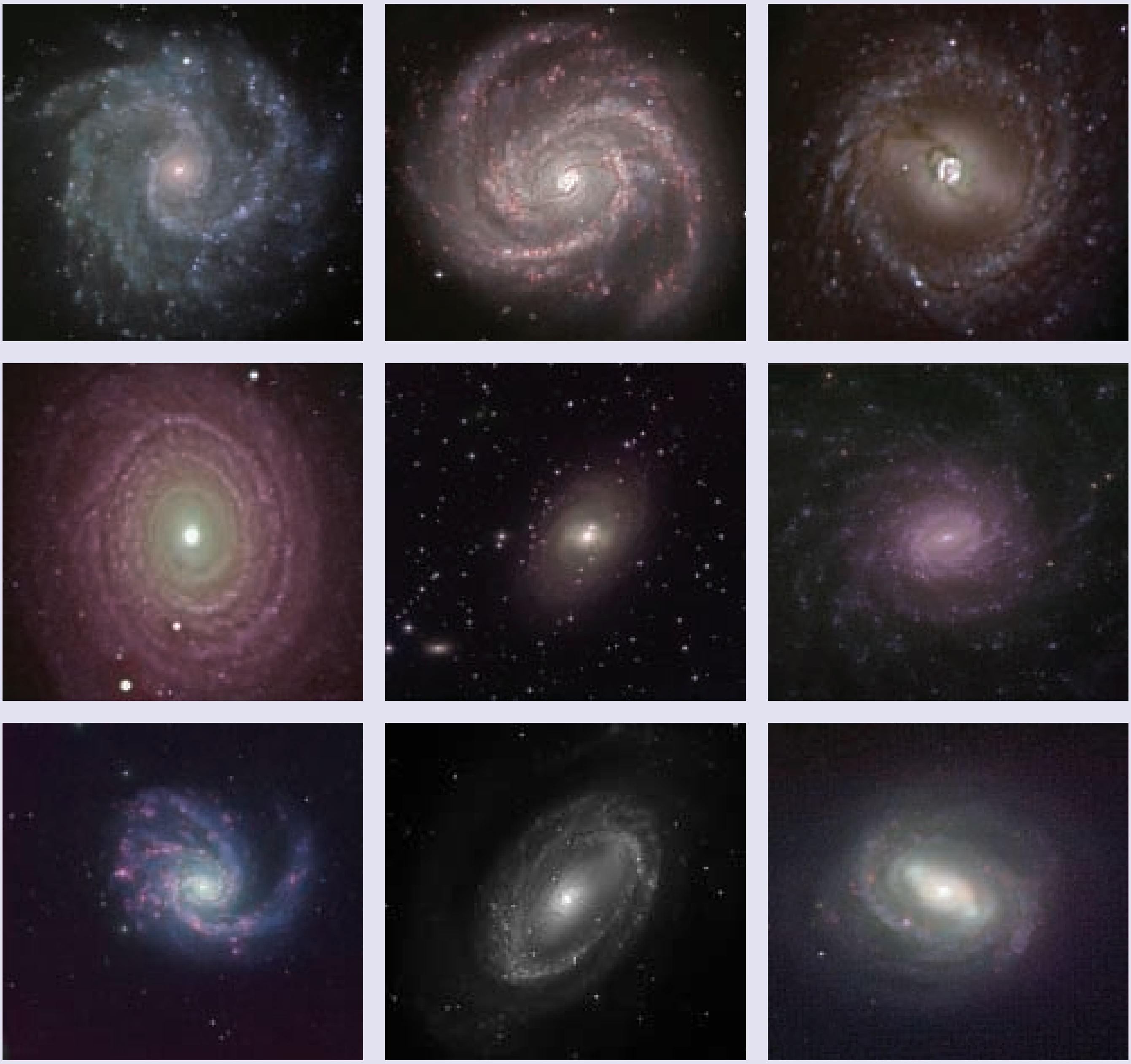

*From left to right and from top to bottom: NGC 3184, NGC 4321, NGC 3351, NGC 488, NGC 1169, NGC 3486, NGC 4254, NGC 4725 (B-band) and NGC 4579.*

To produce the real-colour images, the image sets, originally in FITS format, are read into an image processing package called Maxim DL. This programme allows manipulation of ING images as well as powerful image co-addition, calibration and colour combination/balancing routines. Images are saved in a variety of formats including FITS, TIFF and JPEG. It is our intent to produce a finished result that extracts detail from the core region of galaxies as well as any other features, such as rings, gravitational tails, interacting arms, etc. A variety of processing routines will do this successfully, such as logarithmic scaling, but in our opinion the best routine is that of "Digital Development" a software algorithm created by the Japanese amateur astronomer Dr. Kunihiko Okano. Digital Development applies a hyperbolic transfer function that sits neatly between the standard gamma curve and a logarithmic curve. The Digital Development curve is successful for a number of reasons. The steeply rising curve withholds the brightness value of the sky background and as the curve levels out the effect is to enhance the middle-grey tones, typically information which is contained in the overexposed ("burnt-out") core of the galaxy. As the curve finally levels out and flattens this has the effect of compressing the dynamic range of the image. A sharpening routine known as "unsharp masking" is also applied to enhance detail. There are several user-definable parameters within Maxim DL, as well as a preview screen which displays how the image will appear once Digital Development is applied.

Each of the galaxy image components will be processed using the above method. Best (or certainly most spectacular) images are achieved using standard B, R and V images. Additional wavelength data, such as H-alpha components, can be overlaid at any point. Maxim DL allows the colour addition and registration of the individual files but, in our opinion, the best results are obtained using powerful image-manipulation software such as Adobe Photoshop. The FITS files are converted to 8-bit TIFF files after careful scaling, and combined in registration. Further processing such as colour balancing and the removal of unsightly artifacts such as cosmic ray hits, dust-"donuts" and general CCD defects are easily applied in Photoshop.

It is important to realise that the above processing routines are applied to produce aesthetically pleasing images and perhaps not images that are intended for purely scientific research. To be fair, the Digital Development routine extracts more detail than most other applications and performs spectacularly with the nuclei of galaxies and globular clusters. The ING Archive contains many high-quality images taken with the JKT, INT and WHT and these images can be used to demonstrate the quality of ING equipment and, indeed, the quality of the sky at La Palma (see *Sky & Telescope*, June 2001, pp. 44–45).

We thank Sharon Stedman, Dan Bramich, Stuart Folkes and Javier Méndez for their help in the observations and data reduction and handling. ¤

Nik Szymanek (Nik.Szymanek@tesco.net)

# ING Stick to the Task – Work for the NSST

Gordon Talbot, Maarten Blanken, Alan Chopping, Paul Jolley and Juerg Rey (ING)

ING recently demonstrated the range of services they can offer to other telescopes by completing a contract for the Royal Academy of Sciences, Sweden for mirror handling, pad gluing and aluminising a pair of 1.4 metre diameter mirrors to be installed in the New Swedish Solar Telescope (NSST) on La Palma.

Mirror handling involved the need to invert the mirrors after unpacking, then placing them face down so that a set of eighteen Invar axial pads could be glued to the rear of each one. This involved rehearsing the procedure with the dummy mirror supplied which matched the size and weight of the actual mirrors (1400 mm diameter, 150 mm thick and 600 Kg). Rehearsal of these operations is vital to avoid unforeseen occurrences that could damage optical components; the more so when they are this size and weight. ING's policy for all of this type of work is that we look after the mirrors as if they were our own.

Once the mirrors were in position the template that defined the position of the axial pads on the back of each mirror was aligned. The mirror surface was prepared by carefully cleaning then grinding the Zerodur in the area of each pad before applying a special primer. The surfaces of the axial pads were roughened. The pads were then positioned and aligned using the jigs supplied, before being attached by the specified two-pack flexible epoxy adhesive. The jigs controlled the thickness of the epoxy under each axial pad to 75 microns. One mirror was completed before the template and jigs were transferred to the second mirror.

The work was carried out in the WHT aluminising area. To cure the adhesive, they had to be kept at an elevated temperature of at least 24 degrees C for seven days. To achieve this a 'tent' was created for each mirror using polythene sheeting and scaffolding, which was then warmed with space heaters to reach the required temperature while minimising the transfer of additional heat to the dome.

While the axial pads were being glued to the mirrors a total of three 'test pieces' (one for each day of gluing) were made using some of the actual epoxy mixes used. The test pieces were axial pads glued to steel plates, which had had exactly the same surface treatment as the actual pads and mirrors. These were left to cure alongside the mirrors. After the curing time each test piece was then subjected to a pull-off test. Each test piece was sandwiched between thick steel plates to avoid local distortions. A weighing device was slung from the lifting crane. To this was attached a sling with the test piece shackled underneath, and test weights were progressively added. All three demonstrated they would withstand the specified 100 Kg load.

The mirrors complete with firmly attached axial pads were then turned right side up, before being prepared then coated together in the WHT aluminising plant.

After coating, but while still in the aluminising area, the mirrors were then installed in their cells by NSST staff, then with assistance from ING transported to the telescope for installation.

A large number of ING staff contributed a wide range of skills to this work, principally members of the Mechanical, Site Services and Telescope Operators Groups. Some stages of the work required relatively large numbers of people present, for instance the mirror handling required at least five to co-ordinate all the actions of lifting and rotating the mirror.

The NSST representatives also assisted and of course made the whole thing possible by first of all entrusting their mirrors to ING and with their detail work in the design of the pads, templates and jigs.

Due to the current economic climate ING will be driven in the future to seek to carry out more repayment services in areas where we have special expertise or facilities, with the aim of retaining a wide skills base, while maintaining both our proficiency and facilities by exercising them. These areas extend beyond aluminising which has been the main service in the past, to other areas, (which will include optical fibres) where ING have built up experience from our operations and projects. ¤

Gordon Talbot (rgt@ing.iac.es)

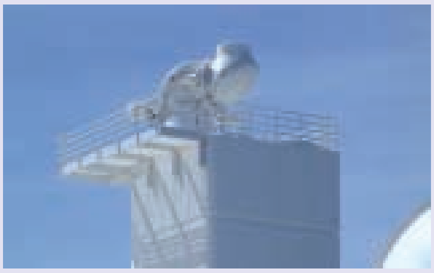

*From top to bottom: one of the NSST mirror blanks in the aluminising area at the WHT, pad gluing in the rear of one of the blanks and the two mirrors assembled on top of the NSST tower.*

# A Euroconference Organised by the ING: "Symbiotic Stars Probing Stellar Evolution", La Palma, 27–31 May 2002

Romano L. M. Corradi (ING)

Half or maybe two thirds of stars in the Universe are binaries. Among them, symbiotic stars are long-period interacting binaries composed of an evolved giant primary and a hot and luminous companion surrounded by an ionised nebula.There are two distinct classes of symbiotic stars: one containing normal red giants and having orbital periods of about 1–15 years, and the other with Mira primaries usually surrounded by a warm dust shell, and orbital periods generally longer than 10 years. Symbiotic stars are thus the interacting binaries with the largest orbital separations, and their study is essential to understand the evolution and interactions of detached or semi-detached binary stars. They are also among the (intrinsically) brightest stars, which makes them excellent observational targets both in our Galaxy and in nearby galaxies.

Mass accretion onto the hot component plays a fundamental role in determining the properties and evolution of symbiotic stars, and involves energetic phenomena relevant to many other astrophysical fields. The hot component of the vast majority of symbiotic systems is in fact a luminous (~1,000 solar luminosities) and hot (100,000 K) white dwarf powered by thermonuclear burning of the material accreted from its companion's wind.

Depending on the accretion rate, these systems can be either in a steady burning configuration or undergo hydrogen shell flashes, which in many cases last for decades due to the low mass of the white dwarf. In addition, in many systems the hot component shows activity on time scales of a few years that cannot be simply accounted for by the thermonuclear models. Possible and promising explanations of this activity involve changes in mass transfer and/or accretion instabilities in a disk.

Surrounding the interacting stars, a rich and luminous circumstellar environment is found, which is the result of the presence of both an evolved giant with a heavy mass loss and of a hot companion copious in ionising photons and often producing its own wind. In particular, strongly different environments are expected, such as ionised and neutral regions, dust forming regions, accretion/excretion disks, interacting winds, bipolar outflows and jets. The best known, spectacular example of a ionised nebula around a symbiotic stars is very likely the Southern Crab (Henize 2–104), whose inner region is displayed in the conference poster shown in the figure. Such a complex multi-component structure makes symbiotic stars a very attractive laboratory to study many aspects of stellar evolution in low-mass binary systems.

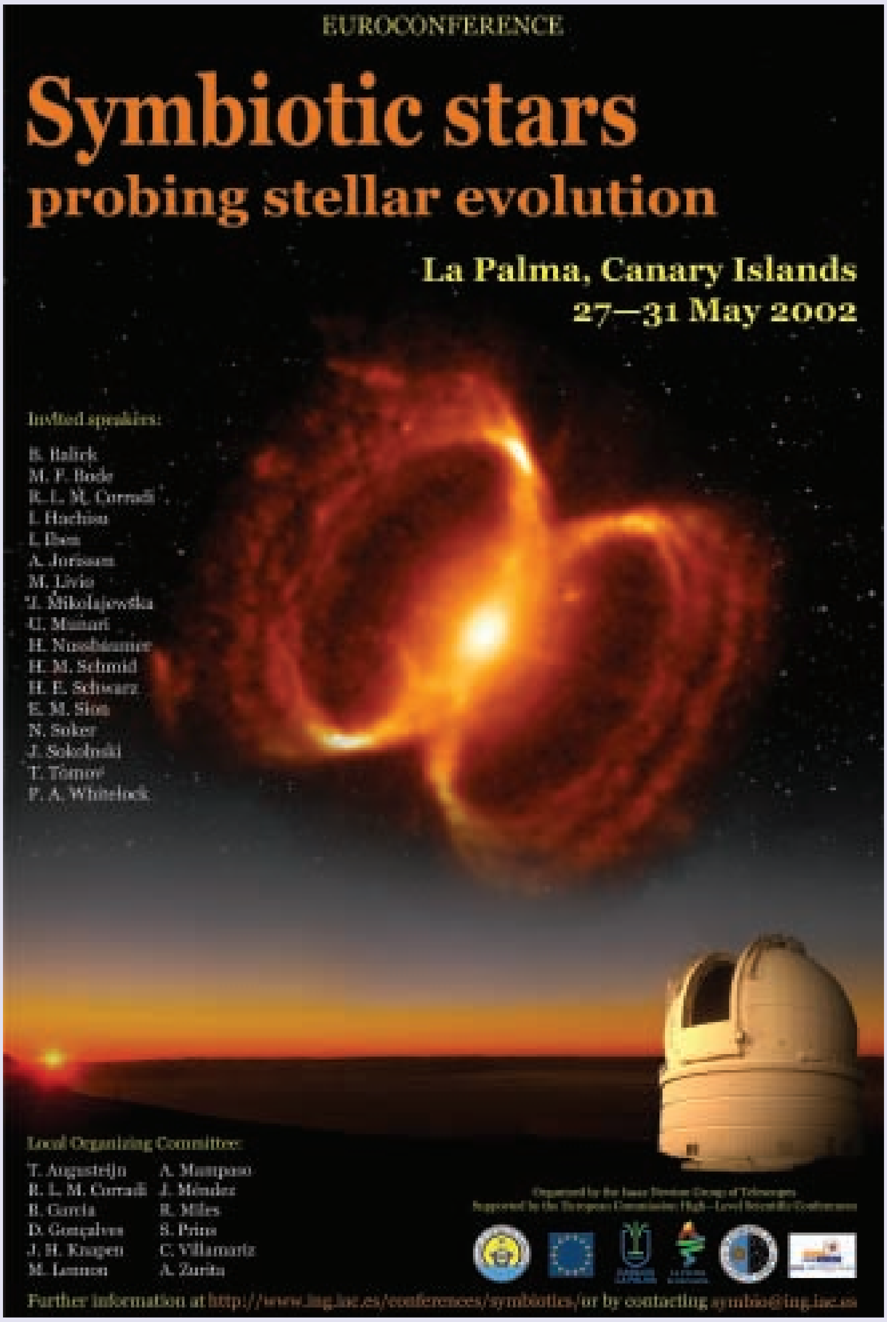


For these reasons, a EuroConference with the title "Symbiotic stars probing stellar evolution" was organised by the ING on La Palma from May 27 to 31, 2002. Financial support to the conference was provided by the ING and the European Commission, High-Level Scientific conferences. The main scientific goal of the conference was to bring together the leading scientists in the world to revise thoroughly the current state of our knowledge in this field. This attracted to La Palma one hundred astronomers from thirty different countries who set, for the first time, firm links between symbiotic stars and related objects, helping to understand for instance the role of such interacting binaries in the formation of stellar jets, planetary nebulae, novae, supersoft X-ray sources, and SN Ia. Many of them are issues concerning the late stages of stellar evolution of which at present little is known, but with important implications for our understanding of the stellar populations and chemical evolution of galaxies, as well of the extragalactic distance scale.

So far, most of the research in the field of symbiotic stars has been conducted by European astronomers, spread among almost every European country. Therefore this Euroconference was also the occasion to strengthen the links and collaborations between researchers from different European institutions. Moreover, more than 50 young researchers and PhD students (especially European) were able to attend the conference thanks to the EU and ING funds. The event was a unique experience for many of them, in which they found guidelines and suggestions to direct their future research toward important issues in modern astrophysics. Special training sessions entirely dedicated to these young researchers were organised with this aim.
The list of invited speakers included: B. Balick (USA), M. Bode (UK), R. Corradi (UK), I. Iben (USA), A. Jorissen (Belgium), J. Mikolajewska (Poland), U. Munari (Italy), H. Nussbaumer (Switzerland), H. M. Schmid (Switzerland), H. Schwarz (Chile), E. Sion (USA), N. Soker (Israel), J. Sokoloski (USA), T. Tomov (Poland), and P. Whitelock (South Africa).

For more information about the conference, visit our web site at `http://www.ing.iac.es/` `/conferences/symbiotics/`. ¤

Romano Corradi (rcorradi@ing.iac.es),
*Chair of LOC and SOC*

# News from the Roque

Although for astronomical observations the weather last winter has been rather poor, this has not hampered fast progress in the construction of the various new facilities, which also continued over the summer. The dome and annex building of the 10-m GTC have made remarkable progress. The dome is nearly fully completed at the time of writing. The dome of this grand facility is now fully silhouetted against the horizon when seen from the ING telescopes site.

The construction of the MAGIC Cherenkov telescope has also been remarkably speedy. The open, unprotected telescope structure was erected in only a few weeks and will soon receive the mirror surface elements. This will most definitely add a bright sparkle to its appearance under the Canarian sunshine. You can't miss it when driving up from the Residencia!

Also the Liverpool Robotic Telescope is making good progress. Following completion of the ground works and foundations, the dome work is now at a very advanced stage. The telescope structure will be erected soon.

Maybe less noticeable but not less impressive are the developments in the Swedish Solar Telescope, where the original telescope has now been replaced by a new telescope within the existing tower. The new telescope's optics, with a 97 cm entrance pupil, is twice the size of the old telescope.

Looking towards the future potential of the ORM site, a site testing tower for solar observations has been erected not far from the WHT. This tower holds a solar DIMM (Differential Image Motion Monitor) and is operated by NOAO in support of a general site testing campaign for a future large solar telescope.

Also in the future plans for an extremely large telescope exist for the ORM. The EURO-50 project, proposing a 50-m optical/IR telescope, is one of several projects that are being studied world-wide. The artist's impression below shows the scale of such an installation in comparison with other facilites on site.

For readers who would like to see progress on some of these facilities for themselves, see the various live web cameras:

GTC: `http://www.gtc.iac.es/webcam_s.asp`
MAGIC: `http://mc5rq.hegra.iac.es/view/view.shtml`
Liverpool Telescope: `http://telescope.livjm.ac.uk/Webcam/`

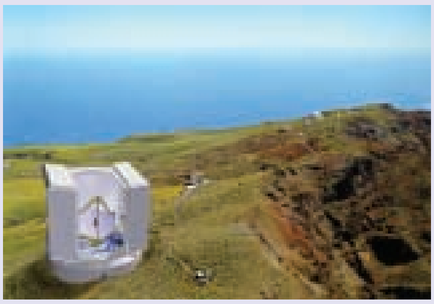

**Haloes of Planetary Nebulae from the INT WFC.** *The images of the three planetary nebulae displayed on the following page were obtained by Romano Corradi at the INT with the Wide Field Camera, that covers a field of view of 34×34 arcmin. They are very deep exposures (one to three hours exposure time) obtained through an Hα+[NII] narrow-band filter, and were aimed at studying the faint haloes that are known to surround a large fraction of planetary nebulae. We believe that these haloes are the trace of the last episodes of mass loss from the stellar progenitors of the nebulae, occurred a few* $10^4$ *years ago when they were in the pulsating red-giant phase that eventually leads to the complete ejection of the stellar envelope and the formation of a planetary nebula. In the case of two of the nebulae (Sh 2–200 and NGC 3242) displayed in the figure, however, the extended and structured emission revealed by the WFC images might not be material lost by the stars in the recent past, but simply interstellar gas located in the proximity of the planetary nebulae and ionized by the energetic radiation from their central stars.*

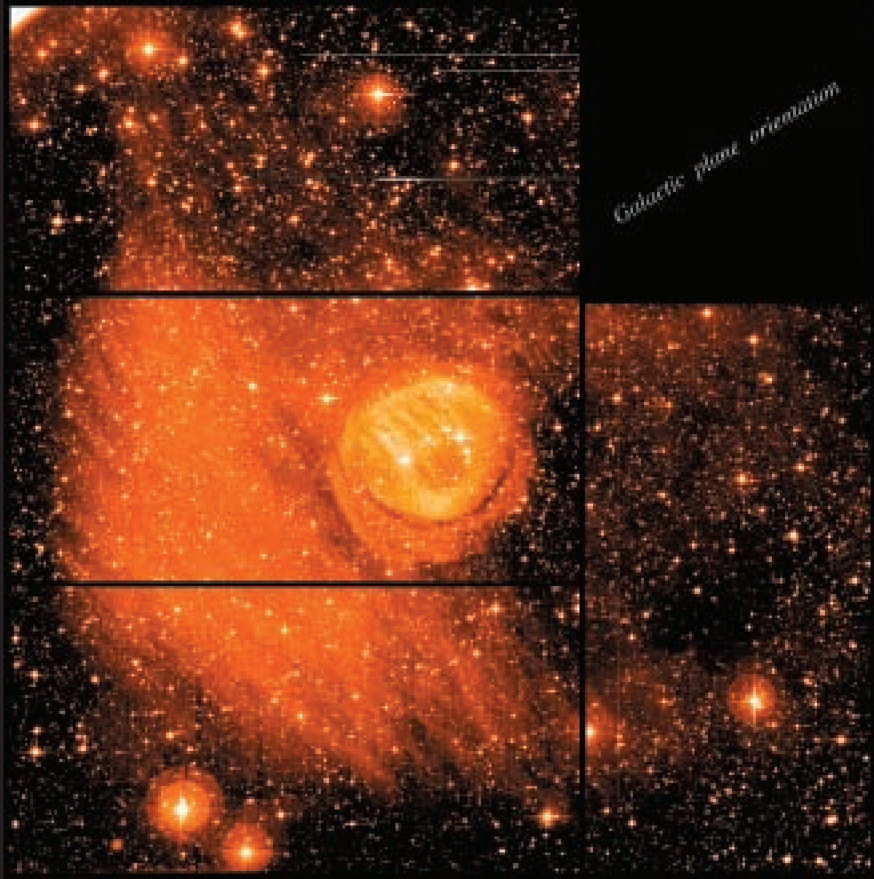


**Planetary Nebula**
**Sh 2 – 200**

**Helix Planetary Nebula**
**NGC 7293**

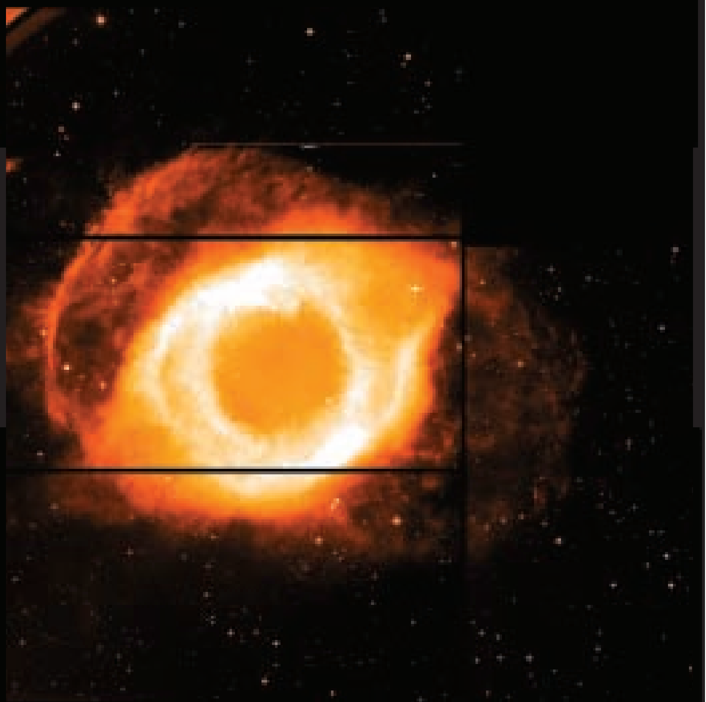

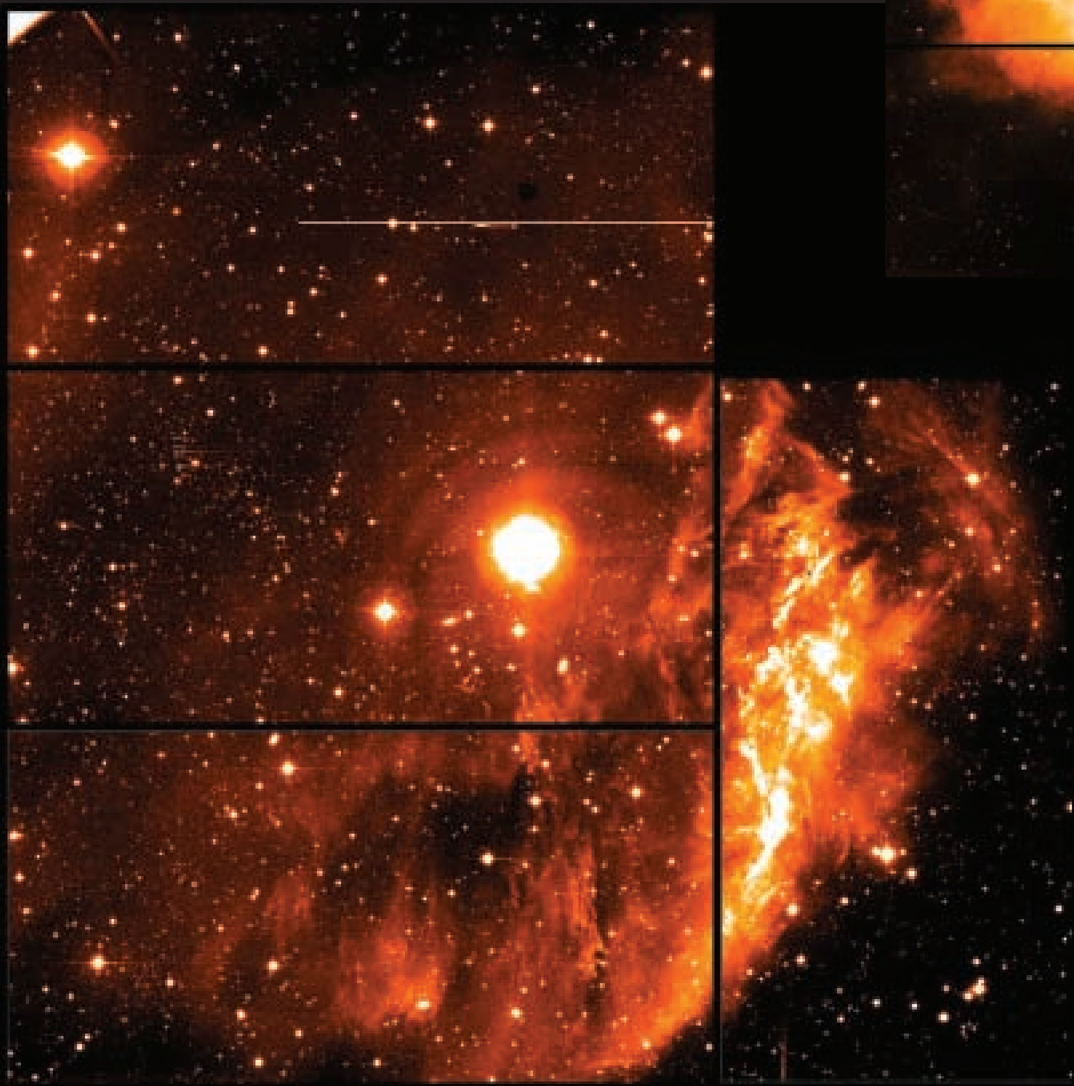

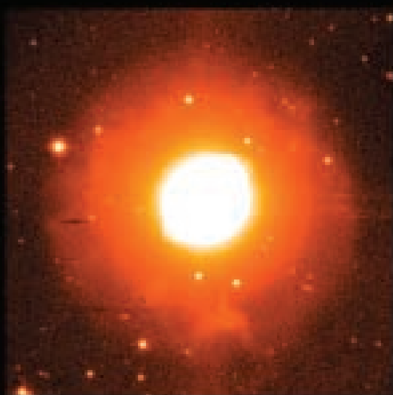

**Planetary Nebula**
**NGC 3242**

# Recent Visits of VIPs

In the last few months ING has received several visits of VIPs: the Spanish Science and Technology Minister, the British Embassador in Madrid, the Industry, Trade, Research and Energy Commission of the EU, the Science and Technology Commission of the Spanish Senate, the Science and Technology Research Committee of the EU (CREST), the Joint Research Centre of the European Commission (JRC) and some ESO representatives involved in the construction of the OWL telescope. In the accompanying photo we can see the representatives of the Industry, Trade, Research and Energy Commission of the EU in the WHT.

## Personnel Movements

After many years at ING **Nic Walton** returned to the UK, to the Institute of Astronomy in Cambridge, where he is involved in the AstroGrid developments. Nic has been at the heart of various developments at the observatory, from which astronomers continue to profit. Grateful for his efforts, we wish him well in his new career.

**Paul Morrall**, who worked in the mechanical section for a number of years, also returned to the UK. He now employs his skills in the field of physics at Daresburry Laboratory.

**Thomas Augusteijn** decided to take up a position as Astronomer in Charge at the Nordic Optical Telescope. Although it is sad to see him leaving ING, it is good that his skills and extensive experience in the observatory 'business' have been retained at the ORM.

ING's second EU-funded Mary Curie Fellow has strengthened our adaptive optics team: **Sebastian Els**, previously at the University of Heidelberg, arrived in La Palma earlier in the year.

**Arami Felipe** and **María Batista** have left the administration group recently to find fortune elsewhere.

**Francisco Prada** and **Javier Licandro** have taken up positions as support astronomers.

**Chris Evans** arrived at ING on a PDRA position to work with Danny Lennon on massive stars.

As part of the financial cutbacks, unfortunately many familiar faces will not be seen at the observatory anymore. I mention **Manuel Acosta**, **Cecilio Alvarez**, **Sheila Crosby**, **Inocencio García**, **Mavi Hernández**, **John Mills**, **Peter Moore**, and **Carlos Ramón** who have all left in recent months. Between them, there are many decades of effort dedicated to the ING telescopes, some going back to the very early days of the construction of the observatory, when neither roads nor Residencia, or even the WHT existed! We wish them all well for the future.

## The ING PR Collections of Images

One of the best ways to advertise the observatory to the public is by showing superb astronomical images obtained at the telescopes. For this reason at ING we have started to collect astonishing images of celestial objects which are then made available on the web. Full credit is given to the observers and the authors of the images.

The images are offered as part of several collections which can be found at `http://www.ing.iac.es/PR/images_index.html`. Here you will also find information on how to participate in this exciting project.

On the following page we show a recent image of M42 and M43 obtained using the Wide Field Camera on the INT. Such an image is already part of our PR collections of images. Credit: Simon Tulloch (ING) and Nik Szymanek (Univ. of Hertfordshire).

Javier Méndez (jma@ing.iac.es)

## Seminars Given at ING

Visiting observers are politely invited to give a seminar at ING. Talks usually take place in the sea level office in the afternoon and last for about 30 minutes plus time for questions afterwards. Astronomers from ING and other institutions on site are invited to assist. Please contact Francisco Prada(`fprada@ing.iac.es`) and visit this web page: `http://www.ing.iac.es/Astronomy/science/seminars.html`, for more details. These were the seminars given in the last six months:

30 August. *The exceptional Dwarf Nova, V485 Cen*, Hannah Worters (Univ. of Sheffield & ING)

30 August. *Star formation in spiral galaxies*, Stuart Folkes (Univ. of Hertfordshire & ING)

27 August. *Planetary Exospheres*, Cesare Barbieri (Padova)

26 August. *A study of B-type line-profile variables in close binaries*, Katrien Uytterhoeven (Leuven/Mercator Telescope)

12 August. *AGN-selected clusters as revealed by weak lensing*, Margrethe Wold (IPAC, USA)

7 August. *Dynamical Processes in the Central Kpc and AGN*, Isaac Shlosman (JILA & Univ. Kentucky, USA)

30 July. *Lucky exposures: diffraction limited CCD imaging*, Bob Tubbs (IoA Cambridge)

18 July. *Red Giants in the Magellanic Clouds*, Maria Rosa Cioni (ESO, Germany)

4 July. *AstroGrid: Creating the UK's Virtual Observatory*, Nic Walton (IoA Cambridge)

3 June. *TASCA: the Tololo All-Sky CAmera*, Hugo Schwarz (CTIO)

24 May. *The EURO-50 project: The world's largest telescope at the ORM*, René Rutten (ING)

21 May. *Double Bars, Inner Disks, and Fossil Nuclear Rings: The Strange and Complex Interiors of Barred Galaxies*, Peter Erwin (IAC)

16 May. *The surface of icy minor planets: trans-neptunian objects, Centaurs, comet nuclei, and trojan asteroids*, Javier Licandro (CGG & TNG)

23 April. *Binary subdwarf-B stars and the origin of Extreme Horizontal Branch stars*, Pierre Maxted (Keele Univ.)

25 March. *Adaptive optics developments on Mauna Kea, Hawaii*, Chris Benn (ING)

21 March. *Lyman-break galaxies: Are they forming bulges?* Sam Rix (IoA Cambridge)

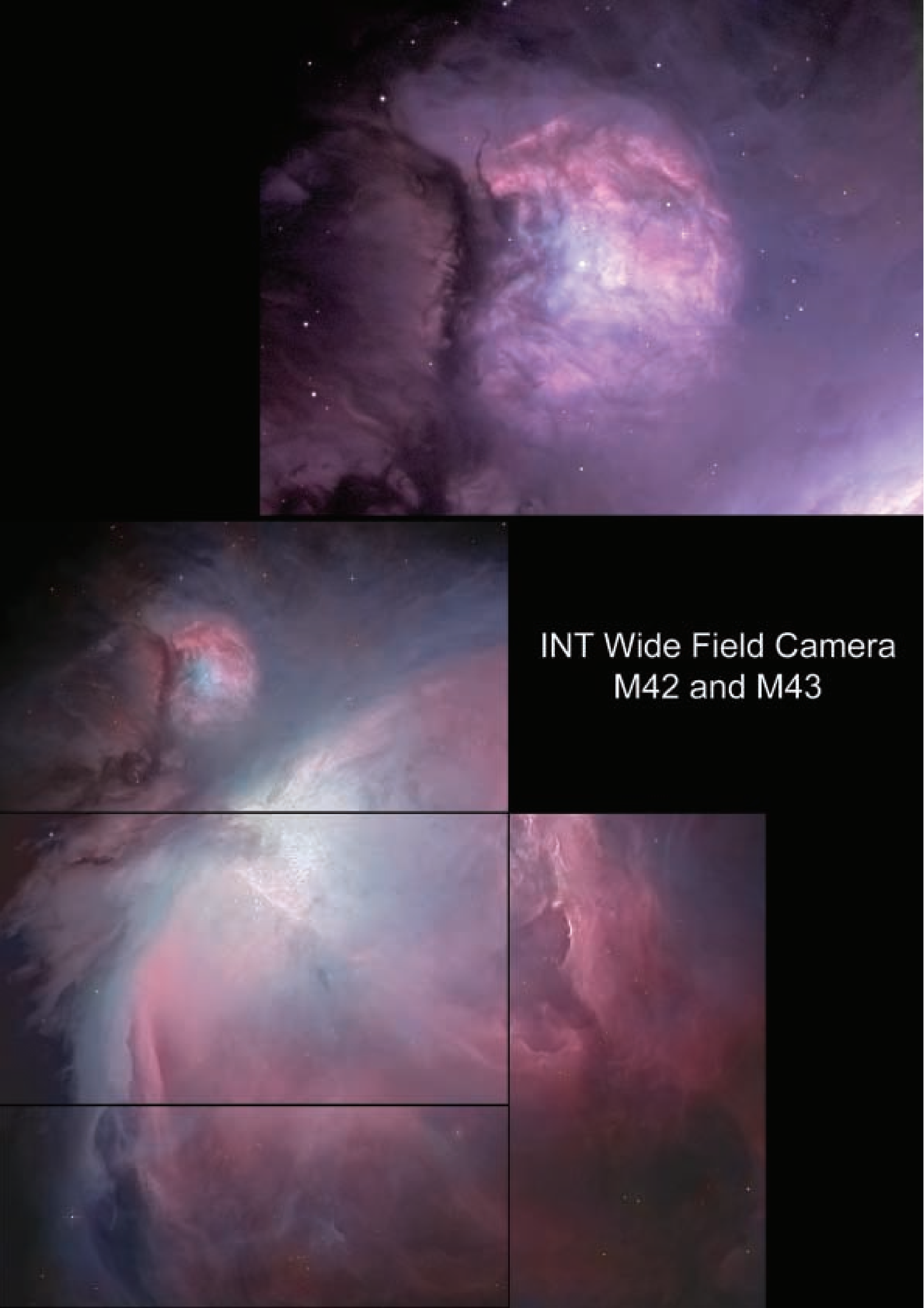
INT Wide Field Camera
M42 and M43

# TELESCOPE TIME

## A New Definition of Dark, Grey and Bright Time at ING

Ian Skillen (ING)

The legacy method used to define dark, grey and bright time at ING is based on the fraction of the night for which the Moon is below the horizon. Although this is perfectly adequate for characterising dark time, it is less so for characterising grey and bright time. As the Moon ages the focus should change to quantifying the enhanced sky surface brightness from scattered moonlight.

The optical sky surface brightness of the moonlit sky in some line-of-sight depends primarily on the Fractional Lunar Illumination, FLI, followed in significance by the angular separation between the line-of-sight and the Moon, and by the altitude of the Moon. The FLI is given to a good approximation by

$$2\times FLI = 1 - \cos\beta \cos(\lambda - \lambda_\odot)$$

where $\lambda$, $\lambda_\odot$ are the longitudes of the Moon and Sun respectively, and $\beta$ is the latitude of the Moon. Partitioning a lunation by the fraction of each night for which the Moon is below the horizon correlates strongly with partitioning the Moon's longitude, since $|\beta| \leq 5.3°$, *but ignores the change in longitude of the Sun by ~1° per day*, and therefore does not give a consistent mapping onto FLI. As a result of this and the non-uniform motion of the Moon in its orbit, the FLI on, for example, the first and last bright nights in a given lunation can be as small as 0.45 and as large as 0.80. The difference in FLI on first and last bright nights exceeds 0.20 in ~30% of lunations, and exceeds 0.30 in ~5% of lunations. An important consequence of this is that the sky surface brightness on first and last bright nights can differ by as much as ~1.2 mag/arcsec$^2$ *with the Moon being present in the sky for the same fraction of each night*. Furthermore, in such asymmetric lunations the sky brightness in the moonlit part of grey nights can be up to ~1 mag/arcsec$^2$ *brighter* than in the moonlit part of the darkest bright night in the same lunation.

Inconsistent partitioning of lunations can lead to a mis-match between observing programme *requirements and actual* conditions. A programme allocated, for example, a specific grey-time award, based on some assumed "typical" grey-time sky background, can be scheduled in significantly brighter conditions, and vice versa, and this is detrimental to observing efficiency. These considerations prompted a reappraisal of the legacy method, and the derivation of a better alternative to it.

### Sky Surface Brightness

The direct way to partition classically-scheduled time is in terms of the sky surface brightness itself, since it is this which impacts the signal-to-noise ratios for observations of a given integration time. The main contributors to the moonless sky optical surface brightness in a line-of-sight and in a specific bandpass are airglow, the zodiacal light and starlight. Benn and Ellison (1998) find the high galactic latitude, high ecliptic latitude, zenith $V_{sky}$ brightness at solar minimum at the ORM to be $V_{sky}$=21.9 mag/arcsec$^2$. The sky is brighter at low latitudes by ~0.4 mag/arcsec$^2$, and at higher airmasses by ~0.3 mag/arcsec$^2$ (at $X$~1.5), and because of variable solar activity, the airglow component is brighter by ~0.4 mag/arcsec$^2$ at solar maximum. There is no dependence on extinction, $A_V$, for $A_V$ < 0.25 mag/airmass. The contribution to the sky surface brightness from scattered moonlight when FLI ≥ 0.15 exceeds the spatial variations from airglow, zodiacal light and starlight, and so to partition classically-scheduled telescope time it is sufficient to partition by the illuminated fraction of the Moon's disc, acting as a proxy for the sky surface brightness from scattered moonlight.

Two scattering mechanisms dominate the background from moonlight; Mie scattering by aerosols and Rayleigh scattering by molecules. Mie scattering is highly forward, and so Rayleigh scattering dominates for scattering angles (i.e. angular distances from the Moon) ≥ 90°. Krisciunas & Schaefer (1991) derived scattering formulae to compute the contribution of moonlight to the sky background at some airmass as a function of lunar phase, lunar zenith distance, distance from the Moon and extinction. The uncertainty in these formulae is estimated to be ~0.25 mag/arcsec$^2$; local prevailing conditions such as enhanced levels of atmospheric dust will of course reduce their precision.

The mean $\Delta V_{Moon}$ from the $V_{sky}$ = 21.9 mag/arcsec$^2$ dark sky is computed from these formulae for the Moon at a zenith distance of 60° (so that scattering angles of up to 120° are accommodated at airmasses ≤ 2), as a function of FLI in increments of 0.1, and at scattering angles ranging from 30° to 120° in increments of 5°, measured both in the azimuthal direction and in altitude (see Figure 1). The computed differences in both directions at a given scattering angle are only a few per cent. These calculations have been normalised to JKT *observations* of the moonlit sky, made by Chris Benn on dust-free nights in 1998. The effect of decreasing the Moon's zenith distance on $\Delta V_{Moon}$ at a given angular distance from it is small, ≲0.1 magnitude, i.e roughly the same size as the points in Figure 1. $\Delta V_{Moon}$ *does* however fall off rapidly by ~1 magnitude/arcsec$^2$ when the Moon is low on the horizon. Therefore, Figure 1 forms a consistent basis for quantifying the effects of moonlight on the sky background at specific scattering angles from the Moon.

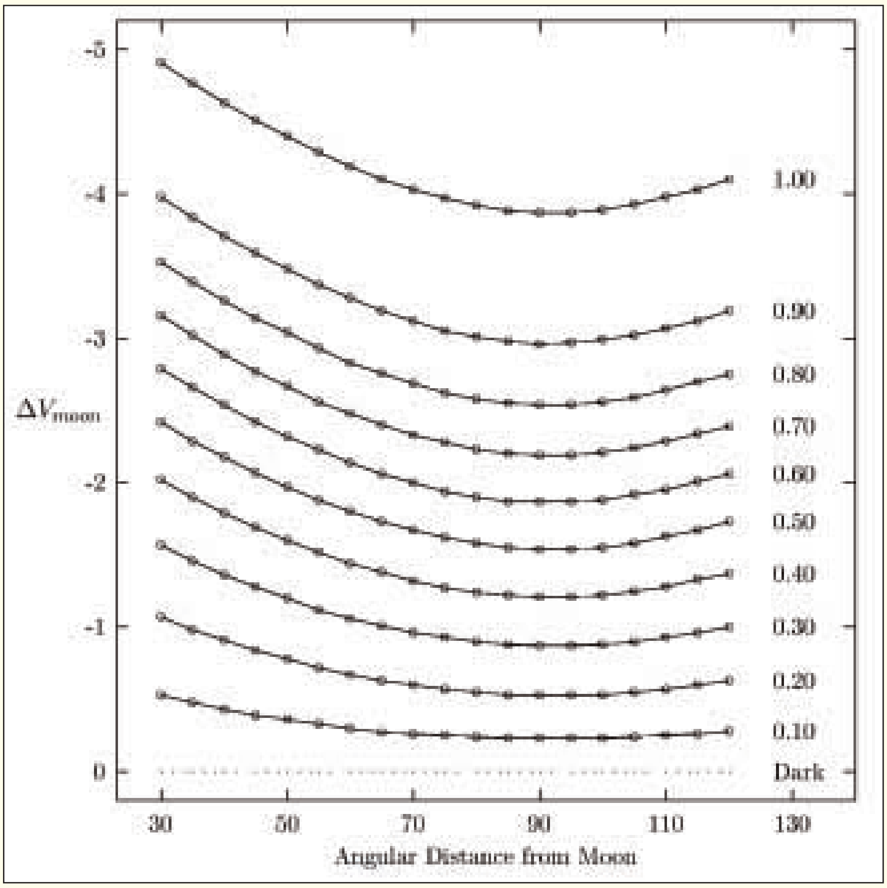


*Figure 1. The brightening of the dark sky ($V_{sky}$=21.9 mag/arcsec$^2$, corresponding to low airmass, high ecliptic and galactic latitude, and solar minimum) by scattered moonlight, calculated as a function of fractional lunar illumination and angular distance from the Moon.*

Several aspects of this Figure are noteworthy. As the scattering angle increases, the contribution of scattered moonlight to the sky surface brightness decreases up to ~90°, and then begins to increase again when Rayleigh scattering dominates. Therefore, in the presence of moonlight, a good strategy for optical observations is to observe in a broad annulus centred ~90° from the Moon whenever possible, in order to minimise the effects of scattered moonlight.

The gradient of scattered moonlight is remarkably flat at scattering angles ~90°. In fact, even at full Moon, the range in scattered moonlight within 70°–110° of the Moon is $\Delta V_{Moon} \lesssim \pm 0.1$. Therefore, it is sensible to quantify the contribution of scattered moonlight to the sky surface brightness in terms of $\Delta V_{Moon}$ computed ~90° from the Moon.

The FLI assumes greater importance in determining the sky surface brightness than angular distance from the Moon, for Moon separations ≳50°. The change in FLI is ~0.1 per day in the neighbourhood of quadratures, and therefore this emphasises the importance of having consistent partitions into grey and bright categories; inconsistent partitions are in general not compensated for by the distribution of targets on the sky in relation to the Moon.

The sky brightness approaching full Moon, i.e. zero lunar phase angle, increases strongly due to the opposition effect, which arises from a combination of shadow-hiding (the shadows of lunar particles are occulted by the particles themselves) and coherent backscattering (multiple scattering of sunlight off lunar dust grains, predominantly in the backward direction to the incident sunlight).

## Dark, Grey and Bright Time

The definition of grey and bright thresholds is to some extent arbitrary. What is important is that the definition is both *sensible* and *consistent*, and that it is understood and agreed by applicants and TAC's, and adhered to in the scheduling process. Consistency in terms of sky surface brightness is achieved by partitioning on the fractional lunar illumination, acting as a proxy for sky surface brightness 90° distant from the Moon. In terms of sensibleness, the numbers of nights in each category should not be greatly different from the legacy method, but a small increase in the number of *grey* nights, at the expense of bright nights, is desirable to better match demand.

Averaged over a Saros cycle (~37 semesters), the *same* number of dark nights (9.6), 0.7 *additional* grey nights (7.9) and 0.7 *fewer* bright nights (12.0) *per lunation* result from the adopted partitioning scheme:

*Dark:* $0.00 \le FLI < 0.25$
*Grey:* $0.25 \le FLI < 0.65$
*Bright:* $0.65 \le FLI \le 1.00$

where the FLI is computed for 0h UT. Illuminated fraction changes by ~0.1 per day in the region of these thresholds, and this "resolution effect" means that inconsistencies in the FLI are constrained to be ≲0.1 at the dark/grey and grey/bright boundaries.

For a given FLI, the fraction of the night for which the Moon is in the sky can vary by as much as ~25%, for the same reasons that the fraction of the night which is moonless does not consistently estimate the FLI. For example, at FLI=0.65 the Moon can be in the sky for between ~65% and ~90% of astronomical darkness. This could be taken into account for each night by scaling the moonlit sky surface brightness by this fraction to give a weighted background for the night, but on balance it is considered better to partition telescope time solely in terms of the *worst case* sky surface brightness computed ~90° from the Moon.

The predicted ranges in the zenith *V* sky surface brightness at high galactic and ecliptic latitudes, and solar minimum, and at an angular distance from the Moon of ~90°, are 21.2–21.9 mag/arcsec$^2$ for dark time, and 19.9–21.2 and 18.0–19.9 mag/arcsec$^2$ respectively for the *moonlit parts* of grey and bright time. For the mean sky, i.e. over all latitudes ~90° from the Moon, these ranges are ~0.5 mag/arcsec$^2$ *brighter* because of the larger contributions of airglow, zodiacal light and starlight.

This definition of dark, grey and bright time will be used in constructing the ING schedules from Semester 2002B onward. The exposure time calculator, `SIGNAL`, has been modified to offer an option specifying 'typical' sky surface brightnesses for dark, grey and bright time, corresponding to $V_{sky}$=21.50, 19.75 and 18.50 mag/arcsec$^2$ respectively.

A longer version of this article is available as *ING Technical Note No. 127*, available at URL `http://www.ing.iac.es/Astronomy/ /observing/manuals/man_tn.html`

## Acknowledgements

It is a pleasure to acknowledge discussions with Thomas Augusteijn, Steve Bell and Rob Jeffries. ¤

References:

Benn, C. R. & Ellison, S. L., 1998, *ING Tech. Note*, **115**.

Krisciunas, K. & Schaefer, B. E., 1991, *PASP*, **103**, 1033.

Ian Skillen (wji@ing.iac.es)

## Important Dates

*Deadlines for submitting applications*

UK PATT:
**15 March, 15 September**

NL NFRA PC:
**31 March, 30 September**

SP CAT: **1 April, 1 October**

ITP: **30 June**

*Semesters*

Semester A:
**1 February – 31 July**

Semester B:
**1 August – 31 January**

# Telescope Time Awards Semester 2002A

For observing schedules please visit this web page:
`http://lpss33.ing.iac.es:8080/cgi-bin/schedules.pl`

ITP Programmes on the ING Telescopes

- Doressoundiram (Paris), Multi-color taxonomy of trans-Neptunian objects. **ITP/2002/1**
- Ruiz-Lapuente (Barcelona), Supernova and the physics of supernova explosions. **ITP/2002/4**

William Herschel Telescope

UK PATT

- Axon (Hertfordshire), The Black Hole Mass-Velocity Dispersion Correlation. **W/2002A/38**
- Barcons (IF Cantabria), An XMM-Newton international survey (AXIS-II): unveiling the hard X-ray source populations. **ITP/2001/2 PB**
- Barnes (St Andrews), Starspot tracking on the W Ursae Majoris system BW Dra. **W/2002A/41**
- Benn, (ING), Adaptive-optics imaging of QSO host galaxies. **W/2002A/6**
- Bower (Durham), The Sauron Deep Survey. **W/2002A/50**
- Boyce (Bristol), K-band imaging of gas-rich low surface brightness galaxies found at 21cm. **W/2002A/52**
- Coggins (Nottingham), Mapping Elliptical Galaxy Mass Distributions using Gravitational Redshift. **W/2002A/35**
- Davies (Durham), Mapping Early Type Galaxies along the Hubble Sequence. **W/2002A/21**
- Dhillon (Sheffield), Coordinated optical and X-ray observations of the eclipsing polar HU Aqr. **W/2002A/9**
- Fitzsimmons (Belfast), The Size Distribution and Colours of Short-Period Comets. **W/2002A/67**
- Gledhill (Hertfordshire), AO imaging of post-AGB circumstellar envelopes. **W/2002A/11**
- Gray (Edinburgh), Combined X-ray and weak lensing mass profiles of the brightest cluster lenses. **W/2002A/80**
- Jeffries (Keele), Low mass stellar populations in the most massive OB associations. **W/2002A/72**
- Kleyna (IoA,Cambridge), Dark matter in the UMi dwarf spheroidal. **W/2002A/46**
- Kodama (Tokyo), History of Galaxy Mass Assembly in the Hierarchical Universe at z~1. **W/2002A/58**
- Marsh (Southampton), Magnetic braking and solar cycles in detached binary stars. **W/2002A/7**
- McMahon (IoA, Cambridge), Constraining the contribution to the UV background from z=3 and z=5 quasars. **W/2002A/78**
- Meikle (Imperial College), Detection and Study of Supernovae in Nuclear Starburst Regions. **W/2001B/34 (Long term)**
- Meikle (Imperial College), Detailed study of the physics of nearby Type Ia Supernovae. **W/2002A/49**
- Merrifield (Nottingham), Determining the Dynamics of Round Elliptical Galaxies. **W/2002A/20**
- Miller (Oxford University), A Survey for wide-separation gravitational lenses from the 2dF QSO Redshift Survey. **W/2002A/33**
- Page (Mullard Space Science Lab/UCL), Optical identification of faint X-ray sources in a deep XMM-Newton/Chandra survey. **W/2002A/43**
- Peroux (IoA, Cambridge), Tracing Galactic Haloes at $3.0<z<4.5$ using CIV Absorption. **W/2002A/14**
- Pettini (IoA, Cambridge), CORALS II: Assessing the Dust Bias in Damped Lyman-α Systems at Intermediate Redshifts. **W/2002A/10**
- Rolfe (Leicester), The Orbital Velocities and Stellar Masses in the Dwarf Nova IY UMa. **W/2002A/28**
- Ryan (Open University), Carbon nucleosynthesis in the first stars. **W/2002A/1**
- Shanks (Durham), A 2dF QSO Lensing Estimate of $\Omega_m$ via Faint QSO Number Counts. **W/2002A/76**
- Smail (Durham), Testing Photometric Redshifts using Cluster Lenses. **W/2002A/5**
- Smith (Durham), Probing the Formation Epoch of Massive Elliptical Galaxies. **W/2002A/56**
- Steeghs (Southampton), The structure of AM CVn binaries and their discs. **W/2002A/31**
- Tanvir (Hertfordshire), Rapid imaging of GRB error boxes and spectroscopy of GRB-related optical/IR transients. **W/2002A/65**
- Unda Sanzana (Southampton), A new structure on U Gem? **W/2002A/51**

NL NFRA PC

– Förster Schreiber (Leiden), Near-infrared Snapshot Survey for Bright Lensed Red High-redshift Galaxies. **w02an002**
– Groot (Nijmegen), Spectroscopic Identification of Old White Dwarf Candidates in the Faint Sky Variability Survey. **w02an001**
– Habing (Leiden), Asymptotic Giant Branch stars in northern Local Group galaxies. **w02an003**
– Kuijken (Groningen), Determining the Dynamics of Round Elliptical Galaxies Using the Planetary Nebula Spectrograph. **w02an005**
– Romanowsky (Groningen), Globular Cluster Kinematics at Large Radii in M49. **w02an006**
– Salamanca (Amsterdam), Rapid imaging of GRB error boxes and spectroscopy of GRB-related optical/IR transients. **w02an008**
– de Zeeuw (Leiden), Mapping Early-Type Galaxies along the Hubble Sequence. **w02an007**

SP CAT

– Balcells (IAC), Estudio de galaxias con formación estelar extrema a alto corrimiento al rojo. **W23/2002A**
– Battaner (Granada), Rotación del sistema estelar en la periferia de galaxias espirales. **W6/2002A**
– Béjar (IAC), La función de masas subestelar en Orión y Praesepe. **W28/2002A**
– Cairós (IAC), Multiwavelength studies of metal-poor Blue Compact Dwarf Galaxies. **W4/2002A**
– Carrera (IAC), Determinación de la relación en cúmulos globulares en destrucción por marea. **W26/2002A**
– Casares (IAC), Optical reprocessing lines as tracers of companion stars in LMXBs. **W19/2002A**
– Castro-Tirado (IAA-CSIC, LAEFF), La naturaleza de las explosiones cósmicas de rayos gamma GRBs. **W27/2002A**
– Colina (IF Cantabria), Integral field spectroscopy of ultraluminous infrared galaxies. **W1/2002A**
– Manchado (IAC), Near infrared imaging of galaxy fields. **W21/2002A**
– Martínez-Delgado (IAC), Destrucción de galaxias enanas en el halo Galactico: cinemática de la corriente Norte de Sagitario. **W25/2002A**
– Mediavilla (IAC), Curvas de extinción en galaxias con redshift intermedios. **W20/2002A**
– Pérez (Madrid Complutense), Spatial analysis of populations in local star-forming galaxies. **W5/2002A**
– Rebolo (IAC), Did very massive stars produce r-elements? **W11/2002A**
– Rebolo (IAC), JOVIAN: detección directa de planetas gigantes alrededor de estrellas y aislados. **W32/2002B [*sic*]**
– Ruiz-Lapuente (Barcelona), Estrellas compañeras de supernovas. **W14/2002A**
– Ruiz-Lapuente (Barcelona), Supernovas a z = 0.35. **W15/2002A**

INSTRUMENT BUILDERS' GUARANTEED TIME

– Packham (Florida), The initial conditions to star formation. **GT/2002A/1**

Isaac Newton Telescope

UK PATT

– Boyce (Bristol), CCD imaging of gas-rich low surface brightness galaxies found at 21cm. **I/2002A/15**
– Feltzing (Lund Observatory), Metallicity distribution functions in Local Group dwarf spheroidal galaxies. **I/2002A/18**
– Fitzsimmons (Belfast), Rapid-response astrometry of potentially hazardous asteroids. **I/2002A/26**
– Gilmore (IoA, Cambridge), Eclipsing K/M Dwarfs and the Low-Mass Stellar M/L Ratio. **I/2002A/20**
– Hilditch (St. Andrews), Accretion Hot Spots in Near-Contact Binaries. **I/2002A/13**
– James (Liverpool), Star formation in the local Universe: Hα imaging of the Virgo cluster. **I/2002A/25**
– Jameson (Leicester), Rigorous limits on the bottom end of the Coma open cluster mass-function. **I/2002A/29**
– Jeffries (Keele), Low mass stellar populations in the most massive OB associations. **I/2002A/32**
– Marsh (Southampton), Subdwarf-B stars: tracers of binary evolution. **I/2002A/4**
– Meikle (Imperial College), Detailed study of the physics of nearby Type Ia Supernovae. **I/2002A/14**
– Oliver (Sussex), The INT SIRTF-Legacy: Extra-galactic Survey (ISLES). **I/2002A/40**
– Tanvir (Hertfordshire), Rapid imaging of GRB error boxes and spectroscopy of GRB-related optical/IR transients. **I/2002A/27**

NL NFRA PC

– Beijersbergen (Groningen), UBR imaging of the Coma cluster periphery. **i02an003**
– Kuijken (Groningen), Sloan standard fields for the photometric calibration of OmegaCAM images. **i02an002**
– Mack (ASTRON/NFRA), Constraining the BL Lac Luminosity Function. **i02an001**
– Salamanca (Amsterdam), Rapid imaging of GRB error boxes and spectroscopy of GRB-related optical/IR transients. **w02an008 [*sic*]**

UK/NL WFS Programmes

– Dalton (Oxford), The Oxford Deep WFC Survey. **WFS/2002A/6**
– Davies (Cardiff), Multi-coloured large area survey of the Virgo cluster. **WFS/2002A/2**
– van den Heuvel (Amsterdam), The Faint Sky Variability Survey II. **WFS/2002A/1**
– McMahon (IoA), The INT Wide Angle Survey. **WFS/2002A/8**
– Walton (ING), The Local Group Census. **WFS/2002A/4**
– Watson (Leicester), An Imaging Programme for the XMM-Newton Serendipitous X-ray Sky Survey. **WFS/2002A/3**

SP CAT

– Balcells (IAC), Estudio de Galaxias con Formación Estelar Extrema a Alto Corrimiento al Rojo. **I8/2002A**
– Casares (IAC), Curva de velocidad radial y función de masa del microcuasar LS5039. **I5/2002A**
– Castro-Tirado (IAA-CSIC, LAEFF), La naturaleza de las explosiones cósmicas de rayos gamma GRBs. **W27/2002A**
– Deeg (IAC), Sample Definition for Exoplanet detection by the COROT SpaceCraft. **I10/2002A**
– Herrero (IAC), Espectroscopía cuantitativa de estrellas O ionizantes. **I11/2002A**
– Herrero (IAC), Preparándose para OSIRIS: población estelar joven de NGC 6946. **I20/2002B [*sic*]**
– Hidalgo (IAC), Estructuras a gran escala en galaxias irregulares. **I19/2002B [*sic*]**
– Lázaro (IAC), Fotometría infrarroja de sistemas Algol. **I14/2002A**
– López (Basel), Nebulosas planetarias intercumulares y estructura del cúmulo de Virgo. **I4/2002A**
– Marín (IAC), Sistemas de cúmulos globulares en galaxias elípticas. **I2/2002A**
– Martínez (IAC), Constrainig the Milky Way dark halo shape from the Sagittarius tidal stream. **I12/2002A**
– Negueruela (Strasburg), Estrellas pre-sequencia-principal de masas intermedias en cúmulos abiertos. **I15/2002A**
– Riera (Politécnica Cataluña), The fragmented wind-blown bubbles around intermediate and massive stars. **I7/2002A**
– Vílchez (IAA), A search for Abundance Gradients in Ring Galaxies. **I6/2002A**

Jacobus Kapteyn Telescope

UK PATT

– Boyce (Bristol), Hα imaging of gas-rich low surface brightness galaxies found at 21cm. **J/2002A/10**
– Burleigh (Leicester), Asteroseismology of a pulsating helium-atmosphere white dwarf star. **J/2002A/16**
– Davies (Edinburgh), Lightcurves of Near Earth Objects. **J/2002A/8**
– Fitzsimmons (Belfast), Rapid-response astrometry of potentially hazardous asteroids. **J/2002A/12**
– Fitzsimmons (Belfast), The size and composition of Near-Earth Objects. **J/2002A/18**
– Green (Open University), Thermo-physical properties of a "cometary" NEO. **J/2002A/6**
– Hodgkin (IoA, Cambridge), Photometry of candidate halo white dwarfs. **J/2002A/17**
– Jeffery (Armagh Observatory), Time-resolved observations of the pulsating sdB star PG1605+072. **J/2002A/7**
– Keenan (Belfast), Four-colour photometry of stars from the Palomar-Green Survey. **J/2002A/1**
– Marsh (Southampton), Cataclysmic Variable Stars from the 2dF QSO survey. **J/2002A/4**
– Marsh (Southampton), Companions to sub-dwarf binary stars. **J/2002A/5**
– Morales-Rueda (Southampton), Measuring orbital periods of dwarf novae. **J/2002A/14**
– Norton (Open University), Multiwavelength Observations of SXTs: Black Hole Accretion Disk Outbursts. **J/2002A/2**
– Seigar (JAC, Hawaii), Optical properties of the disks of spiral galaxies. **J/2002A/3**
– Tanvir (Hertfordshire), Rapid imaging of GRB error boxes and spectroscopy of GRB-related optical/IR transients. **J/2002A/13**

NL NFRA PC

– Röttgering (Leiden), A catalogue of galaxies near bright stars: preparing for VLT-AO and VLTI. **j02an002**
– Salamanca (Amsterdam), Rapid imaging of GRB error boxes and spectroscopy of GRB-related optical/IR transients. **w02an008 [*sic*]**

SP CAT

– Baes (Viena), Tracing the dynamic interplay between the gas-dominated and star-dominated disk components in barred spirals. **J1/2002A**
– Calabresi (Rome), Photometry of Centaur Object Chariklo. **J2/2002A**
– Casares (IAC), Optical reprocessing lines as tracers of companion stars in LMXBs. **JW19/2002A**
– Castro-Tirado (IAA-CSIC, LAEFF), La naturaleza de las explosiones cosmicas de rayos gamma GRBs. **JW11/2002A**
– Kidger (IAC), Definition of an accurate 1-30 micron flux calibration system for the GTC and SIRTF. **J4/2002A, J4/2002B [*sic*]**
– López (Basel), ¿Hay barras lentas en galaxias interactuantes? **J3/2002A**
– Rosenberg (IAC), Calibración Homogénea de Cúmulos Globulares del Halo Externo. **J5/2002B [*sic*]**

# Telescope Time Awards Semester 2002B

For observing schedules please visit this web page:
`http://lpss33.ing.iac.es:8080/cgi-bin/schedules.pl`

ITP Programmes on the ING Telescopes

– Doressoundiram (Paris), Multi-color taxonomy of trans-Neptunian objects. **ITP/2002/1**
– Ruiz-Lapuente (Barcelona), Supernova and the physics of supernova explosions. **ITP/2002/4**

William Herschel Telescope

UK PATT

– Blundell (Oxford), After the trigger: the time-resolved evolution of the hosts of powerful active galaxies. **W/2002B/68**
– Crowther (University College, London), Properties of Wolf-Rayet stars in the metal-rich environment of Andromeda (M31). **W/2002B/60**
– Crowther (University College, London), Direct constraints on the expansion velocity of hot, WN stars. **W/2002B/61**
– Dalton (Oxford), Near Infrared Coverage of the Oxford INT Deep Multicolour Imaging Survey. **W/2002B/32**
– Folha (Porto, Portugal), Excess Emission in T Tauri Stars: the Missing link. **W/2002B/54**
– Gray (Edinburgh University), Combined X-ray and weak lensing mass profiles of the brightest cluster lenses. **W/2002B/74**
– Harries (Exeter), A search for Zeeman polarization in the emission lines of classical T Tauri stars. **W/2002B/43**
– Jeffery (Armagh Observatory), Colorimetric mode identification in pulsating subdwarf B stars. **W/2002B/27**
– Longmore (Royal Observatory, Edinburgh), Structure of and star formation limits in isolated dark globules. **W/2002B/38**
– McLure (Edinburgh University), Black-hole mass measurement and the geometry of the broad-line region in AGN. **W/2002B/63**
– Meikle (Imperial College, London), Detailed study of the physics of nearby Type Ia Supernovae. **W/2002B/23 (Override, long term)**
– Meikle (Imperial College, London), Direct detection and study of supernovae in nuclear starbursts. **W/2002B/56 (Long term)**
– Merrifield (Nottingham), 2000 Planetary Nebulae in M31: A Deep Kinematic Survey. **W/2002B/64**
– Naylor (Exeter), Is there structure in the substellar mass function? **W/2002B/52**
– Nelemans (Cambridge), Testing common envelope theory and SN Ia progenitor models with double white dwarfs. **W/2002B/51**
– Page (MSSL-UCL), A pilot spectroscopic study of serendipitous hard spectrum XMM-Newton source. **W/2002B/47**
– Pettini (Cambridge), CORALS II: Assessing the Dust Bias in Damped Lyman α Systems at Intermediate Redshifts. **W/2002A/10 (Long term)**
– Poggianti (Padova Observatory, Italy), Star formation and morphological evolution of galaxies in nearby clusters with WYFFOS. **W/2002B/28 (Long term)**
– Royer (Leuven, Belgium), A complete survey of the Wolf-Rayet content of M33. **W/2002B/16**
– Smail (Durham), Testing Photometric Redshifts using Cluster Lenses. **W/2002B/7**
– Smith (Hertfordshire), Scattering geometries and the broad-line region in Radio-Quiet Quasars. **W/2002B/20**
– Tanvir (Hertfordshire), Gamma-Ray Bursts: Origin, Physics and use as Cosmological Probes. **W/2002B/62 Override**
– Vink (Imperial College), A search for evidence of accretion in Herbig Be stars. **W/2002B/4**
– Wilkinson (Cambridge), NGC2419 — a radial velocity survey of an unusual stellar cluster. **W/2002B/33**
– Willott (Oxford), The Fundamental Plane and black hole masses of $z=0.5$ radio galaxies. **W/2002B/49**
– Wills (Sheffield), Triggering the Activity in Giant Elliptical Galaxies. **W/2002B/9**

NL NFRA PC

– Förster Schreiber (Leiden), Near-infrared Snapshot Survey for Bright Lensed Red High-redshift Galaxies. **w02bn001**
– Ferguson (Groningen), A Search for Recent Massive Star Formation in Gas-Rich Ellipticals/SOs. **w02bn010**
– Hulleman (Utrecht), The nature of magnetars: UltraCam observations of the Anomalous X-Ray Pulsar 4U 0142+61. **w02bn007**
– Jarvis (Leiden), An unbiased view of the gaseous environments of high-redshift radio galaxies. **w02bn005**
– Kuijken (Groningen), M31 microlensing: checking Mira contamination with nIR AO imaging. **w02bn011**
– Kuijken (Groningen), 2000 Planetary Nebulae in M31: a Deep Kinematic Survey. **w02bn002**
– Mellema (Leiden), Polarization studies of the rings and haloes of Planetary Nebulae. **w02bn008**
– O'Brien (Amsterdam), Optical analogues of X-ray timing phenomena. **w02bn003**
– Van den Heuvel (Amsterdam), The Origin and Physics of Gamma-Ray Bursts. **w02bn004 Override**

ES CAT

– Barrado (LAEFF, Madrid), The Substellar Mass Function: Clues to the Star Formation Process. **W7/2002B**
– Esteban (IAC, Tenerife), Abundancias químicas a partir de líneas de recombinación en nebulosas ionizadas. **W3/2002B**
– Gallego (Complutense, Madrid), The evolution of the Star Formation Rate density of the Universe up to $z=0.8$. **W12/2002B**
– Gutiérrez (IAC, Tenerife), Búsqueda de galaxias de muy alto z a través del efecto lente gravitoria en cúmulos. **W23/2002B**
– Gutiérrez (IAC, Tenerife), Fotometría en Hα y espectroscopía de objetos con corrimientos al rojo anómalos. **WN13/2002B**
– Martínez (Valencia), La masa y la extensión de los halos en galaxias elípticas. **W24/2002B**
– Mathieu (IAA, Granada), Do S0 galaxies follow the Tully-Fisher relation? **W1/2002B**
– Negueruela (Alicante), La órbita de V0332+53. **W9/2002B**
– Paredes (Barcelona), Búsqueda de nuevos microcuásares: confirmación espectroscópica de candidatos. **W19/2002B**
– Prieto (IAC, Tenerife), Estudio de galaxias con formación estelar extrema a alto corrimiento al rojo. **W27/2002B**
– Shahbaz (IAC, Tenerife), High time resolution optical studies of quiescent black hole X-ray transients. **W25/2002B**
– Zapatero (LAEFF, Madrid), Compañeros de objetos ultra fríos de la vecindad solar. **W16/2002B**

IAC

– Cepa (IAC, Tenerife), El proyecto OTELO: Cartografiado profundo en B y R de SA68 y NOAO-2h. **W31/2002B**
– Rebolo (IAC, Tenerife), JOVIAN: detección directa de planetas gigantes alrededor de estrellas y aislados. **IW32/2002B**

TNG

– Fasano (Padova), Star formation and morphological evolution of galaxies in nearby clusters with WYFFOS. **T022**
– Mannucci (Arcetri), A critical test of cosmological models: tracing the elusive filaments of hot intergalactic gas. **T064**
– Moretti (Padova), Ages and metal abundances of star clusters in M33. **T083**

– Saviane (ESO, Chile), Near-infrared luminosities of dwarf galaxies in the M81 group. **T093**

Isaac Newton Telescope

UK PATT

– Baines (Leeds), Spectro-astrometry of Herbig Ae/Be and T Tauri stars. **I/2002B/12**
– Fitzsimmons (Belfast), Rapid-response astrometry of potentially hazardous asteroids. **I/2002B/18 (Override)**
– Gänsicke (Southampton), The cataclysmic variable population of the Hamburg Quasar Survey. **I/2002B/5**
– Irwin (Cambridge), A Panoramic CCD Survey of the Halo and Disk of M31. **I/2002B/24**
– Jameson (Leicester), Population II/III planetary nebulae and the proper motions of Pleiades BD candidates. **I/2002B/8**
– Keenan (Belfast), A search for early-type stars in the haloes of distant galaxies. **I/2002B/1**
– Marsh (Southampton), Identification of faint stellar ROSAT sources. **I/2002B/4**
– Maxted (Keele), Spectroscopy of detached eclipsing binaries in open clusters. **I/2002B/23**
– McLure (Edinburgh University), A photometric redshift study of radio galaxy environments. **I/2002B/27**
– Meikle (Imperial College, London), Detailed study of the physics of nearby Type Ia Supernovae. **I/2002B/9 (Override, long term)**
– Tanvir (Hertfordshire), Gamma-Ray Bursts: Origin, Physics and use as Cosmological Probes. **I/2002B/28 (Override)**
– Williams (Queen Mary, London), The asteroidal population at the equilateral Lagrangian points of Saturn. **I/2002B/2**

NL NFRA PC

– De Jong (Groningen), The MEGA Survey: Mapping Microlensing in M31. **i02bn002**
– Ferguson (Groningen), A Panoramic CCD Survey of the Halo and Disk of M33. **i02bn006**
– Groot (Nijmegen), Beyond the Blue Edge in the Faint Sky Variability Survey. **i02bn004**
– Van den Heuvel (Amsterdam), The Origin and Physics of Gamma-Ray Bursts. **w02bn004 (GRB override)**

UK/NL WFS Programmes

– van den Heuvel (Amsterdam), The Faint Sky Variability Survey II. **WFS/2002A/1**
– McMahon (IoA), The INT Wide Angle Survey. **WFS/2002A/8**
– Walton (ING), The Local Group Census. **WFS/2002A/4**
– Watson (Leicester), An Imaging Programme for the XMM-Newton Serendipitous X-ray Sky Survey. **WFS/2002A/3**

ES CAT

– Aparicio (La Laguna), Large scale distribution of stellar populations in the M33 halo. **I13/2002B**
– Barrado (LAEFF, Madrid), Deep pencil-beam survey in a young, nearby cluster. **I4/2002B**
– Carrero (IAC, Tenerife), Calibración del triplete del CaII como indicador de metalicidad. **I7/2002B**
– Fernández (IAA, Granada), Pérdida violenta de masa en estrellas jóvenes de tipo solar. **I22/2002B**
– Garzón (IAC, Tenerife), Understanding of the structure of the Galaxy. **I23/2002B**
– Herrero (IAC, Tenerife), Preparándose para OSIRIS: población estelar joven de NGC 6946. **I20/2002B**
– Herrero (IAC, Tenerife), Espectroscopía cuantitativa de estrellas O ionizantes. **I5/2002B**
– Hidalgo (IAC, Tenerife), Estructuras a gran escala en galaxias irregulares. **I19/2002B**
– Montes (Complutense, Madrid), Spectroscopic and photometric monitoring with high temporal resolution of flare stars. **I1/2002B**
– Negueruela (Alicante), La distribución espectral de las estrellas Be. **I6/2002B**
– Pohlen (IAC, Tenerife), The outer edge of the Galaxy. **I11/2002B**
– Ribas (Barcelona), Determinación directa de la distancia de M31 a partir de binarias eclipsantes. **I8/2002B**
– Riera (Politécnica de Cataluña), The fragmented wind-blown bubbles around intermediate and massive stars. **I2/2002B**

IAC

– Balcells (IAC, Tenerife), Cartografiado profundo en U, V, e I para COSMOS y OTELO. **I21/2002B**
– Rebolo (IAC, Tenerife), JOVIAN: detección directa de planetas gigantes alrededor de estrellas y aislados. **IW32/2002B**

Jacobus Kapteyn Telescope

UK PATT

– Bucciarelli (Torino Observatory, Italy), Photometric Calibrators for the Palomar Sky Surveys. **J/2002B/3**
– Burleigh (Leicester), Star Spots on Magnetic White Dwarfs. **J/2002B/5**
– Fitzsimmons (Belfast), Rapid-response astrometry of potentially hazardous asteroids. **J/2002B/8 (Override)**
– Keenan (Belfast), Four-colour photometry of stars from the Palomar-Green Survey. **J/2002B/2 (Long term)**
– Littlefair (Exeter), Are young stars really spun down by their discs? **J/2002B/7**
– Marsh (Southampton), Companions to sub-dwarf binary stars. **J/2002B/1**
– Maxted (Keele), Photometry of detached eclipsing binaries in open clusters. **J/2002B/10**
– McBride (Open University), Physical and thermal properties of Near Earth Objects. **J/2002B/6**
– Norton (Open University), Multiwavelength Observations of SXTs: Black Hole Accretion Disk Outbursts. **J/2002A/2 (Override, long term)**
– Tanvir (Hertfordshire), Gamma-Ray Bursts: Origin, Physics and use as Cosmological Probes. **J/2002B/12 (Override)**

NL NFRA PC

– Röttgering (Leiden), A catalogue of galaxies near bright stars: preparing for VLT-AO and VLTI. **j02bn001**
– Tolstoy (Groningen), Photometric Zero Points in Local Group Dwarf Galaxies. **j02bn004**
– van den Berg (Brera Observatory, Italy), Photometry of peculiar X-ray sources in the old open cluster NGC 6940. **j02bn002**
– Van den Heuvel (Amsterdam), The Origin and Physics of Gamma-Ray Bursts. **w02bn004 (GRB override)**

ES CAT

– Fuensalida (IAC, Tenerife), Medida del perfil vertical de turbulencia en el ORM. **J6/2002B**
– Kidger (IAC, Tenerife ), Fotometría de alta precisión de estrellas estándar para CanariCam. **J7/2002B**
– Lara (IAA, Granada), Gas and dust analysis of the Jupiter family comets 30P/Reinmuth 1 and 57P/duToit-Neujmin-Delporte. **J1/2002B**
– López (IAC, Tenerife), Hay barras lentas en galaxias interactuantes? **J2/2002B**
– Montes (Complutense, Madrid), Spectroscopic and photometric monitoring with high temporal resolution of flare stars. **JI1/2002B**
– Rodríguez (IAC, Tenerife), Estudio fotométrico de remanentes de nova débiles y poco estudiados. **J3/2002B**

IAC

– Beckman (IAC, Tenerife), Stromgren photometry of stars from the Hipparcos catalogue within 300 pc of the Sun. **J8/2002B**
– Fuensalida (IAC, Tenerife), Medida del perfil vertical de turbulencia en el ORM. **J6/2002B**
– Kidger (IAC, Tenerife), Definition of an accurate 1–30 micron flux calibration system for the GTC and SIRTF. **J4/2002B**
– Kidger (IAC, Tenerife), Fotometría de alta precisión de estrellas estándar para CanariCam. **J7/2002B**
– Rosenberg (IAC, Tenerife), Calibración homogénea de cúmulos globulares del halo externo. **J5/2002B**

*Abbreviations:*

| | |
|---|---|
| CAT | Comité para la Asignación de Tiempo |
| ES | Spain |
| IAC | Instituto de Astrofísica de Canarias |
| ITP | International Time Programme |
| NFRA | Netherlands Foundation for Research in Astronomy |
| NL | The Netherlands |
| PATT | Panel for the Allocation of Telescope Time |
| PC | Programme Committee |
| SP | Spain |
| UK | The United Kingdom |
| WFS | Wide Field Survey |

# Contents



| Contacts at ING | Name | Tel. (+34 922) | E-mail (@ing.iac.es) |
|---|---|---|---|
| ING Reception | | 425400 | |
| Director | *René Rutten* | 425420 | rgmr |
| Personal Secretary to Director | *Rachael Miles* | 425420 | miles |
| Public Relations | *Javier Méndez* | 425464 | jma |
| Head of Administration | *Les Edwins* | 425418 | lie |
| Head of Astronomy | *Danny Lennon* | 425441 | djl |
| Head of Engineering | *Gordon Talbot* | 425419 | rgt |
| Telescope Scheduling | *Ian Skillen* | 425439 | wji |
| Service Programme | *Saskia Prins* | 425463 | stp |
| WHT Manager | *Chris Benn* | 425432 | crb |
| INT Manager | *Romano Corradi* | 425461 | rcorradi |
| JKT Manager | *Romano Corradi* | 425461 | rcorradi |
| Instrumentation Technical Contact | *Tom Gregory* | 425444 | tgregory |
| Freight | *Juan Martínez* | 425414 | juan |

Isaac Newton Group of Telescopes
Roque de Los Muchachos Observatory, La Palma